STUDY ON VEHICULAR EMISSIONS OF VOCS AND OVOCS BY USING MULTIPLE MEASUREMENT TECHNIQUES IN HONG KONG

CUI LONG

PhD

The Hong Kong Polytechnic University

2018

The Hong Kong Polytechnic University

Department of Civil and Environmental Engineering

Study on Vehicular Emissions of VOCs and OVOCs by Using Multiple Measurement Techniques in Hong Kong

CUI Long

A thesis submitted in partial fulfillment of the requirements for the degree of Doctor of Philosophy

April 2018

CERTIFICATE OF ORIGINALITY

I hereby declare that this thesis is my own work and that, to the best of my knowledge and belief, it reproduces no material previously published or written, nor material that has been accepted for the award of any other degree or diploma, except where due acknowledgement has been made in the text.

_____(Signed)

_____CUI Long_____(Name of student)

ABSTRACT

Hong Kong is one of the most densely populated cities all over the world. It is facing serious air pollution problems during the past twenty years such as the increasing ground level ozone trend and the reduction of visibility year by year. Volatile organic compounds (VOCs) which can be emitted from multiple sources are important precursors of tropospheric ozone and secondary organic aerosols. Vehicular emissions is one of the major contributors to ambient VOCs in Hong Kong. The Hong Kong Special Administrative Region Government (HKSARG) has implemented a series of control measures to reduce local air pollutions from on-road vehicles. In order to investigate the changes of characteristics and source emission of VOCs and oxygenated VOCs (OVOCs), one roadside campaign at Mong Kok Air Quality Monitoring Station (MK AQMS) and one inside tunnel campaign at Shing Mun (SM) Tunnel were undertaken in this study.

The proton transfer reaction–mass spectrometry (PTR-MS) technique was firstly introduced to measure OVOCs and VOCs in an urban roadside area of Hong Kong. The integrated effect of ambient relative humidity (RH) and temperature (T) on formaldehyde measurements by PTR-MS was explored in this study. A Poly 2-D regression was found to be the best nonlinear surface simulation (r = 0.97) of the experimental reaction rate coefficient ratio, ambient RH, and T for formaldehyde measurement. Inter-comparisons were performed between PTR-MS and other

traditional VOC and OVOC measurement techniques, namely, (1) offline 2,4-dinitrophenylhydrazine (DNPH) cartridge sampling followed by high-performance liquid chromatography (HPLC) analysis; (2) online gas chromatography (GC) with flame ionization detection (FID); and (3) offline canister sampling followed by GC with mass spectrometer detection (MSD), FID, and electron capture detection (ECD). In general, good agreements were found between PTR-MS and other analytical techniques for OVOC species (i.e. formaldehyde, acetaldehyde, and acetone etc.) and aromatic hydrocarbons with correlation coefficients no less than 0.75.

The characteristics and source apportionment of roadside VOCs and OVOCs were investigated and analyzed through the field study at MK AQMS. The total mixing ratio of VOCs and OVOCs at MK AQMS was found to be decreased by about 37% after the liquefied petroleum gas (LPG) catalytic convertor replacement programme (CCRP), which was launched by Hong Kong Environmental Protection Department (EPD) from September 2013 and finished by the end of April 2014. LPG vehicular emissions was found to be one of the major sources of roadside VOCs and OVOCs both before (45%) and after (38%) the LPG CCRP, however, the total contribution from LPG vehicular emissions decreased from 30.5 ppbv to 13.8 ppbv. The sum of OFP for the total target VOCs and OVOCs also decreased by 44% after the LPG CCRP.

Updated vehicular VOC and OVOC emission profiles and emission factors were obtained from the tunnel study in 2015. Net concentrations and emission factors of

nearly all gas species decreased a lot compared with previous tunnel study at the same sampling site in 2003. Emission factors of VOCs and OVOCs from diesel-fueled, gasoline-fueled, and LPG-fueled vehicles were reconstructed in this study. And the decrease of emission factors of those different vehicle types' tracers could reflect the controlling effectiveness on vehicular air pollutants emissions in Hong Kong.

Overall, this study firstly introduced PTR-MS to measure urban roadside VOCs and OVOCs in Hong Kong, and explored the integrated effect of ambient RH and T on formaldehyde measurements by PTR-MS. The results of the large decrease of VOCs and OVOCs both at the roadside sampling site and the inside tunnel site could demonstrate the effectiveness of the series of air pollution control measures undertaken during the past twenty years by the Hong Kong government.

PUBLICATIONS

1. **Cui, L.**, Wang, X.L., Ho, K.F., Gao, Y., Liu, C., Hang Ho, S.S., Li, H.W., Lee, S.C., Wang, X.M., Jiang, B.Q., Huang, Y., Chow, J.C., Watson, J.G., Chen, L.-W., 2018. Decrease of VOC emissions from vehicular emissions in Hong Kong from 2003 to 2015: Results from a tunnel study. Atmospheric Environment 177, 64-74.
2. **Cui, L.**, Zhang, Z., Huang, Y., Lee, S.C., Blake, D.R., Ho, K.F., Wang, B., Gao, Y., Wang, X.M., Louie, P.K.K., 2016. Measuring OVOCs and VOCs by PTR-MS in an urban roadside microenvironment of Hong Kong: relative humidity and temperature dependence, and field intercomparisons. Atmospheric Measurement Techniques 9, 5763-5779.
3. Wang, X., Ho, K.-F., Chow, J.C., Kohl, S.D., Chan, C.S., **Cui, L.**, Lee, S.-c.F., Chen, L.-W.A., Ho, S.S.H., Cheng, Y., Watson, J.G., 2018. Hong Kong vehicle emission changes from 2003 to 2015 in the Shing Mun Tunnel. Aerosol Science and Technology, 1-14.
4. Liang, Y., Zha, Q., Wang, W., **Cui, L.**, Lui, K.H., Ho, K.F., Wang, Z., Lee, S.-c., Wang, T., 2017. Revisiting Nitrous Acid (HONO) Emission from On-road Vehicles: A Tunnel Study with a Mixed Fleet. Journal of the Air & Waste Management Association, 67:7, 797-805.
5. Li, H., Huang, T., Lu, Y., **Cui, L.**, Wang, Z., Zhang, C., Lee, S., Huang, Y., Cao, J., Ho, W., 2018. Unraveling the mechanisms of room-temperature catalytic degradation of indoor formaldehyde and its biocompatibility on colloidal TiO2-

supported MnO_x-CeO_2. Environmental Science: Nano.

6. Song, J., Zhang, Y., Huang, Y., Ho, K.F., Yuan, Z., Ling, Z., Niu, X., Gao, Y., **Cui, L.**, Louie, P.K.K., Lee, S.-c., Lai, S., 2018. Seasonal variations of C_1-C_4 alkyl nitrates at a coastal site in Hong Kong: Influence of photochemical formation and oceanic emissions. Chemosphere 194, 275-284.
7. Yun, H., Wang, Z., Zha, Q., Wang, W., Xue, L., Zhang, L., Li, Q., **Cui, L.**, Lee, S., Poon, S.C.N., Wang, T., 2017. Nitrous acid in a street canyon environment: Sources and contributions to local oxidation capacity. Atmospheric Environment 167, 223-234.
8. Li, L., Ho, S.S.H., Chow, J.C., Watson, J.G., Lee, F.S.C., **Cui, L.**, Gao, Y., Dai, W., Ho, K.F., Huang, Y., Cao, J., 2017. Characterization and health risk assessment of $PM_{2.5}$-bound organics inside and outside of Chinese smoking lounges. Chemosphere 186, 438-445.
9. Li, H., Lee, S., Wang, Z., Huang, Y., Ho, W., **Cui, L.**, 2017. Peroxymonosulfate activated by amorphous particulate MnO_2 for mineralization of benzene gas: Redox reaction, weighting analysis, and numerical modelling. Chemical Engineering Journal 316, 61-69.
10. Wang, J., Virkkula, A., Gao, Y., Lee, S., Shen, Y., Chi, X., Nie, W., Liu, Q., Xu, Z., Huang, X., Wang, T., **Cui, L.**, Ding, A., 2017. Observations of aerosol optical properties at a coastal site in Hong Kong, South China. Atmospheric Chemistry and Physics 17, 2653.
11. Yang, F., Kawamura, K., Chen, J., Ho, K., Lee, S., Gao, Y., **Cui, L.**, Wang, T., Fu,

P., 2016. Anthropogenic and biogenic organic compounds in summertime fine aerosols (PM2.5) in Beijing, China. Atmospheric Environment 124, Part B, 166-175.

12. Huang, Y., Ling, Z.H., Lee, S.C., Ho, S.S.H., Cao, J.J., Blake, D.R., Cheng, Y., Lai, S.C., Ho, K.F., Gao, Y., **Cui, L.**, Louie, P.K.K., 2015. Characterization of volatile organic compounds at a roadside environment in Hong Kong: An investigation of influences after air pollution control strategies. Atmospheric Environment 122, 809-818.
13. Cheng, Y., Lee, S.C., Gao, Y., **Cui, L.**, Deng, W., Cao, J., Shen, Z., Sun, J., 2015. Real-time measurements of $PM_{2.5}$, $PM_{10-2.5}$, and BC in an urban street canyon. Particuology 20, 134-140.

ACKNOWLEDGEMENTS

I would like to express my sincere thanks to my supervisor, Prof. S. C. Lee, for his encouragement, patient, invaluable guidance and helpful advice through my entire study period. He is not only the supervisor on science but also on other aspects of a human life. I would also like to thank Mr. W.F. Tam, the technician of our laboratory, for his technical support on lab work. Special thanks are given to Prof. D.R. Blake, Prof. J.C. Chow, Prof. J.G. Watson, S.C., Prof. X.L. Wang, Prof. X.M. Wang, Prof. Y. Huang, Prof. K.F. Ho, and Dr. Y. Cheng for their assistance on review and revision of published journal papers as well as the thesis. I must express my thanks to all of my friends, particularly Zhang Zhou, Gao Yuan, Sun Jian, Li Haiwei, Kenny Lok, Wang Weihao, Gong Han, Yu Chuan, and Yun Hui, for their support and care which helped me overcome setbacks on work and those days when I was sick, and keep focused on my graduate study. Finally, I would like to thank my families for their moral support and endless love.

TABLE OF CONTENTS

LIST OF FIGURES

LIST OF TABLES

Chapter 1. Introduction

1.1 Background and the objectives of this study

Ambient (outdoor) air pollution is a global problem and about 3 million deaths every year are linked to ambient air pollution. Volatile organic compounds (VOCs) are one of the most important air pollutants. VOCs can be easily emitted from multiple natural and anthropogenic sources to the atmosphere because of their relative low boiling point. Both ozone and secondary organic aerosols can be generated by VOCs through a series of photochemical transformation (Haagen-Smit, 1952; Mader et al., 1952).

VOCs and oxygenated VOCs (OVOCs) can be measured by different techniques, such as off-line Gas Chromatography - Mass Spectrometer Detection / Flame Ionization Detection/ Electron Capture Detection (GC-MSD/FID/ECD), off-line High Performance Liquid Chromatography (HPLC), on-line GC-FID, on-line Differential Optical Absorption Spectroscopy (DOAS), on-line Atmospheric Pressure - Chemical Ionization Mass Spectrometer (AP-CIMS), on-line Proton-transfer Ion Trap - Mass Spectrometer (PIT-MS), on-line Selected Ion Flow Tube - Mass Spectrometry (SIFT - MS), and on-line Proton Transfer Reaction - Mass Spectrometry (PTR-MS) (Christian et al., 2004; Herrington et al., 2007; Smith and Španěl, 2005; Warneke et al., 2011a; Warneke et al., 2001; Warneke et al., 2011b; Xue et al., 2014). Only off-line GC-

MSD/FID/ECD, off-line HPLC, and on-line GC-FID have been using to measure the ambient VOC and OVOC levels in Hong Kong before (Chan et al., 2002; Guo et al., 2004a; Ho et al., 2002; Ou et al., 2015). On-line PTR-MS, which has been developed and widely used on atmospheric chemistry research worldwide since the late 1990s (Bon et al., 2011; Gouw et al., 2003; Jordan et al., 2009; Kuster et al., 2004; Lindinger et al., 1998; Rogers et al., 2006), was firstly used to measure ambient VOCs and OVOCs in Hong Kong in this study. Moreover, PTR-MS has been used in chamber studies, urban areas, suburban areas, mountain areas, forest areas, and ocean areas in other countries/cities all over the world, however, it was the first time that PTR-MS was applied on atmospheric study in urban roadside areas in Hong Kong. Therefore, the validation work of PTR-MS and inter-comparison with other measurement techniques which have been used in Hong Kong was conducted in this study.

Hong Kong, one of the most densely populated city all over the world, is experiencing multiple air pollution problems which both reduced visibility and affected public human health during the past two decades (Louie et al., 2013). Local street-level air pollution and reginal smog problem are the two main air pollution issues of Hong Kong. The Hong Kong Special Administrative Region Government (HKSARG) has implemented a series of control measures to reduce local street-level air pollutions, including control emissions from motor vehicles, marine vessels, power plants, and industrial and commercial processes locally. On the other hand, "A Clean Air Plan for Hong Kong" was released by the Environment Bureau (ENB) in March 2013 for regional air

pollution reduction, and an emission reduction plan for the Pearl River Delta (PRD) region was endorsed by the governments of Hong Kong and Guangdong in November 2012. Four major air pollutants, namely sulphur dioxide (SO_2), nitrogen oxides (NO_X), respirable suspended particulates (RSP) and VOC were included in this plan. The emission reduction targets for VOC was -15% to 2020 as compared with 2010 in Hong Kong and -15% ~ -25% to 2020 as compare with 2010 in PRD zone.

Road transport was found to be one the key sources of air pollution in Hong Kong. Based on Hong Kong Air Pollutant Emission Inventory Report, nearly 18% of VOCs were emitted from road transport (HKEPD, 2017). Many studies on VOC source apportionment have been done from the early 2000s in Hong Kong, and vehicular emissions, including diesel/gasoline/LPG-fueled vehicle exhaust and fuel evaporation, were found to consist of 30% ~ 70% of the total measured VOCs (Guo et al., 2011a; Guo et al., 2004b; Huang et al., 2015; Lau et al., 2010; Ling et al., 2011). Liquefied Petroleum Gas (LPG) vehicular emissions became one of the serious air pollution issues in Hong Kong since nearly all taxis and most public light buses were switched from diesel-fuel to LPG-fuel since 2000, an LPG catalytic convertor replacement programme (CCRP) was launched in September 2013 and finished the replacement of more than 80% of taxis and public light buses in Hong Kong till April 2014. PTR-MS, together with other measurement techniques for VOCs and OVOCs, was applied to measure the roadside VOCs and OVOCs, and investigate the characteristic and sources changing before and after the LPG CCRP in this study.

A series of air pollution control measures have been implemented to reduce the air pollutants from vehicular emissions by the local government since 1999 in Hong Kong, such as the incentive programme to replace diesel-fueled taxis/light buses with LPG-fueled vehicles (from 2000 to 2006), the adoption of tighter fuel and vehicle emission standards (from 2001 to 2012), the incentive programme to retrofit old diesel vehicles with particulate reduction devices (from 2000 to 2004), and reduction of first registration tax for environment-friendly vehicles etc (HKEPD, 2017). A field study at Shing Mun (SM) Tunnel has been done in 2003 by our research group to investigate the source profiles and emission factor of air pollutants from on-road vehicles. In this study, a repeated tunnel campaign was conducted at the same sampling location in 2015. Updated information of VOC profiles and emission factors were obtained by the tunnel study, and the changes of VOC emissions from vehicular emissions through twelve years (from 2003 to 2015) was identified to estimate the effectiveness of air pollution control measures in Hong Kong.

This is the first time to apply PTR-MS on measuring ambient VOCs and OVOCs in urban roadside areas in Hong Kong, and a repeated tunnel study was conducted in 2015 to investigate the updated vehicular VOC and OVOC emissions in this study. Therefore, the objectives of this study are:

a) To explore the methodology on using PTR-MS for atmospheric chemistry study in roadside areas of Hong Kong under high temperature and high relative humidity;

b) To compare the difference between PTR-MS and other techniques on measuring ambient VOCs and OVOCs, and the differences of inter-comparison results between this study and other studies worldwide;

c) To identify the characteristics and sources of roadside VOCs and OVOCs before and after the LPG CCRP in Hong Kong, and then to evaluate the effectiveness of this air pollution control programme;

d) To determine the source profiles and emission factors of VOCs and OVOCs from on-road vehicles in Hong Kong through a tunnel study;

e) To quantify the reduction of vehicular VOC and OVOC emissions in Hong Kong from 2003 to 2015;

f) To evaluate the effectiveness of the series of air pollution control measures from the aspect of vehicular VOC and OVOC emissions since the early 2000s in Hong Kong.

1.2 Outline of the Dissertation

This dissertation comprises eight chapters. Chapter 1 provides a brief introduction on vehicular VOC and OVOC emissions status and local air pollution control history in Hong Kong. The objectives of this study are also given in Chapter 1. In Chapter 2, background information on VOCs, introduction of PTR-MS on atmospheric chemistry study, and VOC studies in Hong Kong are reviewed. Methodology on sampling, instrumentation, analytical methods, and modeling are introduced in Chapter 3. Chapter 4 presents the validation of PTR-MS on measuring ambient VOCs and OVOCs under high temperature and high relative humidity in Hong Kong, inter-comparisons between different measurement techniques are discussed in this chapter. In Chapter 5, the characteristics of roadside VOCs and OVCs, and their source apportionment results before and after the LPG CCRP are discussed. In Chapter 6, the emission profiles and emission factors of VOCs and OVOCs from on-road vehicles are quantified, and the effectiveness of the series of air pollution control measures undertaken during the past twelve years in Hong Kong are evaluated. The results of this study are summarized in Chapter 7. And Chapter 8 gives the significance and limitations of this study.

Chapter 2. Literature Review

2.1 Overview of volatile organic compounds

VOCs are organic chemicals which are highly volatile at ordinary room temperature. VOCs include a large amount of different groups, for instance, alkanes, alkenes, alkynes, aromatic hydrocarbons, alcohols, aldehydes, ketones, and halogenated compounds.

There are several different definitions for VOCs based on their effects or physical properties. The United States Environmental Protection Agency (US EPA) applies an additional requirement to limit the large number of VOCs for their interests, emphasizing their ozone formation property and toxicity. Volatile organic compounds are defined as a group of carbon compounds, excluding carbon monoxide, car bon dioxide, carbonic acid, metallic carbides or carbonates, and ammonium carbonate, which are reactive to participate in atmospheric photochemical reaction to form ozone and ozone precursors (USEPA, 2009). VOCs are functionally defined as organic compounds that have a vapour pressure of 0.001 kPa or more at 293.15 K, or have a corresponding volatility under particular conditions of use according to EU Directive 1999/13/EC or Solvent Emissions Directive (EU, 1999). However, boiling point is used by the EU Paint Directive 2004/42/EC (EU, 2004) in the definition of VOCs and it is defined as an organic compound having an initial boiling point lower than or equal to 250 ^{o}C at an atmospheric pressure of 101.3 kPa. The World Health Organization (WHO)

categorizes indoor organic pollutants as (1) Very volatile organic compounds (VVOCs), (2)Volatile organic compounds (VOCs), and (3) Semi-volatile organic compounds (SVOCs) based on the different boiling range. The higher the volatility (lower the boiling point), the more likely the compound will be emitted from a product or surface into the air. Table 2.1 shows the different classes of VOCs according to the WHO (World Health, 1989).

VOCs can be released to the Earth's atmosphere from multiple natural and anthropogenic sources. Natural sources of atmospheric VOCs include emission from vegetation (specifically rural forested areas), oceans, marine environments, phytoplanktons, soil microbiota and geological hydrocarbon reservoirs (Sahu, 2012; Stavrakou et al., 2009). Anthropogenic sources of ambient VOCs mainly include vehicle emissions, solvent usage, industrial sources, and evaporation of fuel.

Through a series of photochemical transformation, VOCs can lead to the formation of both ozone and secondary organic aerosols (Haagen-Smit, 1952; Mader et al., 1952). The life time of VOCs in the atmosphere can range a lot from hours to thousands of years depending on the atmospheric conditions and the reactivity of different compounds (Atkinson and Arey, 2003). With regard to its highly evaporative nature, VOCs can easily escape into the atmosphere and then be breathed into the human respiratory system. Acute and chronic health effects may be induced by everyday exposure in high-level VOC environment. Eye, nose and throat irritation, headaches,

vomiting, dizziness and asthma exacerbation are classified as actual effects, while liver, kidney and central nervous system damage and cancer are chronic effects (Elliott et al., 2006; Kampa and Castanas, 2008; Ware et al., 1993; Zhang and Smith, 2003).

2.2 Volatile organic compounds detection by PTR-MS

2.2.1 Instrument configurations

PTR-MS was developed in the late 1990s by Lindinger and co-workers at the University of Innsbruck in Austria (Hansel et al., 1995; Lindinger et al., 1998). Proton-transfer reaction is used by this technique with H_3O^+ ions to ionize atmospheric VOC and the product ions are analyzed by mass-spectrometric detector. The proton-transfer chemistry takes place in a drift-tube reactor, which enhances the ion kinetic energy and effectively limits cluster ion formation with the abundant water molecules in ambient air. This simplifies both the proton-transfer chemistry and the interpretation of the mass spectra (Warneke et al., 2005).

A quadrupole mass spectrometer was firstly used to select and detect product ions in the original PTR-MS instrument. Several other types of mass spectrometers (i.e. ion traps and time-of-flight analyzers) were incorporated into PTR-MS instrumentation later. In the late 2000s, the development of PTR-MS with the time-of-flight mass spectrometry (TOF-MS) fulfilled a much higher mass resolution ($R = m/\Delta m$, where Δm

is the full width at half-maximum of the isolated ion peak) than the quadrupole mass filters used before (Graus et al., 2010; Jordan et al., 2009) . Importantly, isobaric ions with different elemental compositions could be separately measured by the advantage of PTR-TOF-MS technique. Furthermore, The detection limits of PTR-MS instrument were significantly improved by equipping a quadrupole ion guide for the highly effective transfer of ions from the drift tube to the mass spectrometer, which was called PTR-QiTOF-MS, whereas "Qi" stands for "Quadrupole interface" (Sulzer et al., 2014). Ion-trap mass spectrometry was also used in PTR-MS instruments in order to select product ions by mass and dissociated and the fragment ion spectra could be determined (Mielke et al., 2008; Warneke et al., 2005).

A PTR-MS instrument usually consists of four different parts, namely, ion source, drift tube, ion interfaces, and mass analyzer. High-purity hydronium ions (H_3O^+) are generated by the ion source, and then hydronium ions are introduced into the drift tube for proton-transfer reactions. A VOC specie (R) with higher proton affinity than that of water (165.2 kcal mol^{-1}) can be ionized via proton transfer reaction with H_3O^+ to produce the product ions (RH^+) in the drift tube (equation 2.1). The product ions are then transmitted through the ion interfaces to a mass spectrometry analyzer for detection.

$$H_3O^+ + R \rightarrow RH^+ + H_2O \qquad (2.1)$$

Many versions of PTR-MS instruments have been developed in the past decade. The different versions of PTR-MS introduced by commercial companies (Ionicon Analytik and Kore Technology) or custom-built by various research groups have been summarized and illustrated by Yuan et al. (2017) as in Figure 2.1.

2.2.2 Applications of PTR-MS on atmospheric chemistry

PTR-MS has been successfully applied in atmospheric and environmental chemistry studies from the past decade. A wide range of VOCs and OVOCs in the atmosphere can be measured by using this technique as summarized in Table 2.2 (Yuan et al., 2017). Since VOCs generated from multiple sources have a great impact on atmospheric chemistry, a lot of compounds have been routinely measured by PTR-MS. By coupling with PTR-MS and other techniques to measure air pollutants (i.e. CO, SO_2, NO_x, ozone, and aerosols), a detailed picture of the overall atmospheric physics and chemistry can be drawn.

PTR-MS has also been used in many chamber studies. The atmospheric process can be simulated in a large chamber by controlling air conditions (temperature, relative humidity, light, air exchange rate etc.) and known levels of certain air pollutants like NO_x, ozone, and aerosols. Alternatively, PTR-MS has been applied to study the ambient air in different types of places, such as urban areas (Herndon et al., 2005; Kato et al., 2004; Slowik et al., 2010; Wang et al., 2014), suburban areas (Kuster et al., 2004;

Warneke et al., 2001), mountain areas (Fall et al., 2001; Inomata et al., 2010), forest areas (Müller et al., 2006), and ocean areas (Gouw et al., 2003).

2.3 Characteristic of volatile organic compounds in Hong Kong

2.3.1 Long-term variation of ambient volatile organic compounds in Hong Kong

The Hong Kong Air Pollutant Emission Inventory has been complied by the Hong Kong Environmental Protection Department (EPD) since March 2000. The quantity and the major sources of local air pollutant emissions are analyzed and published by the Hong Kong air pollutant emission inventory report every year. Six major air pollutants are included in the emission inventory report, namely, SO_2, NO_x, RSP, fine suspended particulates ($PM_{2.5}$), VOC and carbon monoxide (CO). Seven emission sources are categorized as public electricity generation, road transport, navigation, civil aviation, other combustion sources, non-combustion sources, and biomass burning. Non-combustion sources for VOC here mainly include paints and associated solvents, consumer products and printing (HKEPD, 2017).

Total VOC emissions has been decreased by about 65% from 1997 (76,510 tonnes) to 2015 (26,610 tonnes) as shown in Figure 2.2. Non-combustion source comprised the most (58% ~ 73%) of total VOC emissions through the past 18 years. Except non-combustion source, road transport is the major source of VOC emissions with the

percentage of 16% ~ 21%. During the past decade, the local government of Hong Kong has taken measures to control VOC emissions with increasing recognition of the adverse health effects of VOCs. On the one hand, VOC emissions from regulated products such as solvent-based paints/coatings, adhesives, sealants, printing inks etc. were controlled by the Air Pollution Control Regulation, and the products imported into Hong Kong and manufactured in Hong Kong with VOC contents exceeding the prescribed limits were prohibited. The VOC Regulation controls the VOC contents of architectural paints/coatings, printing inks and six selected categories of consumer products (air fresheners, hairsprays, multi-purpose lubricants, floor wax strippers, insecticides and insect repellents) in phases starting from 1 April 2007. On the other hand, road transport air pollutant emissions have been controlled by the following four sectors: (1) tightening vehicle emission standards, (2) updating vehicle fuel standards, (3) switching diesel vehicles to liquefied petroleum gas (LPG) vehicles, and (4) retrofitting emission control devices.

2.3.2 Sources of volatile organic compounds in Hong Kong

Source apportionment of ambient VOCs in Hong Kong has been studied from the early 2000s. The principal component analysis (PCA) method has been applied to analyze the sources of VOCs at a rural site in Hong Kong from 2002 to 2003 (Guo et al., 2004b). It was found that vehicle emissions and biofuel burning contributed 71% of the total VOC emissions, gasoline evaporation and solvent emissions contributed about 7%,

biomass burning and industrial emissions contributed about 22% of the total VOC emissions. Another study at a coastal sampling site in Hong Kong found that vehicular emissions, LPG usage, gasoline evaporation, and industrial emissions contributed 39%, 12%, 14%, and 35%, respectively of ambient VOCs by using the PCA method (Guo et al., 2006). The sources of ambient VOCs at four sites ranging from urban to rural areas in Hong Kong from September 2002 to August 2003 were identified by Guo et al. (2007). Vehicular emissions contributed the most for all of the four sampling sites, it comprised about 65% of total ambient VOCs at the urban site, and about 50% at the two-suburban sites (53% and 49%) and the one rural site (48%) (Guo et al., 2007).

The Positive Matrix Factorization (PMF) model has also been widely applied to conduct the source apportionment of VOCs in Hong Kong (Guo et al., 2011a; Huang et al., 2015; Lau et al., 2010; Ou et al., 2015). In 2002–2003, vehicle emissions and marine vessel-related sources contributed 31–48% of ambient VOC concentrations in Hong Kong, and this contribution increased to 40–54% in 2006–2007 (Lau et al., 2010). Ou et al. (2015) has conducted a multi-year study on characterizing sources of VOCs from 2005 to 2013 in Hong Kong. In this study, vehicular exhaust, gasoline evaporation and liquefied petroleum gas (LPG) usage, consumer product and printing, architectural paints, and biogenic emissions were identified as the sources of VOCs. And traffic-related sources including vehicle exhaust, gasoline evaporation and LPG usage were found to be the major source of ambient VOCs which contributed 30% ~ 60% from 2005 to 2013. A field study on VOCs at an urban site in Hong Kong in 2007 found that

vehicular emissions contributed the most to ambient VOCs with the percentage of 48%, followed by solvent use (43%) and biomass burning (9%) (Guo et al., 2011a). Moreover, one study on the roadside VOCs in Hong Kong found that LPG usage, gasoline exhaust, gasoline evaporation, diesel exhaust, and solvent usage contributed 60%, 9%, 6%, 15%, and 11%, respectively to the total VOC emissions (Huang et al., 2015). In summary, vehicular emission is one of the major sources in Hong Kong, and its contribution varied from sampling sites and time

2.3.3 Previous studies on vehicular VOC emissions in Hong Kong

Vehicular emissions are one of the major sources of anthropogenic VOCs from urban to rural areas in Hong Kong. Therefore, it is important to evaluate and quantify the VOC emissions from on-road vehicles.

VOC emissions from vehicles in Hong Kong were evaluated through a study at several typical roadside sites in 2003 (Ho et al., 2013; Ho et al., 2012). Ground-based roadside sampling at six traffic intersections and highway on/off ramps was conducted in order to obtain the comprehensive chemical source profiles for different vehicle types, including gasoline private car, LPG taxi, diesel good vehicles, diesel minibus, diesel double-decked bus, and diesel single-decked bus. A total of 111 VOC species were analyzed in this study. It was found that n-butane (31%), followed by propane (26%), and i-butane (25%) were the dominant species for LPG-fueled dominated samples. For

the gasoline-fueled dominated samples, toluene (16%), ethene (8.4%), pentane (7.1%), and ethyne (6.6%) were the dominant species. Ethene and ethyne were the most dominant species for diesel-fueled dominated samples. A total of fifteen carbonyls were also quantified in the study (Ho et al., 2012). It was found that formaldehyde was the most abundant carbonyl species among all types of fuel dominated sample with the percentage of 55% ~ 61%. Acetaldehyde and acetone also contributed the most to total measured carbonyls next to formaldehyde with the range of 16% ~ 21%, and 8% ~ 13%, respectively.

The chassis dynamometer testing method was used to determine the emissions of VOCs from gasoline-fueled and LPG-fueled vehicles in Hong Kong. The emission profiles at five different driving speeds (0 km h^{-1}, 25 km h^{-1}, 50 km h^{-1}, 70 km h^{-1}, 100 km h^{-1}) were investigated and the emission factors of different VOC species were estimated in the study (Guo et al., 2011b). Ethane, n-butane, i-pentane, n-pentane, 2,2,4-trimethylpentane, ethene, benzene, toluene, m/p-xylene and 1,2,4-Trimethylbenzene were found to be the dominant species for gasoline-fueled vehicles under all driving speeds. However, propane, i-butane, n-butanes and ethane were found to be the most abundant species from LPG-fueled vehicle emissions. Moreover, the emission factors of almost all species were much higher at idle state (0 km h^{-1}) than under the other driving speeds, and this finding was consistent with other studies worldwide (Int Panis et al., 2006; Kean et al., 2003).

A tunnel study was conducted in Hong Kong in 2003 to investigate the vehicular emissions of VOCs and carbonyls in real-world (Ho et al., 2009b; Ho et al., 2007). The total measured VOC emission factors ranged from 67 mg veh^{-1} km^{-1} to 148 mg veh^{-1} km^{-1}. Ethene, toluene, n-butane, propane, and i-pentane were found to be the most abundant VOC species, and they contributed over 38% of the total measured VOCs. Propane and n-butane were found to be highly associated with LPG-fueled vehicles (Ho et al., 2009b). The total measured carbonyl emission factors ranged from 22 mg veh^{-1} km^{-1} to 69 mg veh^{-1} km^{-1}. Formaldehyde was found to be the most abundant carbonyl specie which contributed more than 50% of the total measured carbonyls. The five most abundant carbonyls in vehicles emission at the tunnel were, in decreasing order, formaldehyde (18.8 mg veh^{-1} km^{-1}), acetaldehyde (5.5 mg veh^{-1} km^{-1}), acetone (2.9 mg veh^{-1} km^{-1}), crotonaldehyde (2.5 mg veh^{-1} km^{-1}) and MEK (1.1 mg veh^{-1} km^{-1}). Total measured carbonyl emissions from diesel-fueled vehicles were 71.5 mg veh^{-1} km^{-1}, which were about 7 times higher than those from non-diesel-fueled vehicles (Ho et al., 2007).

Table 2.1 Classification of Inorganic Organic Pollutants (adapted from WHO)

Description	Abbreviation	Boiling Point Range (°C)	Example Compounds
Very volatile (gaseous) organic compounds	VVOC	<0 to 50-100	Propane, butane, methyl chloride
Volatile organic compounds	VOC	50-100 to 240-260	Formalddehyde, s-limonene, toluene, acetone, ethanol, 2-propanol, hexanal
Semi volatile organic compounds	SVOC	240-260 to 380-400	Pesticides (DDT, chlordane, plasticizers (phthalates), fire retardants (PCBs, PBB))

Table 2.2 VOC species identified by PTR-MS adapted from Yuan et al. (2017).

Nominal Masses	Formula	m/z	Species
28	$HCNH^+$	28.018	hydrogen cyanide
31	CH2OH+	31.018	formaldehyde
33	CH4OH+	33.033	methanol
42	C2H3NH+	42.034	acetonitrile
44	CHNOH+	44.013	isocyanic acid
45	C2H4OH+	45.033	acetaldehyde
47	CH2O2H+	47.013	formic acid
	C2H6OH+	47.049	ethanol
54	C3H3NH+	54.034	acrylonitrile
57	C3H4OH+	57.033	acrolein; MTBE
	C4H9+	57.070	butentes
59	C3H6OH+	59.049	acetone; propanal
61	C2H4O2H+	61.028	acetic acid; glycolaldehyde
63	C2H6SH+	63.026	dimethyl sulfide
69	C4H4OH+	69.033	furan
	C5H8H+	69.070	isoprene
71	C4H6OH+	71.049	MVK; MACR
73	C3H4O2H+	73.028	methylglyoxal; acrylic acid
	C4H8OH+	73.065	MEK; butanals
75	C3H6O2H+	75.044	hydroxyacetone; propanoic acid

77	C2H4O3H+	77.023	PAN; peracetic acid
79	C6H6H+	79.054	benzene
81	C6H9+	81.070	monoterpenes and PAH fragment
83	C5H6OH+	83.049	methyl furan
	C6H11+	83.085	methylcyclopentane
85	C4H4O2H+	85.028	furanone
	C5H8OH+	85.065	cyclopentanone
87	C4H6O2H+	87.044	butanedione; methacrylic acid
	C5H10OH+	87.080	MBO; pentanones; pentanal
93	C7H8H+	93.070	toluene
95	C6H6OH+	95.049	phenol
99	C4H2O3H+	99.008	maleic anhydride
	C5H6O2H+	99.044	furfuryl alcohol
	C6H10OH+	99.080	hexenals; cyclohexanone
101	C6H12OH+	101.096	hexanal
103	C5H10O2H+	103.075	pentanoic acid
105	C8H8H+	105.070	styrene
107	C7H6OH+	107.049	benzaldehyde
	C8H10H+	107.086	C8 aromatics
121	C9H12H+	121.101	C9 aromatics
129	C10H8H+	129.070	naphthalene
135	C10H14H+	135.117	C10 aromatics

137	C10H16H+	137.132	monoterpenes
139	C9H14OH+	139.112	nopinone
169	C10H16O2H+	169.122	pinonaldehyde

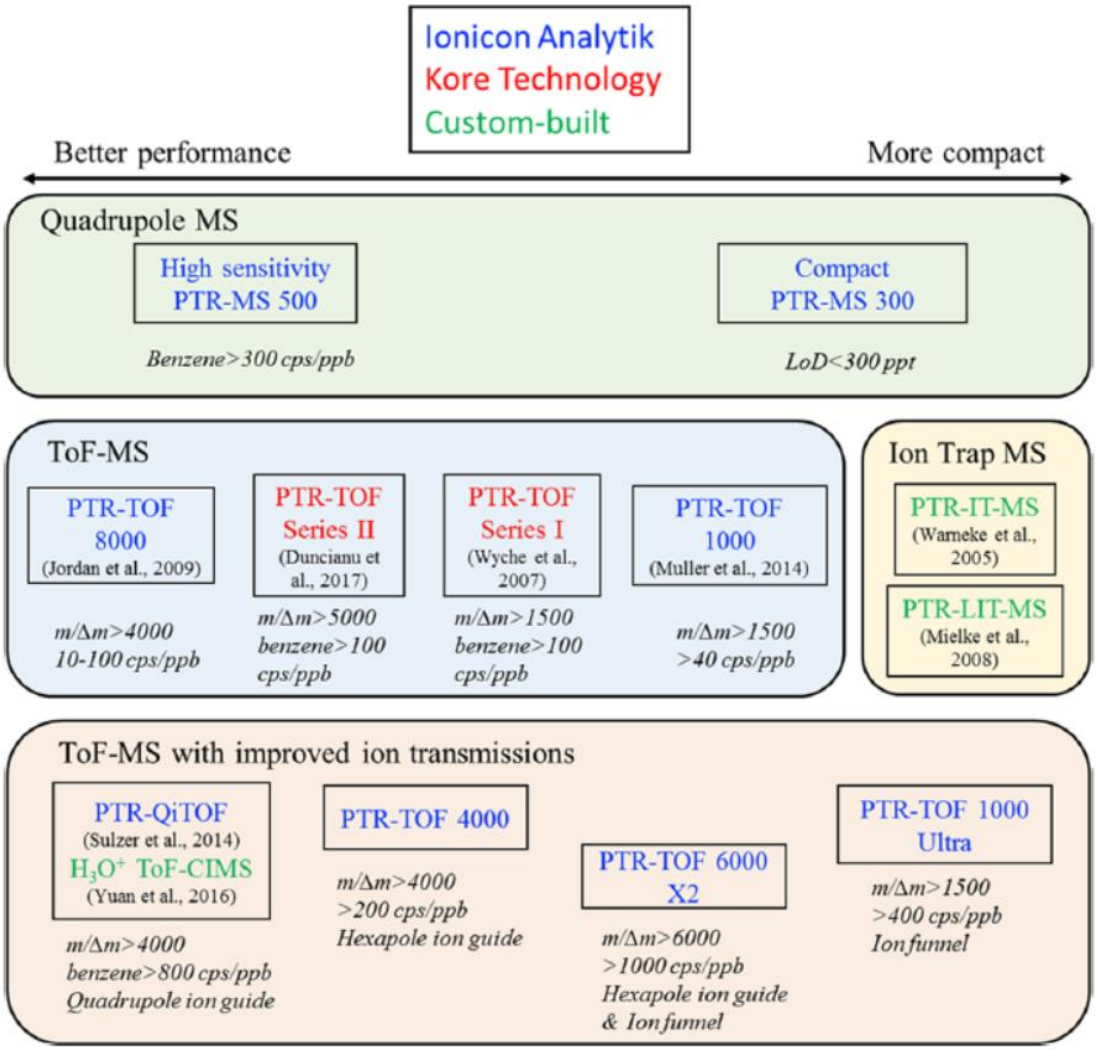

Figure 2.1 Product family of PTR-MS in the literature summarized by Yuan et al. (2017).

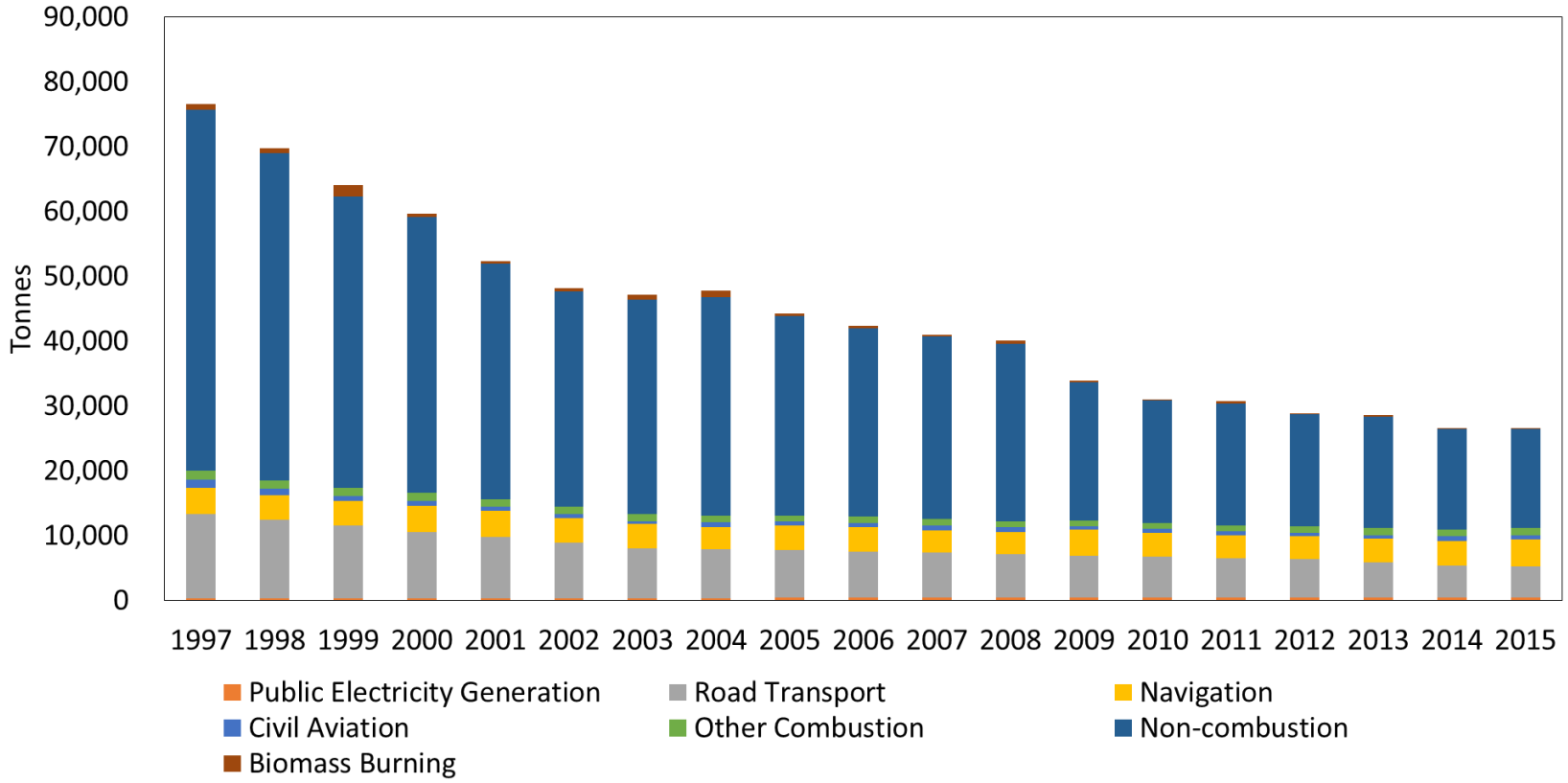

Figure 2.2 Hong Kong Air Pollutant Emission Inventory for VOCs

Chapter 3. Methodology

3.1 Sampling sites

3.1.1 Mong Kok urban roadside sampling site

An urban roadside station, Mong Kok (MK) Air Quality Monitoring Station (AQMS), was chosen as one of the field sampling sites in this study. This sampling site, which is one of the three roadside monitoring stations established by the HK EPD, is located in a mixed commercial and residential area with heavy daily traffic in Hong Kong (see map in Figure 3.1). Briefly, MK AQMS is the best representative of the roadside environment in Hong Kong, and more detailed information can be found elsewhere (Chan et al., 2002; Lee et al., 2002). The field study at this sampling site was conducted in May 2013, August 2013, November 2013, February 2014, May 2014 and August 2014.

3.1.2 Shing Mun (SM) Tunnel

The SM tunnel is a two-bore tunnel on the HK Route 9 expressway connecting Sha Tin and Tsuen Wan urban areas in the New Territories (see map in Figure 3.1). The tunnel is 2.6 km long in total and divided into east and west sections with lengths of 1.6 and 1.0 km, respectively. The cross-sectional area of the tunnel is 70 m^2, and the vehicle

speed limit is 80 km h^{-1}. The tunnel has a 1% grade from the entrance to the exit. The actual vehicle speed was in the range of 60 km h^{-1} ~ 70 km h^{-1}. The ventilation fans were not turned on during this study. Therefore, the air movement in the tunnel was mainly inducted by the piston effect of vehicle movement. There are 80 jet fans and four exhaust fans positioned along the ceiling throughout the tunnel, which are only activated occasionally during morning rush hours. The fans did not activate during this study. The tunnel measurements were conducted in the south bore of Shing Mun tunnel at two sampling sites: one at the inlet (Point A in Figure 3.2), and the other one at the outlet (Point B in Figure 3.2). The SM tunnel has been previously studied by our research group in 2003 (Cheng et al., 2010; Cheng et al., 2006; Ho et al., 2009a; Ho et al., 2009b; Ho et al., 2007). The inlet and outlet sampling sites were 686 m from the entrance and 350 m from the exit of the tunnel, respectively. The selection of the sampling position was based on the following three reasons, (1) inlet and outlet sampling points were set at the same position in 2015 as in 2003 to maintain the consistency, (2) the selection of sampling points should acquire the permission of related managing department, and (3) there can provide sufficient spaces for setting up other sampling instruments.

The experiment was conducted from 19 January to 31 March, 2015 in this study. It should be mentioned here that from late evening to early morning (23:00 – 06:00 local standard time [LST]) of Monday through Thursday, one of the tunnel bores was closed for cleaning and maintenance and the traffic was routed to the other bore. Thus,

experimental data obtained during the tunnel maintenance period were excluded from this study.

3.2 Measurement techniques

3.2.1 On-line measurements of VOCs and OVOCs at MK AQMS

A commercially available PTR-MS instrument (PTR-QMS 500, IONICON Analytik GmbH, Innsbruck, Austria) was used in this study. PTR-MS instrument has been described in detail elsewhere (Gouw et al., 2003; Gouw et al., 2006; Gouw and Warneke, 2007; Lindinger et al., 1998). Model PTR-QMS 500 mainly consists of a discharge ion source, a drift tube and a quadrupole mass spectrometer as presented in Chapter 2. In this study, H_3O^+ was utilized as the reagent ion, the drift tube was operated at 2.2 mbar pressure and the electric field was maintained at 600 V difference. The E/N (E stands for the electric field strength and N stands for the air density inside drift tube) value in the drift tube was kept at 136 Townsend (Td). The electric field maintains a controlled ion velocity in the drift tube so that the clustering of water ions can be reduced. The PTR-MS inlet system and the drift tube were maintained at 60 ^oC to minimize wall losses. The PTR-MS instrument was located in a shelter with an air conditioning system at the MK station. The inlet was located about 2 m above the ground. A 1/8" Teflon line was used as a sample line. The sample air was pumped at a flow rate of 75 mL min^{-1}, with an estimated residence time of 2 s in the inlet line. An in-line particulate filter (4.7

mm Teflon-membrance filter assembly, Whatman Inc., Clifton, NJ,USA) was used to prevent particles from entering the instrument.

Ionimed mix-VOC gas standard (IONICON Analytik GmbH, Innsbruck, Austria) was used for PTR-MS calibration in this study. Seventeen species were contained in the gas standard, namely formaldehyde, methanol, acetonitrile, acetaldehyde, ethanol, acrolein, acetone, isoprene, crotonaldehyde, 2-butanone, benzene, toluene, *o*-xylene, chlorobenzene, *α*- pinene, 1,2-dichlorobenzene and 1,2,4-trichlorobenzene with mixing ratios about 1 ppm for each compound. Standard VOC gas mixtures (Supelco TO-14 Calibration Mix) were used for determining the transmission curve of the PTR-MS instrument. Zero air was generated by a Gas Calibration Unit (GCU) (IONICON Analytik GmbH, Innsbruck, Austria) with a VOC-scrubber installed inside the GCU. Background level was determined by zero air with the frequency of half-hour each day. The relative humidity and temperature of inlet gas were controlled by adjusting the humidification chamber and a dew point mirror inside the GCU. Ionimed mix-VOCs gas standard was diluted with four different ratios (0.08, 0.06, 0.04 and 0.001) to calibrate the PTR-MS. Calibrations were done every six days for ensuring the accuracy of PTR-MS. The relative humidity (RH) and temperature (T) of inlet gas for calibration were set at 80% and 25^{o}C respectively according to the average level (RH = 78.2% and T = 23.5^{o}C) of ambient air in Hong Kong from 1997 to 2012 (shown in Figure 3.3; data were obtained from the Hong Kong Observatory). The accuracy and the measurement precision of the PTR-MS was 3~20% and 1.6~10.0%, respectively.

The accuracy of each species measured by PTR-MS was determined by the percentage difference between measured mixing ratio and actual mixing ratio based on calibrations every six days during the whole campaign. The quantification precision was determined by the experimental standard deviation of respective mass signal intensity at a constant volume mixing ratio (about 1 ppbv in this study) (Graus et al., 2010). The limit of detection (LOD) was determined as the 3σ uncertainty of the 5-min background measurements. The total uncertainty for each species can be determined by the geometric sum of the accuracy and precision (Eerdekens et al., 2009). The LOD, accuracy, precision and total uncertainty for each species measured by PTR-MS is listed in Table 3.1. Table 3.2 is a summary table in which the LOD, accuracy and precision for PTR-MS and the other VOC/OVOC measuring techniques described in following sections are shown.

An on-line GC-FID analyzer (Syntech Spectras GC 955, Series 600/800, the Netherlands), which consists of two separate systems for detection of C_2-C_5 and C_6-C_{10} hydrocarbons was used to collect VOCs speciation data continuously from May 2013 to August 2014. All the on-line GC-FID data used in this study were measured by the HK EPD (http://epic.epd.gov.hk/ca/uid/airdata). Data quality was assured by strict quality assurance and quality control (QA/QC) procedures. Weekly calibrations were conducted by using NPL standard gas (National Physical Laboratory, Teddington, Middlesex, UK). More details about the on-line GC-FID system can be found from

previous studies in Hong Kong (Ou et al., 2015; Xue et al., 2014). The C_2-C_{10} hydrocarbon species included ethane, ethene, ethyne, propane, propene, n-butane, i-butane, 1-butene, trans-2-butene, cis-2-butene, 1,3-butadiene, n-pentane, i-pentane, 1-pentene, trans-2-pentene, n-hexane, 2-methyl pentane, n-heptane, n-octane, i-octane, benzene, toluene, ethylbenzene, m,p-xylene, o-xylene, 1,2,4-trimethylbenzene and 1,3,5-trimethylbenzene. Sampling resolution for the on-line GC-FID analyzer was 30 minutes, and hourly averaged data were used for further analysis. The accuracy and precision of the measurements was 5~20% and 1.2~10.1%, respectively. The accuracy of each species measured by on-line GC-FID was determined by the percentage difference between measured mixing ratio and actual mixing ratio based on weekly span checks and monthly calibrations. The precision was based on the 95% probability limits for the integrated precision check results (Ling et al., 2013; Lyu et al., 2016).

O_2^+ was also tested as the ion source in lab study for the measurement of n-butane and propane. Single standard gas of n-butane and propane were used, and the GCU was used to generate zero air. The measured mass spectrum of n-butane and propane was shown in Figure 3.4, together with the background (zero air) signal. For the n-butane test, the primary ion, i.e. O_2^+, was detected at m/z 32, 34, 33, while NO^+ (m/z 30), NO_2^+ (m/z 46) and H_3O^+ (m/z 19) were the significant contaminant ions in case of O_2^+ reagent ions. Apart from these primary ions, m/z 43 and 41 showed the largest signals and the largest increasing when they were compared with background signals. They were thought to be the most possible product ions of the reaction of n-butane with O_2^+. The

m/z 43 and 41 were assigned to $C_3H_7^+$ and $C_3H_5^+$, respectively. Moreover, the m/z 28, 42 and 39 were also the candidate ions to detect n-butane. As the signals of other m/z, like m/z 26, were less than 10% of the highest signals, they could not be used to quantify n-butane in O_2^+ mode. The product ions of the reaction of n-butane and O_2^+ were: m/z 43 ($C_3H_7^+$, 48%), m/z 41 ($C_3H_5^+$, 40%), m/z 42 ($C_3H_6^+$, 7%) and m/z 39 ($C_3H_3^+$, 5%). The m/z 43 and m/z 41 may be used to quantify n-butane under O_2^+ mode. For the propane test, Similar as n-butane, m/z 43, 41, 39, 42 were the possible product ions of the reaction of propane with O_2^+. Poor correlation coefficient was found for m/z 39. Thus, the product ions of the reaction of propane and O_2^+ were: m/z 43 ($C_3H_7^+$, 50%), m/z 41 ($C_3H_5^+$, 46%) and m/z 42 ($C_3H_6^+$, 4%). The m/z 43 and m/z 41 may also be used to quantify propane under O_2^+ mode. Therefore, both n-butane and propane will be reflected on m/z 43 and m/z 41, as a result, butanes and propane cannot be separated by using this method. Moreover, nearly 30 species produced ions of m/z 41 and 43 were found by other studies under O_2^+ mode. Thus, it is not appropriate to apply PTR-MS on butanes and propane measurements in this study.

3.2.2 Off-line Measurements of VOCs by canister samples at MK AQMS

Twenty-four hour (0:00-23:59) VOC samples were collected using 2-L electropolished, conditioned stainless steel canisters and an ATEC Model 2200 automated sampler (Model 2200, Malibu, CA) once every six days in each sampling month. All canisters used in this study were pre-cleaned and evacuated by the Rowland/Blake group at the

University of California, Irvine (UCI). Detailed information of the preparation and pre-conditioning of the canisters can be found elsewhere (Blake et al., 1994; Simpson et al., 2010). After sampling, canisters with air samples were sent back to the laboratory at UCI for VOCs analysis by a GC-MSD/FID/ECD system within one week of collecting the canister samples. Complete analytical details are given in Colman et al. (2001). Briefly, the sample flow is split into five streams, with each stream chromatographically separated on an individual column and sensed by a single detector, namely: (1) FID with a DB-1 column (60 m, I.D. 0.32 mm, film 1 mm); (2) FID with PLOT (30 m, I.D. 0.53 mm) + DB-1 (5 m, I.D. 0.53 mm, film 1 mm) columns; (3) ECD with a Restek 1701 column (60 m, I.D. 0.25 mm, film 0.50 mm); (4) ECD with DB-5 (30 m, I.D. 0.25 mm, film 1 mm) + Restek 1701 (5 m, I.D. 0.25 mm, film 0.5 mm) columns; and (5) MSD with a DB-5ms column (60 m, I.D. 0.25 mm, film 0.5 mm). This technique was used to measure 55 C_1-C_{10} VOCs, including all those measured by the on-line GC-FID. The accuracy of the VOC measurements was 5% or better, replicate runs of the calibration standards yielded the measurement precision ranged from 0.5-5% (Colman et al., 2001; Ling and Guo, 2014; Lyu et al., 2016).

3.2.3 Off-line Measurements of VOCs by canister samples at SM tunnel

A total of 46 pairs of VOC samples were collected in stainless steel canisters during the sampling period. One pair of samples was collected at the inlet and outlet sites simultaneously. Tunnel air was sampled from inlets located at 1.5m above the ground

through Teflon tubing and collected into pre-cleaned and pre-evacuated 2 L stainless steel canisters at a flow rate of 27.3 mL min^{-1} for 2 hours by a multi-port canister sampler (Model 8001, ATEC, California, USA). The sampling periods covered morning rush hour (8:00–10:00), midday (11:00–13:00 and, 14:00–16:00), and afternoon rush hour (17:00–19:00). Air samples inside canisters were firstly preconcentrated in a pre-concentrator (Model 7100, Entech Instruments Inc., California, USA) and then analyzed by a gas chromatography-mass selective detector/flame ionization detector (GC-MSD/FID) system (Model 5973N, Agilent Technologies, California, USA). Detailed analysis procedures are described elsewhere (Wang and Wu, 2008; Zhang et al., 2012). Briefly, preconcentrated air samples were firstly separated by a HP-1 column (60 m × 0.32 mm × 1.0 μm, Agilent Technologies, USA), and then separated into two streams: one went through a PLOT-Q column (30 m × 0.32 mm × 2.0 μm, Agilent Technologies, USA) which was detected by FID detector, and the other one went through a 65 cm × 0.1 mm stainless steel line followed by the MSD detector. The accuracy of the measurement was 0.5–5%, and the detection limit was 3–57 pptv for individual species.

3.2.4 Off-line Measurements of OVOCs by DNPH cartridges

Twenty-four hour (0:00-23:59) OVOC samples were collected by an ATEC Model 2200 automated sampler (Model 2200, Malibu, CA) once every six days in each sampling month at MK AQMS. An ozone scrubber (Sep-Pak; Waters Corporation, Milford, MA)

was used to remove ozone during carbonyl sampling with 2,4-dinitrophenylhydrazine (DNPH) cartridges (Waters Sep-Pak DNPH-silica, Milford, MA). The flow rate was regulated at 0.7 L min^{-1} by a mass flow controller. For the field study at SM tunnel, 40 pairs of DNPH cartridges (Waters Sep-Pak DNPH-silica, Milford, MA) were collected for carbonyls analysis in total. DNPH cartridge samples were collected at the flow rate of 0.7 L min^{-1} with 2 hours duration for each sample. All cartridge samples at both sampling sites were analyzed according to the United States Environmental Protection Agency (USEPA) Method TO-11A (USEPA, 1999).

A High Performance Liquid Chromatography (HPLC) system (Perkin Elmer Series 2000, Massachusetts 02451, USA) coupled with an ultra-violet (UV) detector operating at 360 nm was used for chemical analysis. The column for separation was a 4.6 × 150 mm Hypersil ODS 5 m reversed phase column (Alltech, Deerfield, IL) at room temperature (Huang et al., 2011). The mobile phase consisted of two solvent mixtures: (A) 6:3:1 (v/v/v) water/acetonitrile/tetrahydrofuran, and (B) 4:6 (v/v) water/acetonitrile. The gradient program was 80% A/20% B for 1.5 min, followed by a linear gradient to 50% A/50% B in 8 min, and finally 100% B for 10 min. The flow rate was 2.0 mL min-1 throughout the run. All solvents and water used were HPLC grade (Duksan Pure Chemicals Co., Ltd, Gyeonggi-do, Korea) and Milli-Q grade, respectively. The calibration curve was established by five concentration points covering the levels of interest. One calibration standard was run for every ten samples to ensure the stabilization of the instrument. Carbonyls were identified and quantified by their

retention times and peak areas of the corresponding calibration standards (Cheng et al., 2014). Formaldehyde, acetaldehyde, acrolein, acetone, propionaldehyde, crotonaldehyde, 2-butanone, i-/n-butyraldehyde, benzladehyde, i-valeraldehyde, valeraldehyde, o-tolualdehyde, m-tolualdehyde, p-tolualdehyde, hexaldehyde, and 2,5-dimethylbenzaldehyde were detected by this method. The detection limits for target carbonyls were below 0.45 ppbv. The accuracy was 15% or better which was determined by measuring the recovery of a spiked sample. Sample precision is measured by the analysis of ambient duplicate samples, and the precision of the measurements was less than 10%.

3.2.5 Continuous measurements of trace gases and traffic count analysis at SM tunnel

Carbon monoxide (CO), and nitrogen oxides ($NO/NO_2/NO_x$) concentrations were measured continuously every minute) at both inlet and outlet sampling sites. CO was monitored with CO analyzers (Model 300E, Teledyne API, California, USA), and $NO/NO_2/NO_x$ was measured by $NO/NO_2/NO_x$ analyzers (Model T200, Teledyne API, California, USA). The sampling inlets of trace gas analyzers were set at 1.5m above the ground with the sampling flow rates both at 1.0 L min^{-1}.

Traffic compositions and volume were determined by manual counts at the entrance of the tunnel tube at 15-minute intervals during the sampling periods. Video-recording was

also taken for data validation and review purposes. The vehicle types were classified into three major categories, namely diesel-fueled vehicle (heavy goods vehicle, light goods vehicle, double deck bus and single deck bus), gasoline-fueled vehicle (motor cycle and private car), and LPG-fueled vehicle (taxi and public light bus). The age and mileage distribution of vehicles were not obtained in this study.

3.3 Model used in this study

3.3.1 Positive Matrix Factorization (PMF) model

USEPA PMF 5.0 model (Norris et al., 2014) was used to conduct the source apportionment of VOCs and OVOCs at MK AQMS in this study. This model was firstly developed in 1994 by Paatero and Tapper (1994), and non-negative constraints are utilized for obtaining physically realistic meanings in this model. Detailed description and application of this model can be found elsewhere (Manousakas et al., 2017; Shao et al., 2016; Wang et al., 2015). In general, the budget of ambient VOCs is determined by the emissions from different sources, the deposition of chemical and physical processes. Based on the fundamental assumption of mass conservation of species from the emissions sources to the receptor site, the concentration of one specific VOC could be proportional to its emission amounts from different sources in the certain atmospheric volume (Shao et al., 2016). According to the above assumption, data set in the PMF model can be represented as a data matrix X of i by j dimensions, where i

number of samples and j chemical species (VOCs and OVOCs) were measured by equation 3.1 (Paatero, 2000). The function of the PMF model is to identify the number of emission sources and the species profile of each source, and to attribute the amount of mass from each source to each species in each individual sample by an analyst based on the measured data at the receptor site, which could presented by equation 3.1. Therefore, two metrics, i.e., factor contributions and factor profiles, were included and exported in the PMF results.

$$x_{ij} = \sum_{k=1}^{p} g_{ik} f_{kj} + e_{ij} \qquad (3.1)$$

where x_{ij} is the j species concentration measured in the I sample, g_{ik} is the species contribution of the k source to the I sample, f_{kj} is the j species fraction from the k source, e_{ij} is the residual for each sample/species, and p is the total number of independent sources (Paatero, 2000).

In the PMF application, the uncertainties for each sample/species were calculated using the following equation: (US EPA, 2008):

For concentrations below detection limit (DL):

$$\text{Uncertainty} = 5 \times \text{DL}/6 \qquad (3.2)$$

For concentrations no less than detection limit:

$$\text{Uncertainty} = (\text{DL}^2 + \text{Precision}^2)^{0.5} \qquad (3.3)$$

where the Precision accounts for the relative measurement error determined by calibration of the instruments. The DLs equal five times the baseline noise of the species' chromatograms, whereas the Precisions are the relative standard deviations of six repeated measurements of a real-air standard in the range of ambient concentrations. Data below the DL are replaced by half the DL values. Missing data are replaced by the geometric mean of the measured concentrations of that species, and their uncertainties are set as four times the geometric mean.

3.3.2 Photochemical reactivity of VOCs

The maximum incremental reactivity (MIR) and propene-equivalent concentrations (Prop-Equiv) were often used to estimate the photochemical reactivity of VOCs (Carter, 1994; So and Wang, 2004). The MIR value developed by Carter (2009) is used in this study to assess the ozone formation potential (OFP) of individual VOCs according to the following equation,

$$OFP_j = Conc_j \cdot MIR_j \qquad (3.4)$$

where OFP_j is the ozone formation potential of specie j in ppbv O_3; $Conc_j$ is the mixing ratio of specie j in ppbv; and MIR_j is the maximum incremental reactivity value of specie j in ppbv O_3 per ppbv organic compound.

The Prop-Equiv of specie j can be defined by the following equation,

$$\mathrm{Prop-Equiv_j} = \mathrm{Conc_j} \times \frac{k_{OH(j)}}{k_{OH(propene)}} \qquad (3.5)$$

where $Conc_j$ is the concentration of specie j in ppbC; $k_{OH(j)}$ and $k_{OH(propene)}$ are the reaction rate constants between specie j or propene and OH radical.

3.3.3 Emission factor model

Emission factors (in mg veh^{-1} km^{-1}) of specific pollutants from vehicular emissions is the mass of the pollutants emitted over a certain distance normalized by the vehicle number and distance. (Pierson and Brachaczek, 1982; Pierson et al., 1996)

$$EF_{veh} = \frac{(C_{outlet} - C_{inlet}) \cdot A \cdot U \cdot t}{N \cdot L} \qquad (3.6),$$

where EF_{veh} is the average emission factor in mg veh^{-1} km^{-1}; C_{outlet} and C_{inlet} are the mass concentrations on of specific pollutants at the outlet and inlet sampling sites in mg m^{-3}; A is the cross section area of the tunnel in m^2; U is the wind speed in m s^{-1}; t is the sampling duration in s; N is the total number of vehicles pass through the tunnel during the sampling period; and L is the distance between outlet and inlet sampling sites in km.

The emission factors of VOCs calculated by the above equation reflect the fleet-average emission factors of specific VOCs from mixed vehicle types during the sampling period. Multiple linear regression (MLR) method can be used to estimate the EFs of individual VOCs for non-diesel vehicles (NDVs) and diesel vehicles (DVs) according to the following equation (Grosjean et al., 2001; Ho et al., 2007; Pierson et al., 1996)

$$EF_i = \alpha_i EF_{NDV} + \beta_i EF_{DV} \qquad (3.7),$$

where EF_i is the measured individual VOC EFs in time interval i; α_i, β_i are the fractions of NDV and DV passing through the tunnel during the time interval i, respectively, and $\alpha_i + \beta_i = 1$; EF_{NDV} and EF_{DV} are estimated EFs for NDV and DV, respectively.

Table 3.1 Detection limit, accuracy, precision and total uncertainty of the PTR-MS for individual VOCs in gas standard.

Component	m/z	LOD (pptv)	Accuracy	Precision	Uncertainty
Formaldehyde	31	296	11.9%	3.1%	12.3%
Methanol	33	162	5.3%	2.7%	5.9%
Acetonitrile	42	17	7.4%	2.0%	7.7%
Acetaldehyde	45	101	3.0%	1.7%	3.4%
Ethanol	47	237	19.9%	10.0%	22.3%
Acrolein	57	23	11.8%	2.4%	12.0%
Acetone	59	31	4.2%	1.7%	4.5%
Isoprene	69	40	18.0%	3.4%	18.3%
Crotonaldehyde	71	25	15.5%	2.1%	15.6%
2-Butanone	73	18	6.3%	1.6%	6.5%
Benzene	79	12	4.6%	1.8%	4.9%
Toluene	93	30	7.1%	2.0%	7.4%
o-Xylene	107	25	7.4%	1.7%	7.6%
α-Pinene	137	29	9.9%	2.2%	10.1%
Dichlorobenzenes	147	21	7.8%	2.7%	8.3%
Trichlorobenzenes	181	96	10.0%	3.3%	10.5%

Table 3.2 Summary of detection limit, accuracy, and precision of different techniques used in this study.

Method	Measured parameters	LOD (pptv)	Accuracy	Precision
PTR-MS	VOCs and OVOCs	12~296	3~20%	1.6~10.0%
DNPH-HPLC	OVOCs	20~450	1~15%	0.5~10.0%
On-line GC-FID	VOCs	15~1186	5~20%	1.2~10.1%
Off-line GC-MSD/FID/ECD	VOCs	1~10	1~5%	0.5~5.0%

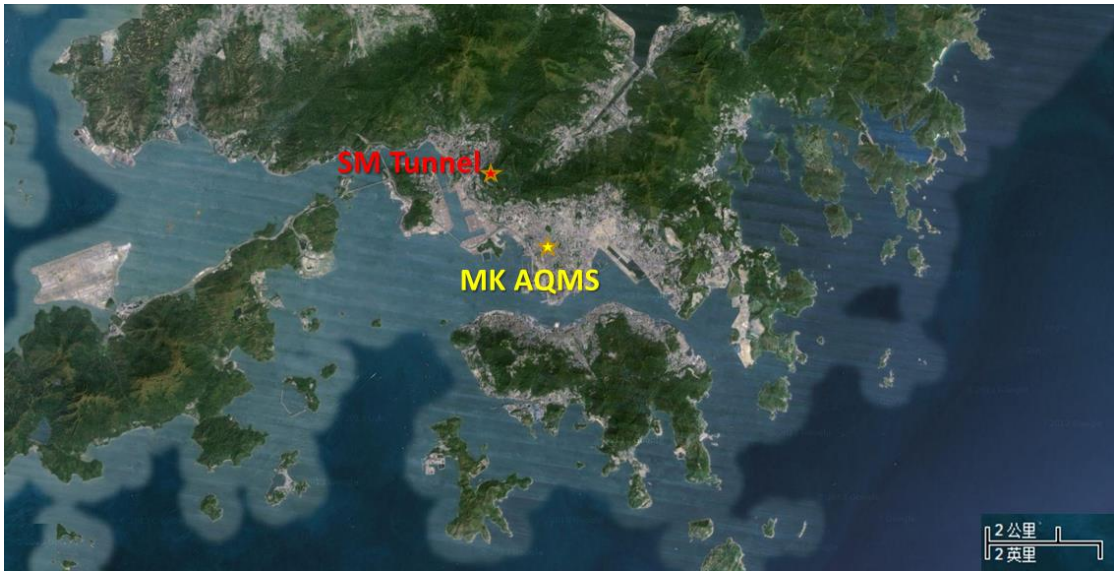

Figure 3.1 Location of the two sampling sites in this study.

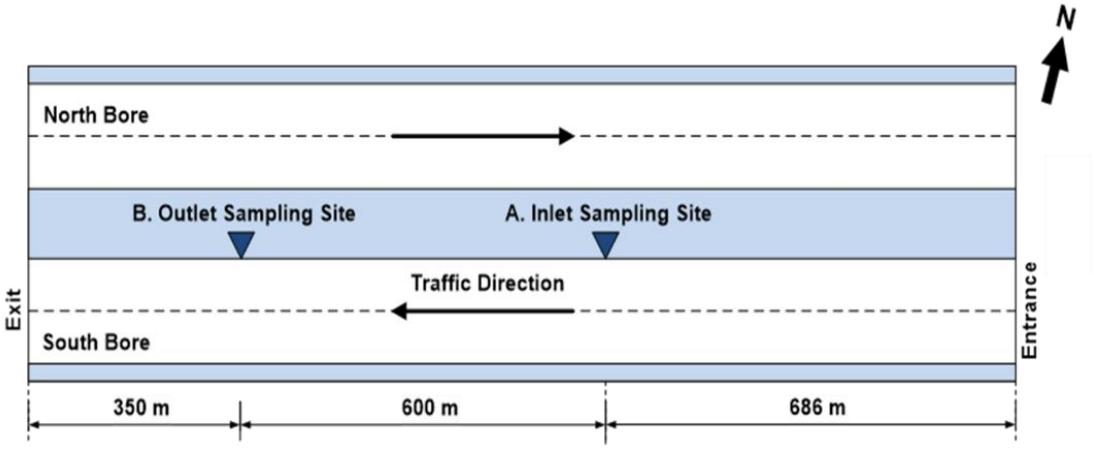

Figure 3.2 Schematic diagram of SM Tunnel and sampling sites in the south bore.

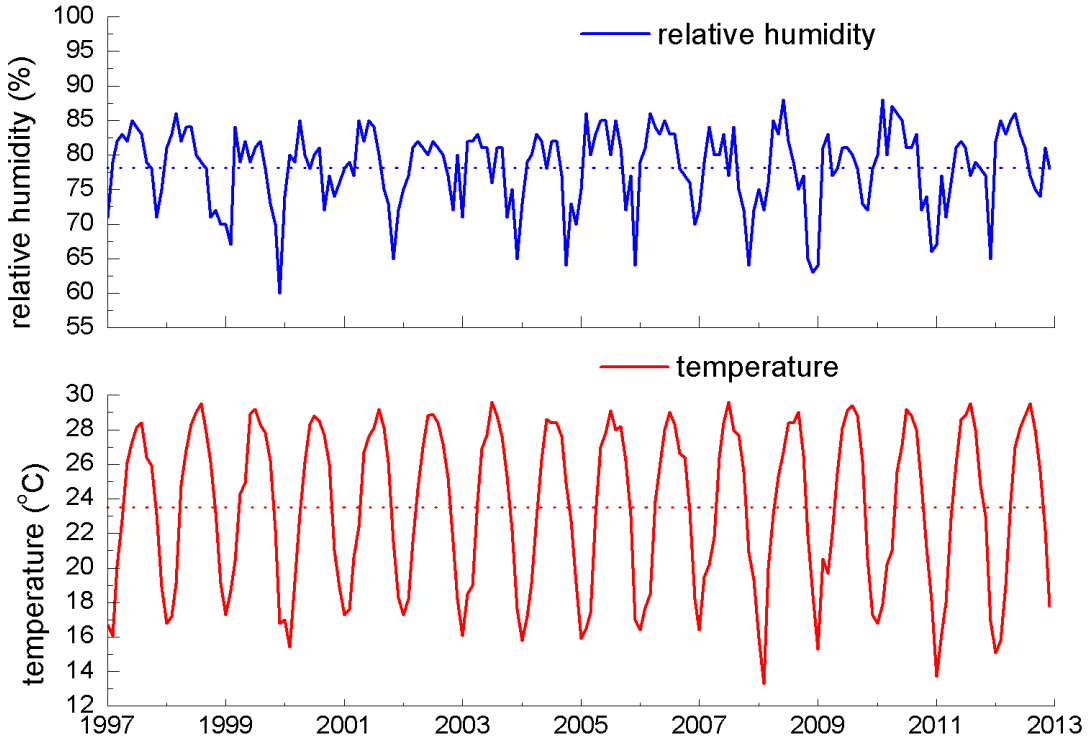

Figure 3.3 Statistics of relative humidity and temperature of Hong Kong from 1997 to 2012, dashed lines represent the average levels of RH and T (data were obtained from the Hong Kong Observatory).

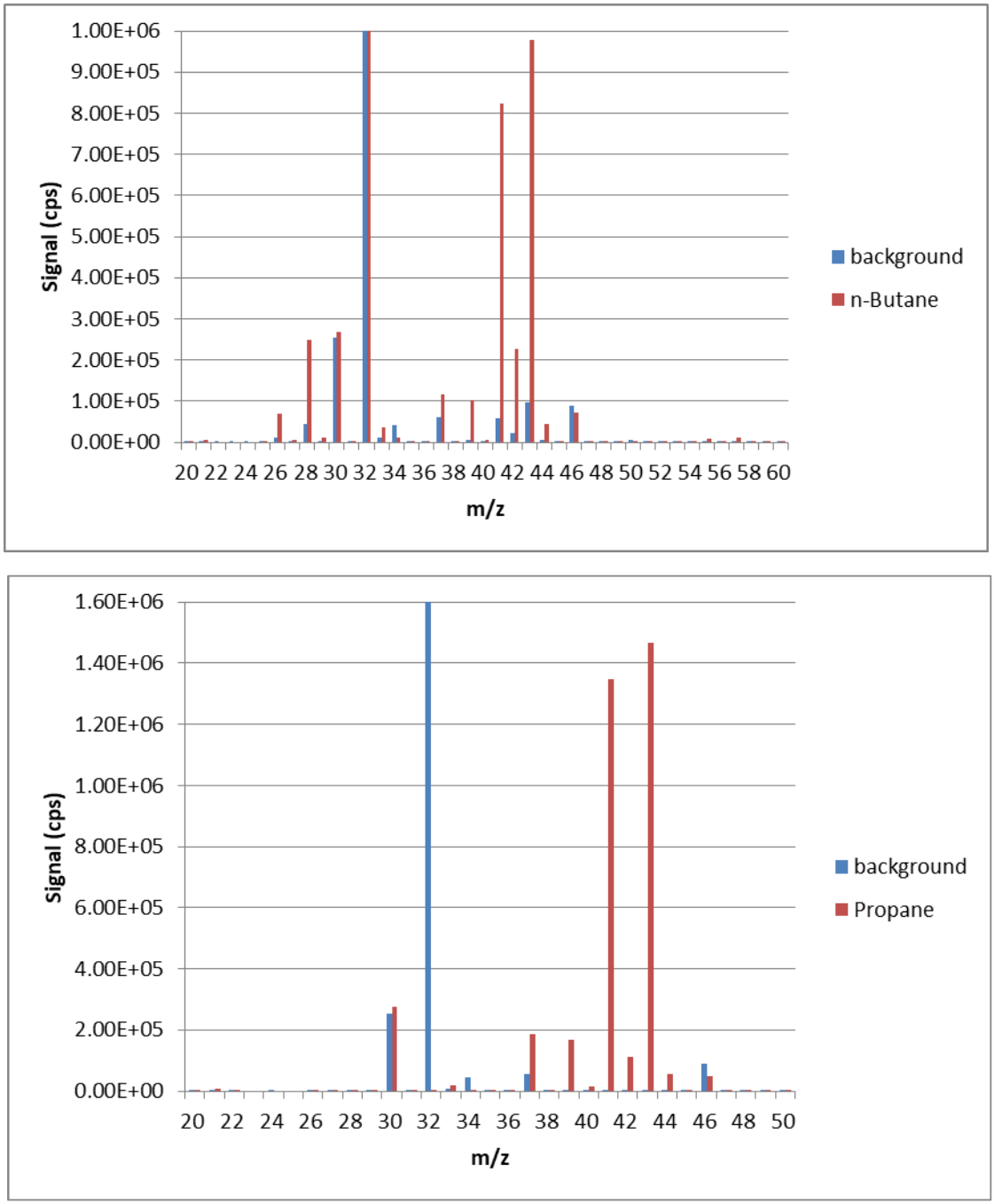

Figure 3.4 Measured mass spectrum of n-butane and propane, together with the background (zero air) signal

Chapter 4. The Application of PTR-MS on Measuring Roadside VOCs and OVOCs in Hong Kong

4.1 Introduction

VOCs which are important precursors of tropospheric ozone and secondary organic aerosols (SOAs) (Sillman, 2002), can be emitted from multiple anthropogenic sources (e.g., vehicular emissions, industrial emissions and solvent usage) and biogenic sources (Atkinson and Arey, 2003; Watson et al., 2001). VOCs also have adverse impact on human beings (Lelieveld et al., 2015; von Schneidemesser et al., 2010). As one of the most densely populated cities in the world, Hong Kong has over 7.2 million people and more than 699,540 registered vehicles in an area of 1,104 km^2 as of December in 2014 (HKTD, 2014). Special attention has been paid to the characteristics of roadside VOCs and their impacts on the local air quality of Hong Kong during the past years (Guo et al., 2007; Ho et al., 2004; Lee et al., 2002; Ling and Guo, 2014; Louie et al., 2013). Previous studies showed that vehicular emissions is one of the major contributors to ambient VOCs in Hong Kong (Guo et al., 2007; Huang et al., 2015; Lau et al., 2010; Ou et al., 2015).

In order to investigate urban roadside VOCs in Hong Kong, multiple sampling and analytical techniques were used, such as off-line DNPH cartridge sampling followed by HPLC analysis for OVOCs, on-line GC-FID, and off-line canister sampling

followed by GC-MSD/FID/ECD for VOCs (Cheng et al., 2014; Ho et al., 2013; Ho et al., 2012; Lyu et al., 2016). These techniques, however, can be impacted by their relatively low sampling resolution that may lead to the underestimation or overestimation of ambient VOC and OVOC concentration levels (Jobson and McCoskey, 2010; Wang et al., 2014; Wisthaler et al., 2008). Moreover, since there is no single technique that can measure all VOCs and OVOCs simultaneously, so different kinds of sampling and analytical techniques are usually used to obtain the measurements of these species (Ambrose et al., 2010; Jobson and McCoskey, 2010; Warneke et al., 2011a; Wisthaler et al., 2008).

PTR-MS is a relatively novel method that can fulfill on-line measurements of VOCs and OVOCs at trace levels in ambient air. Proton transfer enables soft ionization of chemical species that have a higher proton affinity (PA) than that of the reagent species (i.e. H_2O). PTR-MS does not need any sample treatment such as drying and/or precondensation like gas chromatographic analysis, and it is available for monitoring OVOCs which are quite difficult to quantify from canister samples. Hence, PTR-MS has recently been widely used in atmospheric chemistry research (Gouw and Warneke, 2007; Jobson and McCoskey, 2010). PTR-MS has been used in China for environmental studies throughout these years (Wang et al., 2016; Wang et al., 2014). But PTR-MS was firstly used in an urban roadside microenvironment of Hong Kong to measure ambient VOCs and OVOCs in this study.

Formaldehyde (HCHO) is one of the most abundant OVOCs in Hong Kong (Cheng et al., 2014; Ho et al., 2012; Louie et al., 2013). The lifetime of HCHO in the boundary layer is estimated to be only several hours when photolysis and its reaction with OH radical occur with sunlight. Because HCHO is carcinogenic (Kerns et al., 1983), it is one of the OVOCs of most interest in urban areas. Only off-line DNPH cartridge sampling analyzed by HPLC has previously been used to determine the level of ambient formaldehyde in Hong Kong (Cheng et al., 2014; Guo et al., 2004a; Ho et al., 2002; Louie et al., 2013). PTR-MS was introduced to measure ambient concentrations of formaldehyde continuously in this study. HCHO can be protonated by the following reaction (Ra):

$$HCHO + H_3O^+ \rightarrow HCHO \cdot H^+ + H_2O \qquad (Ra)$$

$$HCHO \cdot H^+ + H_2O \rightarrow HCHO + H_3O^+ \qquad (R\text{-}a)$$

However, because the PA of formaldehyde (170.4 kcal mol^{-1}) is just slightly higher than that of water (165.2 kcal mol^{-1}), the backward reaction (R-a) of protonated formaldehyde with H_2O can lead to an underestimation of HCHO by PTR-MS (Hansel et al., 1997). Jobson and McCoskey (2010) found that the sensitivity to HCHO can be improved by removing water vapor from the air sampling inlet. Correction for absolute humidity effects on HCHO measurement by PTR-MS was further discussed by Vlasenko et al. (2010). However, the previous studies did not fully discuss the effect of ambient RH and/or T separately and integratively on HCHO measurements by PTR-

MS. In addition, few studies have reported inter-comparisons between PTR-MS and DNPH-HPLC during field studies, especially in urban roadside areas.

In this study, PTR-MS was applied in Hong Kong to measure ambient VOCs and OVOCs coupled with other measurement techniques. The effect of ambient conditions (RH and T) on VOC and OVOC measurements by PTR-MS are discussed in this chapter. Detailed comparisons of PTR-MS, DNPH-HPLC, on-line GC-FID and off-line canister sampling followed by GC-MSD/FID/ECD for VOC and OVOC measurements at an urban roadside site in Hong Kong are conducted.

4.2 Effect of ambient RH and T on PTR-MS measurement

As described in Chapter 3, four-point calibrations were conducted to get the calibration curves. The experimental reaction rate coefficient (k) of each compound was obtained by the original input k value (typically $2.0 \cdot 10^{-9}$ cm^3 s^{-1}) multiplied by the slope of the measured concentration to the diluted concentration of standard gas, because the volume mixing ratio (VMR) of each species is inversely related to its reaction rate coefficient (k) (see equation 4.1) (Gouw and Warneke, 2007). Experimental k values of selected VOC and OVOC species were obtained under different ambient conditions, and RH ranged from 25% to 100% and T ranged from 5 ºC to 25 ºC through this method.

$$VMR = \frac{\mu_0 N_0}{kL} \times \frac{E}{N^2} \times \frac{I_{RH^+} \times TR_{H_3O^+}}{I_{H_3O^+} \times TR_{RH^+}} \qquad (4.1)$$

where,

VMR - the volume mixing ratio, ppbv;

μ_0 - the reduced mobility, cm V^{-1} s^{-1};

N_0 - the gas number density at standard pressure (1 atm) and temperature (273.15 K);

k - the reaction rate coefficient, 10^{-9} cm^3 s^{-1};

L - the length of the drift tube, 9.3 cm in this study;

E - the electric field strength, V m^{-1};

N - the air density in the drift tube, m^{-3};

I - the numbers of detected ions, cps;

TR - the transmission factor of respective ions.

Figure 4.1 shows the effect of ambient RH on the sensitivity and experimental *k* value of HCHO and benzene. The temperature of inlet air was kept at 25 ºC during the series of various RH tests. A significant decrease (about 40%) of sensitivity and calibrated k value was found when the RH of inlet air increased from 25% to 100% for HCHO (m/z 31). However, the sensitivity and experimental *k* value of benzene (m/z 79) did not vary much while the RH of inlet air changed with a variance of less than 5%. The variation patterns of sensitivity and experimental *k* value for the other species were similar to benzene. Therefore, only benzene is plotted to represent other species in the gas standard. HCHO was found to have lower sensitivity (less than 2.0 ncps $ppbv^{-1}$) than benzene (about 20 ncps $ppbv^{-1}$), since the backward reaction of protonated

formaldehyde with H_2O is not negligible, and the ratio between the forward and backward reaction was determined to be about 6000 by Spanel and Smith (2008). Beauchamp et al. (2013) used a similar mixed gas standard for PTR-MS calibration, low sensitivity of HCHO was also found below 2 ncps $ppbv^{-1}$ when the RH ranged from 20% to 100%. Moreover, strong nonlinear dependence on RH for HCHO was found by Beauchamp et al. (2013), and the sensitivity of HCHO significantly decreased by about 50% when the RH of inlet air increased from 20% to 100%, which is comparable to this study. The effect of ambient temperature on sensitivity and experimental *k* value of HCHO and benzene is plotted in Figure 4.2 under different RH. Both the sensitivity and experimental *k* value significantly dropped by 30 ~ 40% when the temperature of inlet air increased from 5 ºC to 25 ºC. Both sensitivity and experimental *k* value maintained a relatively stable level (variance less than 5%) for benzene when the temperature of inlet air was changed under the given RH, and the same for the other species in the standard gas excluding HCHO. A quadratic polynomial fit was found to be the best fit model (r^2 >0.98) for the experimental *k* value of HCHO with a single variable (RH or T of inlet air). Because the RH and T of inlet gas for calibration were set at 80% and 25ºC respectively, $R_{(RH,T)}$ (the ratio of *k* value under given ambient conditions to the experimental *k* value under 80% and 25ºC) was chosen to explore the integrated effects of ambient RH and T on experimental *k* value. Poly2D regression, which used a binary quadratic equation, was found to be the best nonlinear surface simulation of $R_{(RH,T)}$, ambient RH and T for HCHO in this study, and the following equation (equation 4.2) shows the relationship between them.

$$R_{(RH,T)} = r_0 + a \cdot RH + b \cdot T + c \cdot RH^2 + d \cdot T^2 + f \cdot RH \cdot T \qquad (4.2)$$

where,

$R_{(RH,T)}$ - the ratio of experimental reaction rate under given RH & T to calibrated reaction rate under 80% and 25ºC;

RH - the relative humidity of inlet gas/air;

T - the temperature of inlet gas/air.

The constant term r_0 and coefficients a, b, c, d, and f, as well as the correlation coefficients of all species in the gas standard are listed in Table 4.1. The difference of $R_{(RH,T)}$ was within 10% for all species except HCHO (m/z 31) when the condition of inlet air changed within controlled range for RH (25% ~ 100%) and T (5ºC ~ 25ºC). The $R_{(RH,T)}$ for formaldehyde differs significantly because of humidity effects on HCHO measurement by the PTR-MS. Excellent correlation was found between $R_{(RH,T)}$, ambient RH and T for HCHO (m/z 31) with a correlation coefficient of 0.97. The relationship between these three factors is plotted in Figure 4.3.

The relationship of experimental *k* value and absolute humidity (AH) in sample air for HCHO is plotted in Figure 4.4. The best simulation ($r = 0.92$) was found following the function: $k_{(AH)} = 0.0007 \cdot AH^2 - 0.0568 \cdot AH + 1.8139$, where $k_{(AH)}$ stands for the experimental *k* value of HCHO, AH stands for the absolute humidity in sample air. Fig. 6 shows the comparison between concentrations of HCHO measured during the

campaign at MK after correction by $R_{(RH,T)}$ and $k_{(AH)}$ separately. Good agreement during the field sampling for HCHO was found between the above two correction methods with a slope of 1.02 and a correlation coefficient of 0.99 (as shown in Figure 4.5).

A relationship between the normalized detection sensitivity, S (ncps $ppbv^{-1}$), of HCHO and its humidity dependence at a certain E/N condition was raised by Inomata et al. (2008b) as follows:

$$S = \frac{m}{n} \cdot \frac{a}{[H_2O]_{sample} + b} \cdot \frac{1}{88.0} \qquad (4.3)$$

where,

m - the detection sensitivity of HCHO by direct introduction, ncps $ppbv^{-1}$;

n - the detection sensitivity of HCHO by Dynamic dilution, ncps $ppbv^{-1}$;

a, b – fitting parameters obtained from the simulation equation $y = a / (x + b)$ for the signal intensity of HCHO,

$[H_2O]_{sample}$ - the water vapor concentration in sample air, mmol mol^{-1}.

Ion counts are divided by 88.0 because the humidity dependence was measured with HCHO of 88.0 ppbv in the dynamic dilution method in this study. The relationship of the signal intensity of HCHO and the water vapor concentration in sample air is plotted in Figure 4.6. Simulated fitting parameters, a and b, are 5404 ± 72 (ncps mmol mol^{-1}) and 26 ± 0.4 (mmol mol^{-1}), respectively. The value of m/n is 1.09 in this study, and it is about 1.2 times of the $(k_a/k_{-a})/a$ value. This result agrees with the study of Inomata et al.

(2008b). Hence, the normalized detection sensitivity of HCHO in this study can be determined as a function of the water vapor concentration in sample air as equation 4.4.

$$S = \frac{67.18}{AH_{sample} + 26.04} \qquad (4.4)$$

Figure 4.7 shows the comparison of the measured detection sensitivity of HCHO and the normalized detection sensitivity obtained from equation 4.4. Good agreement was found between the measured detection sensitivity and the normalized detection sensitivity of HCHO with a slope of 1.18 ± 0.01 (r = 0.998). Since the normalized detection sensitivity of HCHO was 1.18 times of the measured detection sensitivity, lower HCHO concentration will be obtained by using the normalized detection sensitivity with a percentage of about 15.3%.

4.3 Comparisons between PTR-MS and other measurement techniques

4.3.1 PTR-MS versus DNPH-HPLC

Daily averaged PTR-MS data were used to compare the ambient OVOC measurements by PTR-MS and by DNPH-HPLC. As shown in Figure 4.8, good linear correlations were found for formaldehyde, acetaldehyde and MEK with correlation coefficients of 0.79, 0.75, 0.93, respectively, and with slopes of 1.00 ± 0.10, 1.10 ± 0.33, and 0.88 ±

0.058, respectively. For acetone, the slope is 0.76 ± 0.23 (PTR-MS to HPLC) with a correlation coefficient of 0.60. Concentrations of HCHO measured by the PTR-MS in Figure 4.8B were the corrected data by the Poly 2D regression of RH and T. Since the conditions of inlet air for calibration were set at RH = 80% and T = 25ºC, which were close to the average level of ambient air in Hong Kong from 1997 to 2012, uncorrected concentrations of HCHO measured by PTR-MS were only slightly lower than that by DNPH-HPLC with a percentage of 8.0% (r = 0.68). Corrected concentrations of HCHO by absolute humidity in sample air also correlated well with that by DNPH-HPLC (slope = 0.91, r = 0.77), because of the excellent correlation between these two different correction methods discussed above. However, correction for HCHO concentrations by Poly 2D regression of RH and T which has a better slope than the others is a better choice. Moreover, it is easy to measure RH and T of ambient air for further correction of HCHO data by PTR-MS in practice.

Wisthaler et al. (2008) reported the inter-comparison between PTR-MS and DNPH-HPLC in an atmosphere simulation chamber, good agreement was found between PTR-MS and DNPH-HPLC while ambient air was introduced into the chamber, but the concentration of HCHO measured by DNPH-HPLC was less than by PTR-MS, which could be caused by some interferences for DNPH-HPLC method or the varying performance of the KI ozone scrubber. Overestimation of DNPH-HPLC for HCHO in the presence of NO_2 was also reported by (Herrington and Hays, 2012), because NO can be oxidized to NO_2 in the upstream ozone scrubber, and NO_2 will react with DNPH

to form 2,4-dinitrophenylazide (DNPA), which has the similar chromatographic properties with the formaldehyde-DNP-hydrazone. Hence, the intercept of -0.03 for HCHO inter-comparison between PTR-MS and DNPH-HPLC in this study may be explained by the interference of NO_2 because of the high NO_x levels at the roadside sampling site.

Low acetaldehyde collection efficiencies (CEs), ranging from 1% to 62% was found by Herrington et al. (2007) for the typical 24-hour sampling period which can lead to the underestimation of acetaldehyde by DNPH-HPLC method. And this artifact is consistent with the result for acetaldehyde inter-comparisons in this study. It was found that ketone (acetone and MEK) concentrations determined by DNPH-HPLC method could be underestimated by 35% ~ 80% under high RH (>50%) condition when the temperature is about 22ºC (Ho et al., 2014). This DNPH issue could explain the 12% difference between PTR-MS and DNPH-HPLC for MEK and the relative bad agreement for acetone in our study.

4.3.2 PTR-MS versus on-line GC-FID

Hourly data were used for conducting inter-comparison between PTR-MS and on-line GC-FID. Because the ion signal at m/z 107 reflects C_2-benzenes (the sum of *p*-xylene, *m*-xylene, *o*-xylene, ethylbenzene and benzaldehyde) (Gouw and Warneke, 2007), C_2-benzenes measured by on-line GC-FID were compared with the ion signal at m/z 107

of PTR-MS. Time series concentrations of benzene, toluene, and C_2-benzenes measured by PTR-MS and on-line GC-FID are plotted in Figure 4.9. Excellent correlation was found for toluene with a slope of 1.01 ± 0.01 and a correlation coefficient of 0.96. Good linearities were observed for benzene and C_2-benzenes between PTR-MS and online GC-FID, with correlation coefficients of 0.92 and 0.96, respectively. However, the concentration of benzene detected by PTR-MS was 65% higher than that by on-line GC-FID, and the concentration of C_2-benzenes detected by PTR-MS was 17% lower than that by on-line GC-FID. The significant difference of benzene detected by PTR-MS and on-line GC-FID could mainly be due to the fragments from ethylbenzene and propylbenzene to m/z 79. Rogers et al. (2006) raised an equation (equation 4.5) to calculate the contributions from ethylbenzene and propylbenzene to m/z 79.

$$[\text{Benzene}] = [\text{M79}] - \frac{S_{\text{Ethylbenzene}}}{S_{\text{Benzene}}} BF_{\text{Ethylbenzene}} [\text{Ethylbenzene}] - \frac{S_{\text{Propylbenzene}}}{S_{\text{Benzene}}} BF_{\text{Propylbenzene[Propylbenzene]}} \quad (4.5)$$

where,

[Benzene] - volume mixing ratio of benzene;

[M79] - volume mixing ratio of m/z 79;

[Ethylbenzene] - actual volume mixing ratio of ethylbenzene;

[Propylbenzene] - actual volume mixing ratio of propylbenzene;

$S_x/S_{Benzene}$ – ratio of the ionization efficiencies;

BF – fraction of m/z 79 ion product that each produces upon ionization.

Since propylbenzene was not measured in this study, only ethylbenzene was used to correct the concentrations of benzene and C_2-benzenes measured by PTR-MS following equation 4.6 and equation 4.7:

$$[\text{Benzene}] = [\text{M79}] - 0.2235\,[\text{M107}] \qquad (4.6)$$

$$[C_2\text{-benzenes}] = 1.2235\,[\text{M107}] \qquad (4.7)$$

where,

[C_2-benzenes] - volume mixing ratio of C_2-benzenes;

[M107] - volume mixing ratio of m/z 107;

Time series of benzene, toluene and C_2-benzenes results obtained by on-line GC-FID and PTR-MS during the sampling period were plotted in Figure 4.9. Figure 4.10 (A and C) shows the correlation between corrected concentrations of benzene and C_2-benzenes based on equation 4.6 and equation 4.7 for PTR-MS and their measured concentrations by on-line GC-FID at MK AQMS. The agreement between the two different sampling techniques for benzene is better after correction by equation 4.6 with a slope of 1.23 ± 0.01 and the correlation coefficient of 0.95. Excellent agreement (slope = 1.02 ± 0.01, r = 0.96) between the two different sampling techniques for C_2-benzenes is achieved using the corrected concentrations of C_2-benzenes by PTR-MS. Since toluene to benzene ratio is one of the key indicators of determining VOC sources and C_2-benzenes are related to vehicular emissions and solvent usage, accurate measurements are required in studies on source apportionment of ambient VOCs. Above two equations

(equation 4.6 and equation 4.7) could offer a good correction method for the concentrations of benzene and C_2-benzenes measured by PTR-MS in urban roadside area of Hong Kong.

4.3.3 PTR-MS versus off-line GC-MSD/FID/ECD

The inter-comparison between the PTR-MS data averaged over the 24-hour canister sampling interval and off-line GC-MSD/FID/ECD analysis of the canisters are displayed in Figure 4.11. Corrected concentrations of benzene and C_2-benzenes by the PTR-MS were used for comparison. Acceptable linear regressions were found for benzene, toluene and C_2-benzenes between the PTR-MS and the off-line GC-MSD/FID/ECD with correlation coefficients of 0.62, 0.96 and 0.92, respectively. However, the mixing ratios of toluene and C_2-benzenes measured by PTR-MS were lower than that measured by off-line canister samples with percentages of 22%, 33%, respectively. The maximum offsets from the 1:1 line were usually found at high concentrations, which could be mainly caused by the different sampling time resolution for each sample of the PTR-MS and canister samples. The canister samples were 24-hour samples with constant flow, while PTR-MS detected a total group of 17 different species with a 30 seconds cycle. From previous studies on comparison between the PTR-MS and the GC-MSD/FID/ECD, the slope for toluene ranged 0.52 ~ 1.18, and the slope for C_2-benzenes ranged 0.58 ~ 3.20 (Christian et al., 2004; Gouw et al., 2003; Kato et al., 2004; Warneke et al., 2001), hence, PTR-MS and off-line GC-

MSD/FID/ECD analysis were comparable for aromatic hydrocarbon measurements in this study.

4.6 Comparison with other studies

Inter-comparisons between PTR-MS and other alternative technologies are summarized in Table 4.2. Most studies were conducted in urban areas, suburban areas, coastal areas, forested areas, or the free troposphere. Overall, most of the slopes of PTR-MS to alternative methods agreed to within less than the PTR-MS measurement accuracy of 20%.

Few studies have conducted inter-comparisons between PTR-MS and alternative methods for OVOCs (e.g. HCHO, acetaldehyde, acetone and MEK). Even fewer studies have investigated inter-comparison between PTR-MS and DNPH-HPLC. In most studies, a DOAS instrument and Hantzsch monitor were usually used to measure ambient HCHO. Good agreement was found between PTR-MS and DOAS in both mountain areas (slope = 1.01) (Inomata et al., 2008b) and urban areas (slope = 1.17) (Warneke et al., 2011b). HCHO measurement by DNPH-HPLC was compared to PTR-MS in an atmosphere simulation chamber by Wisthaler et al. (2008), and significant lower HCHO levels by DNPH-HPLC was observed in dry synthetic air because of hydrazine-to-hydrazone conversion. PIT-MS, AP-CIMS, GC-MS/FID were chosen as alternative monitoring methods for acetaldehyde, acetone and MEK. Relatively higher

acetaldehyde levels by PTR-MS was found while PTR-MS versus PIT-MS (Warneke et al., 2011a) and PTR-MS versus on-line GC-MS (Gouw et al., 2003) with slopes of 1.25 and 1.56, respectively. Better agreement was obtained between PTR-MS and DNPH-HPLC for acetaldehyde (slope = 1.10, r = 0.75) in our study. PTR-MS agreed well with AP-CIMS, online GC-MS and on-line GC-MS-FID for acetone, with slopes ranging from 1.00 to 1.18. In this study, however, the slope is 0.76 (PTR-MS to HPLC) with the offset of 1.88, which could have resulted from other interferences on m/z 59. The slopes of MEK varied in a large ranger (0.85 - 2.51) in previous studies, but a reasonable correlation between PTR-MS and DNPH-HPLC for MEK (slope = 0.88, r = 0.93) was found in this study.

Inter-comparisons between PTR-MS and alternative methods (both on-line and off-line methods) for benzene, toluene and C_2-benzenes have been conducted by previous studies in various areas. For benzene, PTR-MS was always reasonably comparable to other on-line or off-line techniques, with slopes ranged from 0.82 to 1.22. In this study, PTR-MS correlated well with off-line canister measurements for benzene (slope = 1.05), but a higher slope of 1.23 was found between PTR-MS and on-line GC-FID, which could be due to interferences (e.g. propylbenzene) at m/z 79. Lower toluene levels measured by PTR-MS as compared to off-line canister measurements was found in this study, with a slope of 0.78 (r = 0.96). Lower toluene levels measured by PTR-MS was also reported between PTR-MS versus DOAS (Jobson and McCoskey, 2010) and PTR-MS versus on-line GC-FID (Kato et al., 2004) in an urban area. Similarly, lower C_2-

benzenes levels measured by PTR-MS to off-line canister measurements was found with a slope of 0.67 (r = 0.92) in this study, which could be resulted from the much longer sampling resolution of off-line canister sample. The slopes of C_2-benzenes varied from 0.59 to 3.20 in previous studies with different area types.

4.7 Chapter summary

The effect of ambient RH and T on HCHO measurements by PTR-MS was further investigated in this study. Due to the backward reaction of protonated HCHO with H_2O, the sensitivity of HCHO decreased significantly when ambient RH and/or T varied. Meanwhile, calibrated reaction rate coefficient of HCHO and H_3O^+ also decreased significantly. The combined effect of RH and T on HCHO measurement by PTR-MS was explored in this study. A Poly 2D regression was found to be the best nonlinear surface simulation of $R_{(RH,T)}$, ambient RH and T for HCHO, following the equation $R_{(RH,T)} = 1.63 - 3.81 \cdot 10^{-3} \cdot RH + 1.92 \cdot 10^{-2} \cdot T + 5.10 \cdot 10^{-5} \cdot RH^2 - 6.41 \cdot 10^{-4} \cdot T^2 - 3.76 \cdot 10^{-4} \cdot RH \cdot T$. Through a field sampling study at an urban roadside area at MK AQMS, correction of HCHO concentrations by both ambient RH and T and by absolute humidity in sample air agreed well with each other (slope = 1.02, r = 0.99).

A field study of VOCs and OVOCs using the PTR-MS was conducted at MK in Hong Kong from May 2013 to August 2014. Good agreement was found between PTR-MS and DNPH-HPLC for formaldehyde (slope = 1.00, r = 0.79), acetaldehyde (slope =

1.10, r = 0.75) and MEK (slope = 0.88, r = 0.93). For acetone, the relative bad agreement (slope = 0.76, r = 0.60) should be resulted from the DNPH issue, since there is huge underestimation (35% ~ 80%) for ketones measured by the DNPH-HPLC method when RH > 50%. Moreover, correction for HCHO concentrations by Poly 2D regression of ambient RH and T was found to be better than directly correcting by absolute humidity in the sample air. Aromatic hydrocarbons measurements by PTR-MS were inter-compared with on-line GC-FID and off-line canister measurements using GC-MSD/FID/ECD. After correcting benzene and C_2-benzenes levels that were measured by the PTR-MS, which could be affected by fragments from ethylbenzene and propylbenzene at m/z 79, good agreements were found between PTR-MS and on-line GC-FID for toluene (slope = 1.01, r = 0.96) and C2-benzenes (slope = 1.02, r = 0.96), but higher benzene level was still detected by the PTR-MS when compared with that by on-line GC-FID (slope = 1.23, r = 0.95). For the inter-comparisons between PTR-MS and off-canister measurements using GC-MSD/FID/ECD, benzene showed good agreement with a slope of 1.05 (r = 0.62), underestimated toluene and C2-benzenes levels by PTR-MS were obtained with slopes of 0.78 (r = 0.96) and 0.67 (r = 0.92), respectively. In summary, the PTR-MS instrument can be used in urban roadside areas for VOC and OVOC measurements. But further inter-comparisons between PTR-MS and other off-line analytical techniques need to be conducted with higher sampling time resolutions of off-line analytical techniques.

Table 4.1 Poly 2D simulation results of different species in gas standard for the PTR-MS.

Component	m/z	*r*	Value					
			r_0	a	b	c	d	f
Formaldehyde	31	0.97	1.63E+00	-3.81E-03	1.92E-02	5.10E-05	-6.41E-04	-3.76E-04
Methanol	33	0.68	9.43E-01	1.16E-03	-6.16E-04	-7.23E-06	-8.01E-05	2.44E-05
Acetonitrile	42	0.72	9.77E-01	6.82E-04	-1.63E-03	-3.01E-06	-3.62E-05	1.80E-05
Acetaldehyde	45	0.70	1.04E+00	-5.07E-04	-3.97E-03	1.24E-06	4.83E-07	3.74E-05
Ethanol	47	0.67	1.16E+00	-3.30E-03	-1.83E-02	-6.65E-06	1.67E-04	2.35E-04
Acrolein	57	0.74	9.94E-01	-4.42E-04	-5.98E-03	-1.47E-06	2.32E-05	8.29E-05
Acetone	59	0.77	1.04E+00	-6.97E-04	-2.27E-03	6.21E-06	-4.00E-05	2.17E-05
Isoprene	69	0.92	1.00E+00	-1.38E-03	-8.82E-03	7.97E-06	1.13E-04	9.88E-05
Crotonaldehyde	71	0.79	8.69E-01	2.03E-03	-2.91E-04	-7.67E-06	-2.55E-05	1.57E-05
2-Butanone	73	0.74	9.77E-01	6.06E-04	-1.20E-03	-2.06E-06	-4.10E-05	1.41E-05
Benzene	79	0.81	1.03E+00	-3.93E-04	5.65E-03	1.17E-05	-1.53E-04	-6.35E-05
Toluene	93	0.84	1.03E+00	1.91E-04	4.66E-03	7.32E-06	-1.67E-04	-5.62E-05
o-Xylene	107	0.86	1.03E+00	1.06E-03	2.15E-03	-1.75E-06	-1.05E-04	-4.56E-05
α- Pinene	137	0.76	9.60E-01	1.56E-03	3.61E-03	-3.53E-06	-1.01E-04	-4.75E-05
Dichlorobenzenes	147	0.74	1.08E+00	6.93E-04	4.18E-03	2.16E-06	-1.56E-04	-7.19E-05
Trichlorobenzenes	181	0.55	8.66E-01	5.20E-03	1.18E-02	-2.23E-05	-2.91E-04	-1.23E-04

Table 4.2 Inter-comparisons between PTR-MS and alternative methods in this Study and the comparison with previous other studies

Compound	m/z	Alternative method	Slope	Intercept (ppbv)	*r*	Sampling area type	Reference
Formaldehyde	31	MAX-DOAS	1.01	-0.02	N.A.	mountain area	(Inomata et al., 2008a)
		DOAS	1.17	N.A.	0.84	urban area	(Warneke et al., 2011c)
		Hantzsch	1.35	N.A.	0.74	urban area	(Warneke et al., 2011c)
		DNPH-HPLC	N.A.	N.A.	N.A.	in chamber	(Wisthaler et al., 2008)
		DNPH-HPLC	1.00	-0.03	0.79	urban roadside area	This study
Acetaldehyde	45	PIT-MS	1.25	N.A.	0.87	in chamber	(Warneke et al., 2011a)
		on-line GC-MS	1.56	-0.17	0.93	on ship	(de Gouw et al., 2003)
		DNPH-HPLC	N.A.	N.A.	N.A.	in forest	(Müller et al., 2006)
		DNPH-HPLC	1.10	0.83	0.75	urban roadside area	This study
Acetone	59	AP-CIMS	1.18	0.06	0.94	in flight	(Sprung et al., 2001)
		on-line GC-MS	1.00	-0.05	0.98	on ship	(de Gouw et al., 2003)
		on-line GC-MS/FID	1.03	-0.44	0.90	urban area	(Wang et al., 2014)
		DNPH-HPLC	N.A.	N.A.	N.A.	in forest	(Müller et al., 2006)
		DNPH-HPLC	0.76	1.88	0.60	urban roadside area	This study
MEK	73	on-line GC-MS	2.51	0.02	0.95	on ship	(de Gouw et al., 2003)
		off-line canister	0.85	0.06	N.A.	in flight	(de Gouw et al., 2006)
		on-line GC-MS/FID	1.39	-0.18	0.89	urban area	(Wang et al., 2014)
		DNPH-HPLC	0.88	0.36	0.93	urban roadside area	This study
Benzene	79	off-line canister	0.82	0.11	0.91	suburban area	(Warneke et al., 2001)
		on-line GC-MS	1.12	0.00	0.96	on ship	(de Gouw et al., 2003)
		on-line GC-ITMS	0.85	0.00	0.97	suburban area	(Kuster et al., 2004)
		on-line GC-QMS	0.97	0.00	0.92	suburban area	(Kuster et al., 2004)

		on-line GC-FID	0.82	0.03	N.A.	suburban–urban area	(Kato et al., 2004)
		off-line canister	0.96	0.07	0.98	urban area	(Rogers et al., 2006)
		off-line canister	1.08	0.01	0.87	in flight	(de Gouw and Warneke, 2007)
		off-line canister	1.05	-1.16	0.65	urban area	(Jobson et al., 2010)
		DOAS	1.22	0.39	0.61	urban area	(Jobson et al., 2010)
		on-line GC-MS/FID	0.80	0.07	0.96	urban area	(Wang et al., 2014)
		on-line GC-FID	1.23	-0.03	0.95	urban roadside area	This study
		off-line canister	1.05	-0.03	0.62	urban roadside area	This study
Toluene	93	off-line canister	1.18	-0.07	0.96	suburban area	(Warneke et al., 2001)
		on-line GC-MS	1.08	0.01	0.99	on ship	(de Gouw et al., 2003)
		on-line GC-ITMS	0.91	0.00	0.98	suburban area	(Kuster et al., 2004)
		on-line GC-QMS	0.81	0.10	0.95	suburban area	(Kuster et al., 2004)
		on-line GC-FID	0.52	0.16	N.A.	suburban–urban area	(Kato et al., 2004)
		off-line canister	0.99	0.02	0.99	urban area	(Rogers et al., 2006)
		off-line canister	0.88	0.00	0.90	in flight	(de Gouw and Warneke, 2007)
		off-line canister	0.94	-0.43	0.66	urban area	(Jobson et al., 2010)
		DOAS	0.60	0.81	0.55	urban area	(Jobson et al., 2010)
		on-line GC-MS/FID	0.94	0.05	0.99	urban area	(Wang et al., 2014)
		on-line GC-FID	1.01	0.02	0.96	urban roadside area	This study
		off-line canister	0.78	0.19	0.96	urban roadside area	This study
C_2-benzenes	107	on-line GC-MS	3.20	0.01	0.98	on ship	(de Gouw et al., 2003)
		on-line GC-ITMS	1.02	0.00	0.97	suburban area	(Kuster et al., 2004)
		on-line GC-FID	0.58	0.00	N.A.	suburban–urban area	(Kato et al., 2004)
		off-line canister	0.86	0.00	0.91	in flight	(de Gouw et al., 2006)
		off-line canister	1.31	-0.40	0.99	urban area	(Rogers et al., 2006)
		off-line canister	0.86	-0.01	0.91	in flight	(de Gouw and Warneke, 2007)

	off-line canister	0.91	0.18	0.61	urban area	(Jobson et al., 2010)
	DOAS	0.59	0.04	0.58	urban area	(Jobson et al., 2010)
	on-line GC-MS/FID	0.87	0.09	0.98	urban area	(Wang et al., 2014)
	on-line GC-FID	1.02	0.31	0.96	urban roadside area	This study
	off-line canister	0.67	0.38	0.92	urban roadside area	This study

*N.A. - Not available

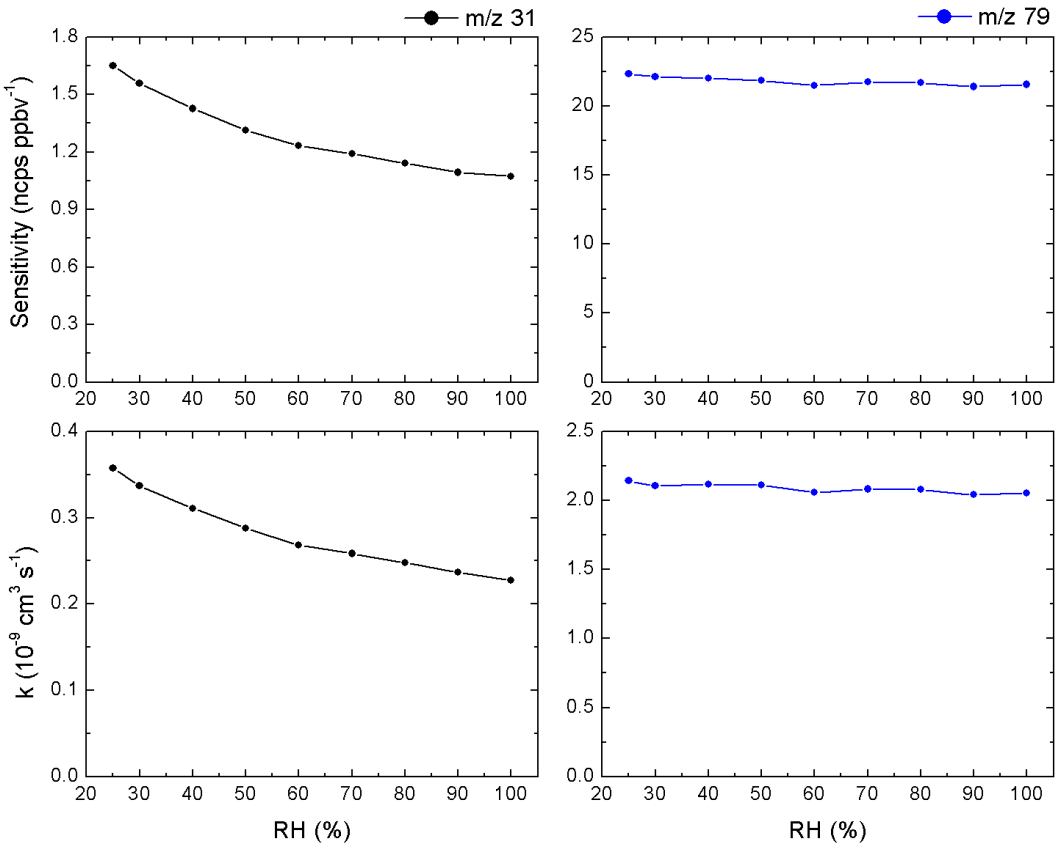

Figure 4.1 The effect of ambient RH on sensitivity and experimental k value of HCHO (m/z 31) and benzene (m/z 79).

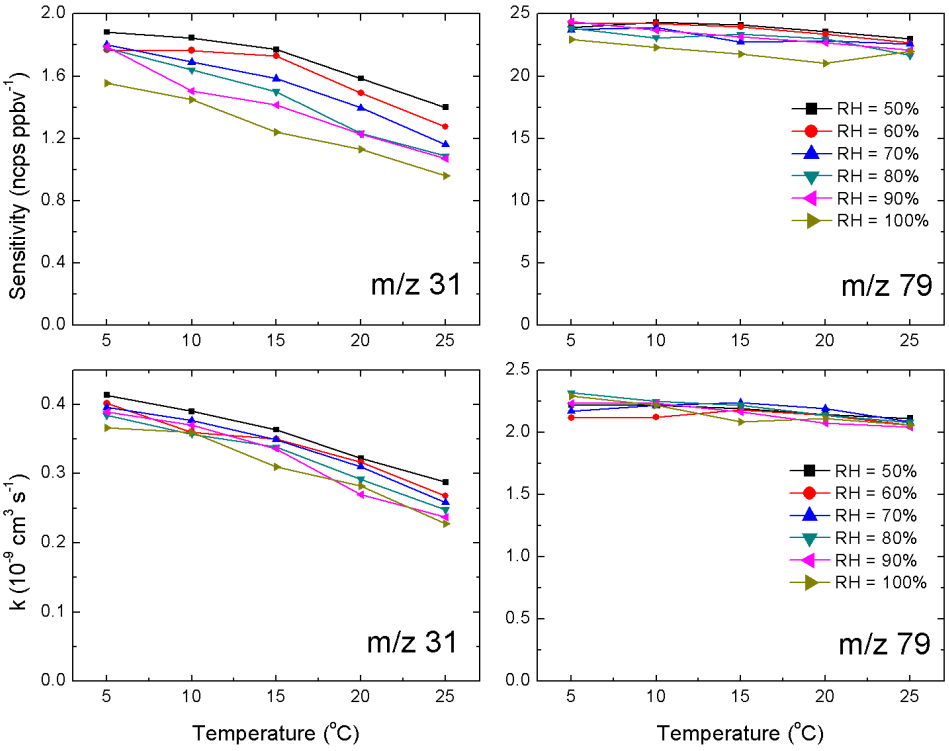

Figure 4.2 The effect of ambient temperature on sensitivity and experimental k value of HCHO (m/z 31) and benzene (m/z 79) under different RH.

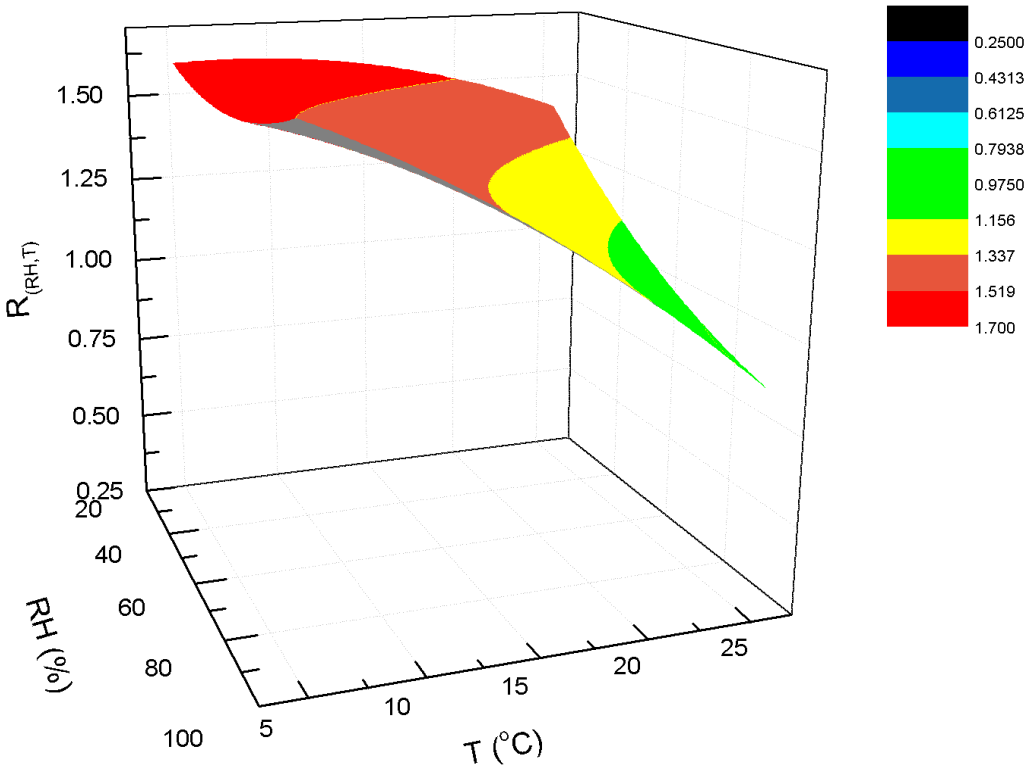

Figure 4.3 Simulation of experimental reaction rate coefficient, ambient relative humidity (RH) and temperature (T) for HCHO (m/z 31).

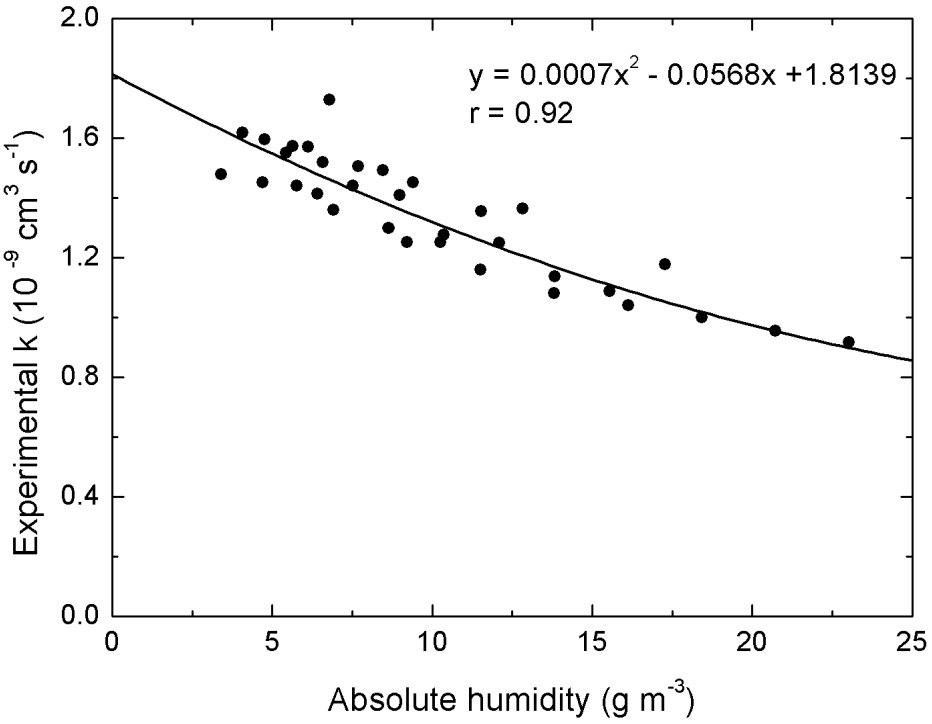

Figure 4.4 Experimental k value of HCHO (m/z 31) as a function of absolute humidity in sample air.

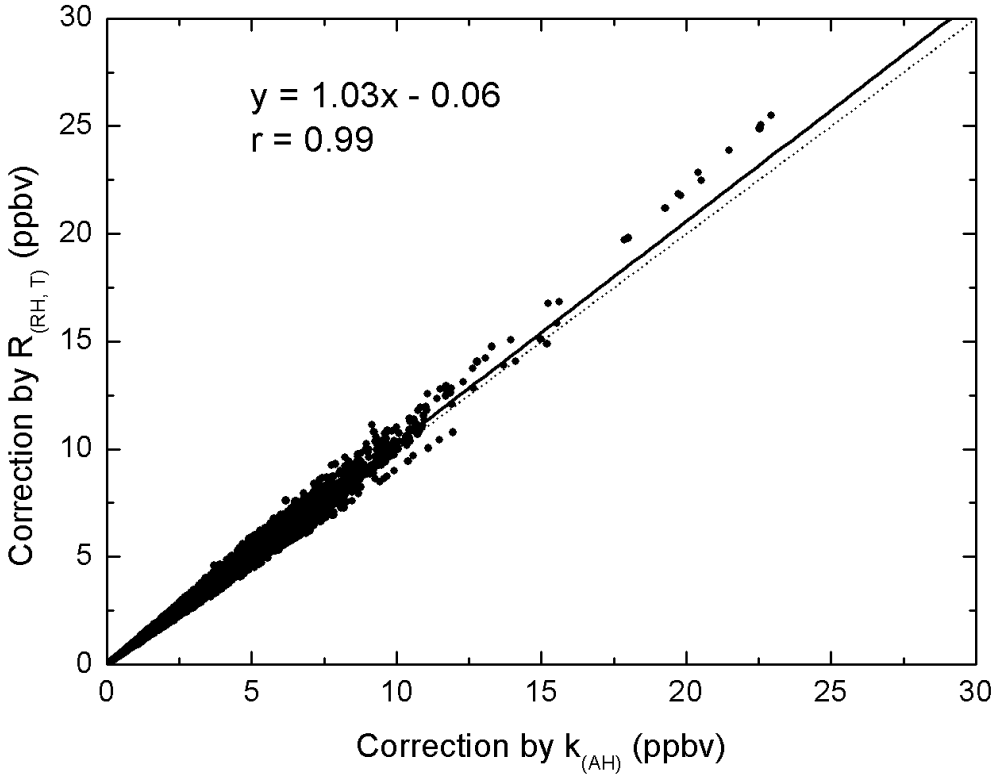

Figure 4.5 Linear regression of two correction methods for HCHO concentrations during the field study at MK in Hong Kong.

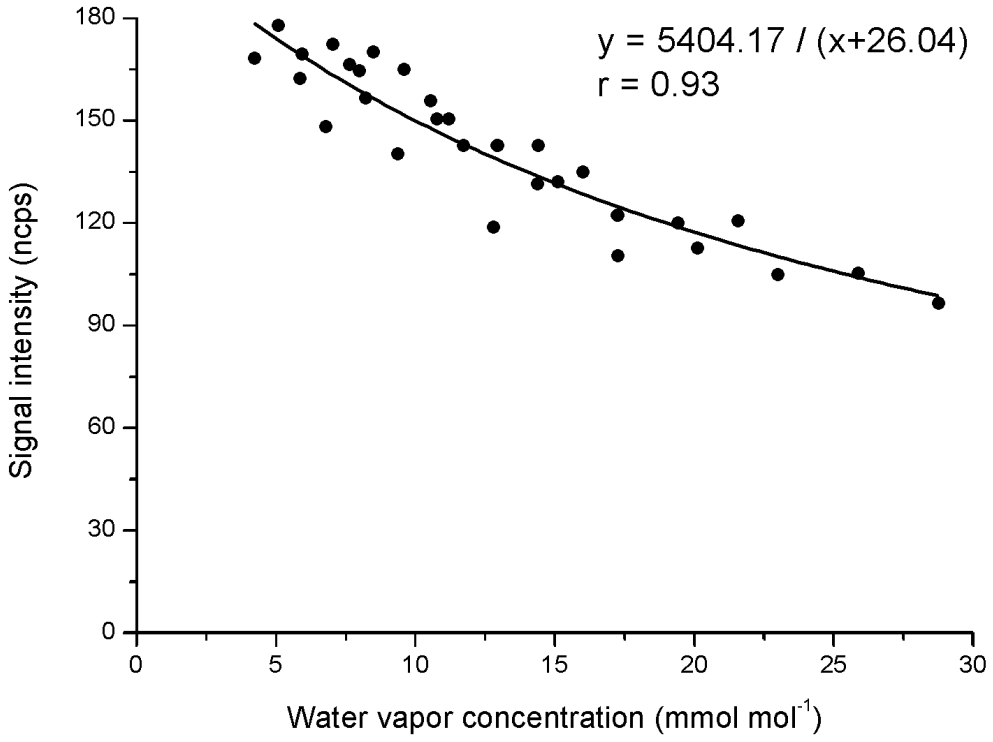

Figure 4.6 The relationship of the signal intensity at m/z 31 and the water vapor concentration in sample air.

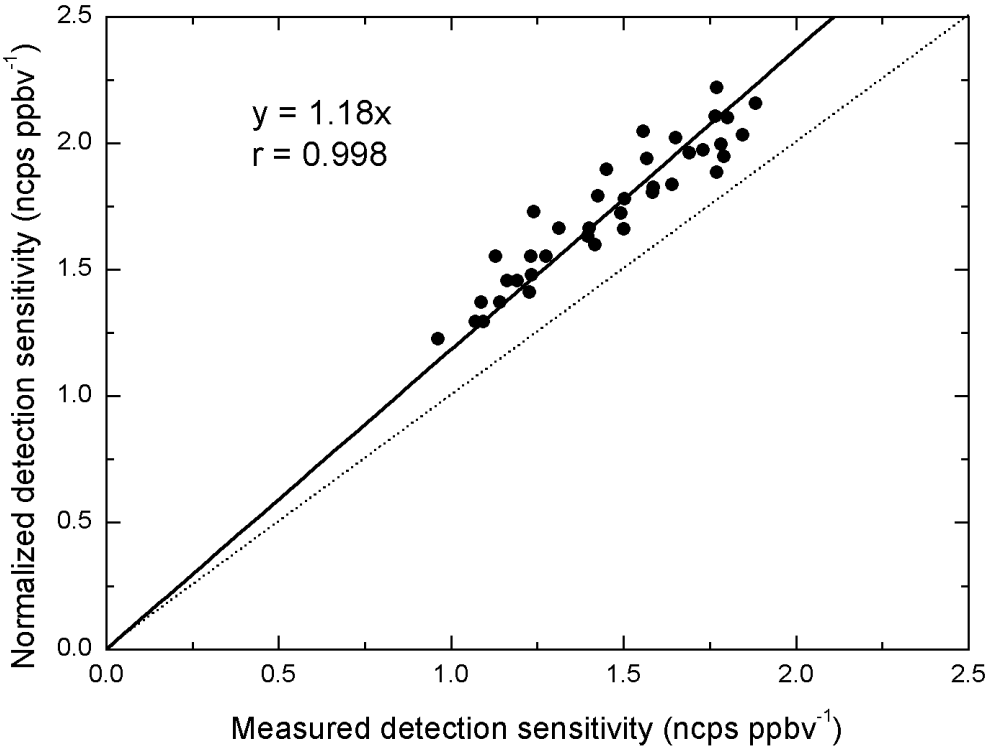

Figure 4.7 Linear regression of the measured detection sensitivity of HCHO and its normalized detection sensitivity by water vapor concentration in sample air.

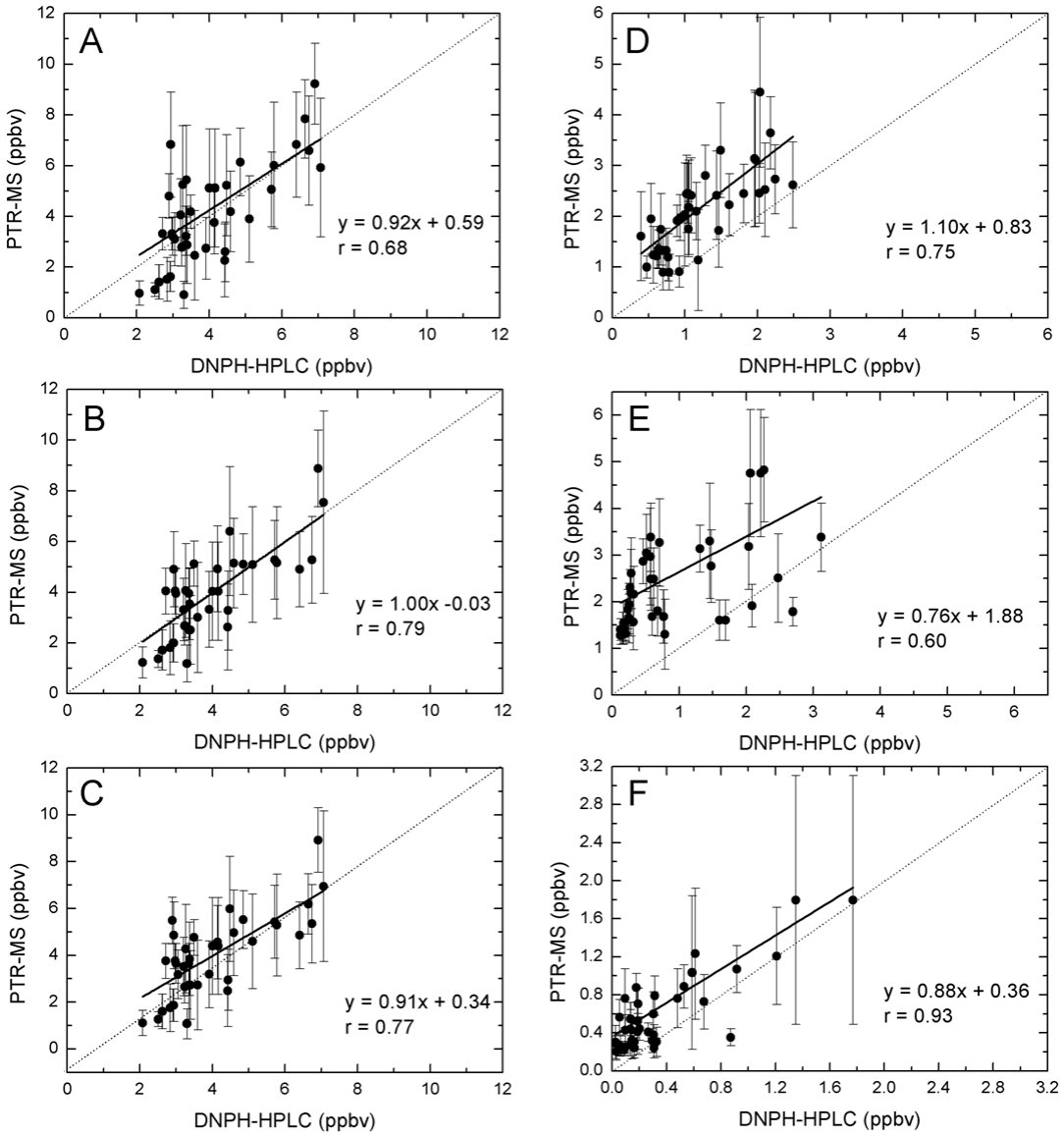

Figure 4.8 Inter-comparison between ambient OVOC measurements by PTR-MS and by DNPH-HPLC during the field study at MK in Hong Kong: (A) formaldehyde without correction, (B) formaldehyde corrected by R(RH,T), (C) formaldehyde corrected by k(AH), (D) acetaldehyde, (E) acetone, and (F) MEK. Linear regression fits are indicated by the solid black line. Error bar stands for the standard deviation of 24-hour averaged PTR-MS data. Dashed line is the 1:1 line for reference.

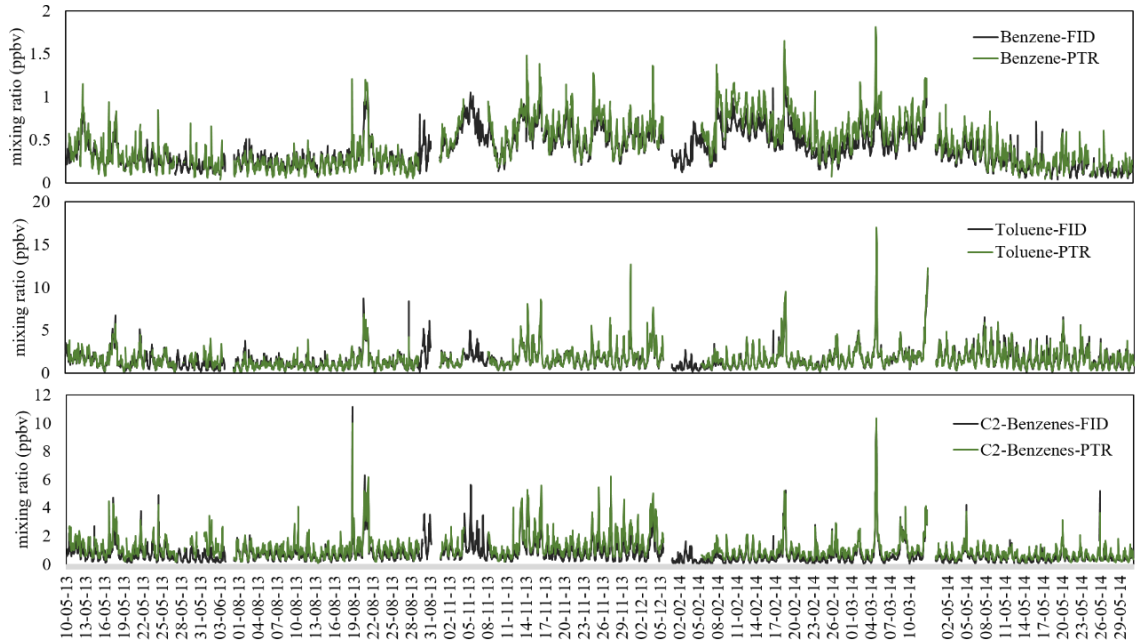

Figure 4.9 Measurement results for benzene, toluene and C_2-benzenes obtained during the field study at MK in Hong Kong. The black lines show the on-line GC-FID data, and the green lines show the PTR-MS results.

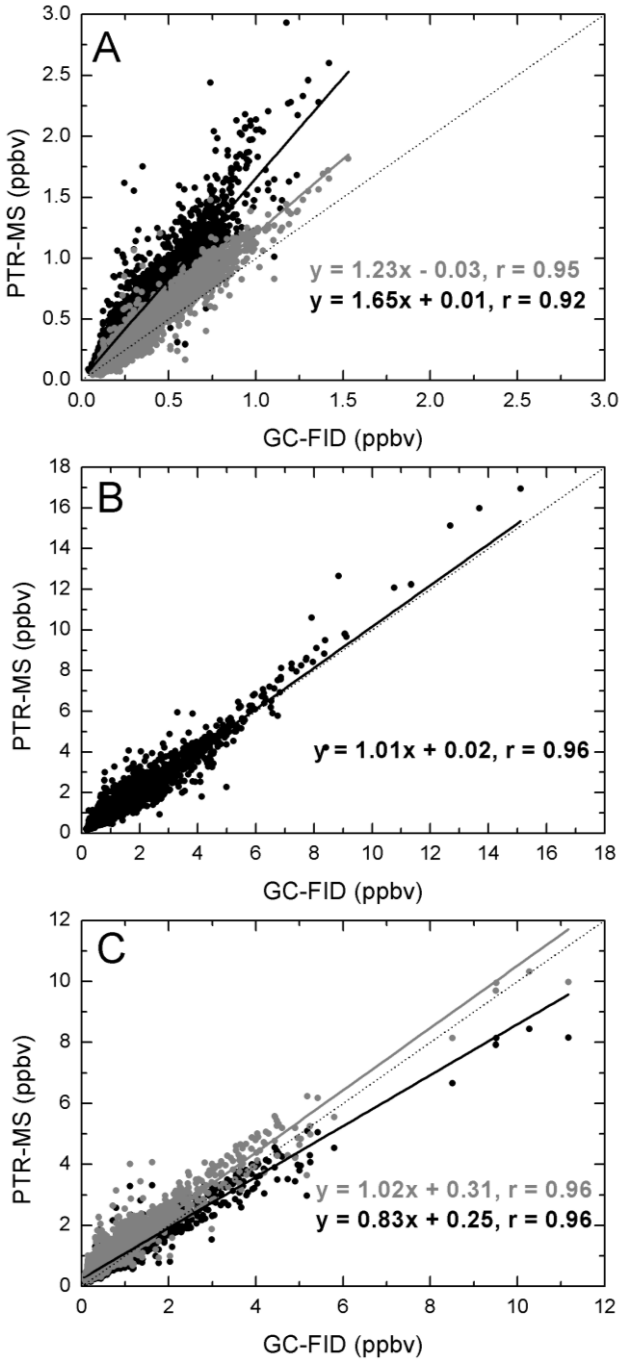

Figure 4.10 Inter-comparison between ambient aromatic hydrocarbon measurements by PTR-MS and by on-line GC-FID during the field study at MK in Hong Kong: (A) benzene, (B) toluene, and (C) C_2-benzenes. Original data are plotted in black dots, grey dots represent the corrected data based on Eq. (6) and Eq. (7). Linear regression fits for original and corrected data are indicated by the solid black line and the solid grey line respectively. Dashed line is the 1:1 line for reference.

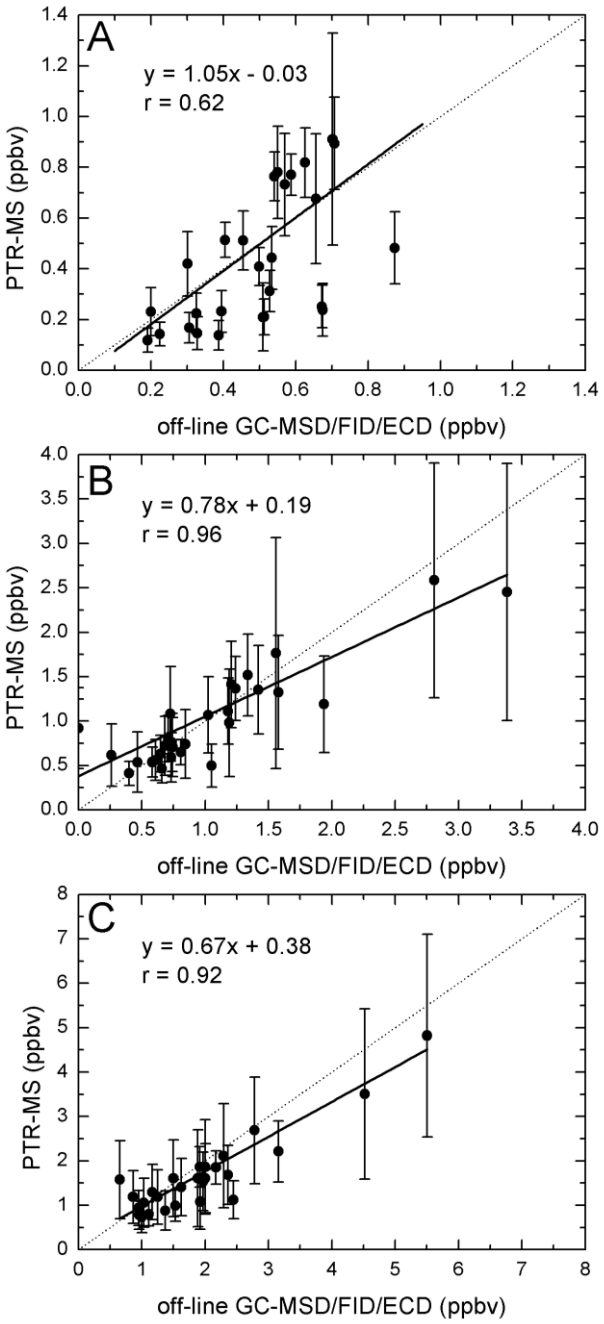

Figure 4.11 Inter-comparison between ambient aromatic hydrocarbon measurements by PTR-MS (corrected based on Eq. (6) and Eq. (7)) and by off-line canister measurements using GC-MSD/FID/ECD during the field study at MK in Hong Kong: (A) benzene, (B) toluene, and (C) C_2-benzenes. Linear regression fits are indicated by the solid black line. Error bar stands for the standard deviation of 24-hour averaged PTR-MS data. Dashed line is the 1:1 line for reference.

Chapter 5 Characteristics and Sources of Roadside VOCs and OVOCs in Hong Kong

5.1 Introduction

Hong Kong is one of the most densely populated cities in the world, and it is experiencing an increasing ozone trend and regional photochemical smog problem, which reduces visibility, adversely affects human health during the past twenty years (Louie et al., 2013; Wang et al., 2009; Yuan et al., 2013a). The total licensed vehicle number of Hong Kong has increased by about 40% from 517,599 in 2003 to 722,012 in 2015. Vehicular emissions has been found to be one of the major sources of air pollutants (i.e. PM, VOCs, CO, CO_2, SO_2, NO_x) in urban areas. The characteristics and source profiles of VOCs have changed substantially because of the air pollution control measures. For instance, the most abundant VOC species has switched from toluene to *i*/*n*-butane as a results of nearly all taxies and public light buses has been changed from diesel-fueled to LPG-fueled since 2000 (Guo et al., 2007; Ho et al., 2004; Huang et al., 2015; Ou et al., 2015).

An LPG CCRP has been launched from September 2013 and finished in April 2014 in order to control LPG vehicular emissions in Hong Kong. One of the aims of this study is to estimate the effectiveness of the LPG CCRP on reducing VOC and OVOC emissions. PTR-MS was firstly used to continuously measure the ambient VOC and

OVOC levels in Hong Kong, and the data file obtained from PTR-MS combined with other measurement techniques were applied to conduct source apportionment of roadside VOCs and OVOCs

5.2 VOC characteristics in the roadside environment

5.2.1 Mixing ratios and compositions

Since the purpose of this study is to assess the effectiveness of LPG CCRP on reducing VOC emissions, the data obtained before LPG CCRP (in May 2013) and after LPG CCRP (in May 2014) were used for comparison and source attribution. Average mixing ratios of total and individual species of VOCs before and after LPG CCRP are shown in Table 5.1. The average mixing ratio of total measured VOCs decreased by 36.7% after LPG CCRP (43.9 ± 6.5 ppbv) than before LPG CCRP (69.3 ± 12.6 ppbv) at MKAQMS. Before LPG CCRP, alkanes were the most dominant species (54.9%) to the total measured VOC mixing ratios, followed by OVOCs (22.7%), alkenes (12.2%), aromatics (5.4%), alkyne (4.2%), and other (0.6%). While after LPG CCRP, alkanes were still the most dominant species (46.5%), followed by OVOCs (25.1%), alkenes (12.8%), alkyne (8.0%), aromatics (7.2%), and other (0.6%). The group compositions were comparable before and after LPG CCRP for most groups, while the contribution of alkanes to total VOCs average mixing ratio decreased from 54.9% to 46.5% after LPG CCRP due to the large decrease of three most abundant species, namely propane

(before: 10.2 ± 5.8 ppbv; after: 4.6 ± 2.3 ppbv), i-butane (before: 8.3 ± 5.1 ppbv; after: 4.0 ± 2.0 ppbv), and n-butane (before:15.4 ± 9.0 ppbv; after: 6.3 ± 3.3 ppbv) among total measured VOCs. Even though the group percentage of OVOCs were slightly higher after LPG CCRP, the average mixing ratios of all individual OVOC species decreased after LPG CCRP with the decreasing rate ranged from 11.1% to 55.5%.

Propane, i-butane, and n-butane are the tracers of LPG emissions in Hong Kong (Tsai et al., 2006). In this study, propane, i-butane, and n-butane, which were the three most abundant species among total measured VOCs comprised 49.0% of total VOCs before LPG CCRP. High levels of the three LPG tracers were also observed at the same sampling site in 2011 with the mixing ratios of 8.1 ± 0.5 ppbv (propane), 6.7 ± 0.5 ppbv (i-butane), and 1.1 ± 0.8 ppbv (n-butane), respectively, and the sum of three LPG tracers accounted for 50.3% of the total quantified VOCs in 2011 (Huang et al., 2015). The percentage (50.3%) in 2011 was comparable with the sum contribution (49.0%) before LPG CCRP (in 2013) in this study. However, the sum contribution of LPG tracers to total quantified VOCs decreased to 34.0% after LPG CCRP, which can reflect the effectiveness of the control measures on reducing LPG vehicular emissions.

5.2.2 Photochemical reactivity of VOCs

After LPG CCRP, total OFP and total Prop-Equiv concentration of all quantified VOCs decreased by 36.6%, and 31.2%, respectively as shown in **Figure 5.1**. Alkenes

comprised the most of total OFP and total Prop-Equiv concentration both before and after LPG CCRP at MKAQMS (as shown in Figure 5.1). OVOCs and alkanes were also important contributors to O_3 formation following alkenes in this study.

Top 10 VOC species contributing to ozone formation based on the MIR scales at MKAQMS before and after LPG CCRP are listed in Table 5.2. The contributions to OFP, in decreasing order, were formaldehyde (12.7%), ethane (10.9%), n-butane (10.3%), propene (9.8%), C_2-benzenes (8.4%), acrolein (6.9%), isoprene (6.3%), toluene (6.0%), i-butane (5.9%), and acetaldehyde (5.7%) before LPG CCRP. Ethene contributed the most to OFP after LPG CCRP with the percentage of 12.6%, followed by toluene (10.0%), formaldehyde (8.9%), acetaldehyde (7.9%), acrolein (7.8%), propene (7.5%), C_2-benzenes (7.2%), isoprene (7.2%), n-butane (6.6%), and i-butane (4.5%). Both absolute OFP values and rankings of n-butane and i-butane decreased significantly after LPG CCRP than before LPG CCRP. Similar trends were also found for Prop-Equiv concentrations of n-butane and i-butane in Table 5.3, the Prop-Equiv concentrations of n-butane and i-butane decreased from 5.54 ppbC to 2.25 ppbC, and from 2.68 ppbC to 1.30 ppbC, respectively. The large decrease of absolute values and rankings of n-butane and i-butane indicate the significant reduction of LPG emissions resulted from the LPG vehicular emissions control programme.

5.3 Changing ratios of two paired species

The ratios of some paired VOCs were always used as the indicators to evaluate the changing source contributions. The ratio of m,p-xylenes to ethylbenzene is commonly used to indicate the photochemical age (Guo et al., 2007; Ho et al., 2004; Min et al., 2011; Nelson and Quigley, 1983). The ratio of m,p-xylenes to ethylbenzene was 1.35 ± 0.02 before LPG CCRP and 1.75 ± 0.03 after LPG CCRP in this study, and these ratios were in the normal range 1.3-1.8 in urban/rural sampling sites in Hong Kong. Moreover, previous studies found that the air mass at MKAQMS was mainly affected by local source (Guo et al., 2011a; Ling and Guo, 2014; Ou et al., 2015). Therefore, the significant change of the ratios of two paired species should mainly attributed to the change of local VOC emissions. If the difference of photochemical age can be ignored, the observed ratio of two paired species is linked to their emission sources. The average ratio of specific VOC specie to CO, which is a widely used non-complete combustion sources tracer, can be used to estimate the change of combustion source (Huang et al., 2017; Warneke et al., 2012). The average ratios of propane, i-butane, and n-butane to CO are shown in Figure 5.2. The average propane/CO ratio decreased by 65.0% from 22.51 before LPG CCRP to 7.89 after LPG CCRP. Similar to propane/CO ratio, i-butane/CO and n-butane/CO significantly decreased by 69.4% (from 19.04 to 5.78), and 69.2% (from 34.05 to 4.05), respectively. The large decrease of three LPG tracers (propane, i-butane, and n-butane) to CO ratios at the roadside sampling site could demonstrate the significant reduction of LPG vehicular emissions in Hong Kong after

the LPG CCRP.

5.4 Source apportionments of VOCs at the roadside site

Four major sources were identified through PMF source attribution at the roadside sampling site in this study (Figure 5.3), including diesel and gasoline vehicular emissions (D&G VE), LPG vehicular emissions (LPG VE), solvent usage (SU), and secondary and biogenic emissions (S&BE).

Factor 1 contributed the largest to ethene, ethane, i-pentane, n-pentane, with significant amounts of CO, benzene, toluene, and OVOCs. Ethene, ethane, ethyne, i-pentane, and n-pentane are typical tracers for diesel-related and gasoline-related emissions (Liu et al., 2008a; Yuan et al., 2013b). Diesel vehicles were also found to emit a large amount of OVOCs (i.e. formaldehyde, acetaldehyde and acetone) (Ho et al., 2007; Ho et al., 2012). Therefore, this factor is identified as diesel and gasoline vehicular emissions.

Factor 2 was found to be dominated by propane, i-butane, and n-butane, which are the key tracers of LPG fuel (Ho et al., 2009b; Lyu et al., 2016; Tang et al., 2007). Thus, this factor is regarded as LPG vehicular emissions.

Factor 3 was considered to be solvent usage because it was dominated by ethylbenzene, m, p-xylene, and o-xylene, which are commonly used in industrial solvents and emitted

from the use of sealant, inks, paints, and varnish for architecture and decoration (Borbon et al., 2002; Liu et al., 2008b; Ou et al., 2015; Seila et al., 2001). Moreover, Poor correlations were also found between CO, which is a combustion tracer, and these aromatic hydrocarbon species in this factor.

Factor 4 comprised abundant isoprene and OVOC species. Isoprene is the indicator of biogenic emissions (Guenther et al., 1995). OVOC species such as formaldehyde, acetaldehyde, methanol, and acetone can be generated through secondary photochemical formations (Bon et al., 2011; Li et al., 2015; Yuan et al., 2012). Hence, this factor was identified as secondary and biogenic emissions.

Mixing ratios of VOCs from different sources at MK AQMS before and after LPG CCRP are plotted in Figure 5.4. LPG vehicular emissions had the highest mixing ratio both before and after LPG CCRP, followed by diesel and gasoline vehicular emissions, secondary and biogenic emissions, and solvent usage. LPG vehicular emissions generated 30.5 ppbv VOCs and OVOCs in total before LPG CCRP, however, it sharply dropped to 13.8 ppbv by about 55% after LPG CCRP. Mixing ratios of VOCs from diesel and gasoline vehicular emissions, secondary and biogenic emissions, and solvent usage all dropped by 22%, 50%, and 59%, respectively. LPG vehicular emissions contributed the most roadside VOCs and OVOCs both before and after LPG CCRP (as shown in Figure 5.5), however, its relative contributing percentage has decreased from 44.7% to 37.8%. Vehicle-related emissions were still the major source of roadside

VOCs and OVOCs in Hong Kong both before (69%) and after (46%) LPG CCPR. Since OVOC data obtained from PTR-MS were firstly applied in the source apportionment of VOCs, secondary and biogenic emissions were identified in this study, and our results showed that they were also important contributors of roadside VOCs in Hong Kong. Secondary emissions together with biogenic emissions were found to comprise about 17% of total roadside VOCs in Hong Kong.

5.5 Contributions of ozone formation potential from different emission sources

The sum of OFP for the total target VOCs and OVOCs in this study was 193.3 ppbv O_3 $ppbv^{-1}$, and 108.5 ppbv O_3 $ppbv^{-1}$, respectively, before and after LPG CCRP. The large reduction of total OFP can be attributed to the large decrease of VOC mixing ratios, especially for formaldehyde, ethene, n-butane, and propene. The three species were the top 3 contributors of total OFP before LPG CCRP, however, the OFPs of formaldehyde, ethene, n-butane, and propene all decreased by more than 50% after LPG CCRP.

The contributions of OFP by different VOCs emission sources based on the PMF data analysis were illustrated in Figure 5.6. LPG vehicular emissions accounted for 30.3% of the total OFP before LPG CCRP, followed by secondary and biogenic emissions (28.3%), diesel and gasoline vehicular emissions (24.6%), and solvent usage (16.8%). After LPG CCRP, diesel and gasoline vehicular emissions contributed the most of total

OFP with the percentage of 46.4%, followed by LPG vehicular emissions (23.8%), secondary and biogenic emissions (21.3), and solvent usage (8.5%). The sequence of the contributions to OFP by each VOC emission source is slightly different from their contributions to total VOC mixing ratios in Figure 5.5, indicating that the reactivity of VOCs is a key factor to be considered during the implementation of VOC control strategies.

5.6 Chapter summary

The characteristics of roadside VOCs and OVOCs were studied at MK AQMS in Hong Kong from 2013 to 2014. PTR-MS was firstly utilized to measure ambient VOCs and OVOCs in Hong Kong coupled with other measurement techniques through this study. The changes of VOCs and OVOCs were investigated before and after the LPG catalytic convertor replacement programme. The average mixing ratio of total measured VOCs decreased by 36.7% after LPG CCRP (43.9 ± 6.5 ppbv) than before LPG CCRP (69.3 ± 12.6 ppbv) at MKAQMS. The three LPG tracers (propane, i-butane, and n-butane) comprised 49% of the total measured VOCs and OVOCs before LPG CCRP, but their contribution to total measured VOCs and OVOCs decreased to 34% after LPG CCRP. In terms of the reactivity, both absolute OFP values and rankings of n-butane and i-butane decreased significantly after LPG CCRP, and similar trends were also found for Prop-Equiv concentrations of n-butane and i-butane.

After LPG CCRP, the average propane/CO, i-butane/CO, and n-butane/CO ratios decreased by 65.0%, 69.4% and 69.2%, respectively. Moreover, source apportionment of roadside VOCs and OVOCs were conducted in this study. LPG vehicular emissions was found to be the largest contributor both before and after LPG CCRP, however, its contribution decreased from 44.7% to 37.8%. The OFP of VOCs and OVOCs from LPG vehicular emissions also decreased from 58.6 ppbv O_3 $ppbv^{-1}$ to 25.8 ppbv O_3 $ppbv^{-1}$. All of these changes indicate that the fulfillment of the LPG catalytic convertor replacement programme was effective on reducing LPG vehicular emissions and improve the air quality of Hong Kong.

Table 5.1 The mixing ratios (in ppbv) of trace gases and VOCs measured at MK AQMS before and after the LPG CCRP

		Before LPG CCRP (n = 528)				After LPG CCRP (n=744)			
Group	**Species**	**Average**	**S.D.**	**Max**	**Min**	**Average**	**S.D.**	**Max**	**Min**
Alkanes	Ethane[a]	1.90	0.49	3.89	1.02	4.00	1.29	9.03	0.55
	Propane[a]	10.23	5.84	40.03	2.89	4.64	2.28	17.38	1.02
	i-Butane[a]	8.32	5.07	35.02	2.09	4.02	1.99	18.23	1.10
	n-Butane[a]	15.44	8.97	63.01	4.23	6.27	3.29	27.28	1.44
	i-Pentane[a]	1.10	0.68	4.83	0.00	0.78	0.56	8.28	0.11
	n-Pentane[a]	0.52	0.32	2.06	0.00	0.32	0.30	5.74	0.00
	i-hexane[a]	0.10	0.22	1.74	0.00	0.15	0.26	1.56	0.00
	n-Hexane[a]	0.24	0.30	3.40	0.00	0.07	0.22	2.26	0.00
	i-Octane[a]	0.11	0.10	0.81	0.00	0.11	0.11	0.79	0.00
	n-Heptane[a]	0.10	0.14	1.18	0.00	0.02	0.09	0.90	0.00
	n-Octane[a]	0.01	0.04	0.31	0.00	0.00	0.02	0.25	0.00
	Sub-Total	*38.08*	*11.89*			*20.40*	*4.71*		
Alkenes	Ethene[a]	4.35	1.15	8.76	2.07	3.17	1.58	7.31	0.00
	Propene[a]	2.01	0.73	4.50	0.65	0.97	0.37	2.64	0.28
	trans-2-Butene[a]	0.01	0.04	0.27	0.00	0.32	0.15	1.21	0.00
	1-Butene[a]	0.38	0.17	1.19	0.00	0.01	0.03	0.16	0.00
	cis-2-Butene[a]	0.10	0.07	0.40	0.00	0.04	0.05	0.43	0.00
	1,3-Butadiene[a]	0.13	0.06	0.36	0.00	0.07	0.05	0.39	0.00
	trans-2-Pentene[a]	0.08	0.09	0.66	0.00	0.03	0.07	0.84	0.00
	1-Pentene[a]	0.17	0.17	1.29	0.00	0.03	0.08	1.29	0.00
	Isoprene[b]	0.88	0.35	2.08	0.27	0.63	0.25	1.61	0.19
	Monoterpenes[b]	0.39	0.15	0.97	0.14	0.34	0.15	1.58	0.11

	Sub-Total	*8.49*	*1.44*			*5.61*	*1.66*		
Alkyne	Ethyne[a]	2.89	2.01	21.70	0.00	3.49	3.28	26.11	0.00
Aromatics	Benzene[b]	0.33	0.18	1.15	0.03	0.28	0.16	0.91	0.04
	Toluene[b]	1.64	0.91	5.78	0.21	1.73	1.05	6.19	0.24
	C_2-Benzenes[b]	1.19	0.69	4.45	0.17	0.65	0.40	3.73	0.12
	1,3,5-Trimethylbenzene[a]	0.00	0.01	0.07	0.00	0.00	0.02	0.22	0.00
	1,2,4-Trimethylbenzene[a]	0.08	0.07	0.40	0.00	0.05	0.08	0.51	0.00
	1,2,3-Trimethylbenzene[a]	0.00	0.01	0.11	0.00	0.00	0.01	0.26	0.00
	Chlorobenzene[b]	0.12	0.08	0.38	0.00	0.14	0.06	0.36	0.05
	Dichlorobenzene[b]	0.29	0.11	0.74	0.10	0.21	0.10	0.88	0.02
	Trichlorobenzene[b]	0.07	0.09	0.94	0.02	0.09	0.03	0.34	0.00
	Sub-Total	*3.72*	*1.17*			*3.15*	*1.15*		
OVOCs	Formaldehyde[b]	4.49	2.29	12.62	0.17	2.00	1.21	8.13	0.24
	Methanol[b]	4.38	1.54	10.48	1.30	3.31	1.47	22.35	1.29
	Acetaldehyde[b]	1.99	1.03	5.92	0.00	1.74	0.82	5.70	0.42
	Acrolein[b]	1.67	0.74	4.29	0.08	1.20	0.52	3.54	0.38
	Acetone[b]	2.45	0.94	5.79	0.92	2.18	0.89	6.88	0.90
	MVK&MACR[b]	0.29	0.14	0.77	0.05	0.21	0.10	0.57	0.05
	MEK[b]	0.46	0.25	1.33	0.08	0.37	0.19	1.27	0.11
	Sub-Total	*15.73*	*3.19*			*11.00*	*2.32*		
Other	Acetonitrile[b]	0.42	0.09	0.75	0.21	0.25	0.06	0.63	0.10
	Total	**69.32**	**12.61**			**43.91**	**6.51**		

[a] Measured by on-line GC-FID

[b] Measured by PTR-MS

Table 5.2 Top 10 VOC species contributing to ozone formation based on the MIR scales at MK AQMS before and after LPG CCRP

	Before LPG CCRP			After LPG CCRP		
Rank	Species	OFP (ppbv/ppbv)	Percentage	Species	OFP (ppbv/ppbv)	Percentage
1	Formaldehyde	26.54	12.7%	Ethene	16.65	12.6%
2	Ethene	22.87	10.9%	Toluene	13.28	10.0%
3	*n*-Butane	21.52	10.3%	Formaldehyde	11.80	8.9%
4	Propene	20.57	9.8%	Acetaldehyde	10.43	7.9%
5	C_2-Benzenes	17.60	8.4%	Acrolein	10.42	7.8%
6	Acrolein	14.52	6.9%	Propene	9.94	7.5%
7	Isoprene	13.18	6.3%	C_2-Benzenes	9.60	7.2%
8	Toluene	12.58	6.0%	Isoprene	9.52	7.2%
9	*i*-Butane	12.40	5.9%	*n*-Butane	8.74	6.6%
10	Acetaldehyde	11.92	5.7%	*i*-Butane	5.99	4.5%

Table 5.3. Top 10 VOC species contributing to ozone formation based on the Prop-Equiv concentration at MK AQMS before and after LPG CCRP

	Before LPG CCRP			After LPG CCRP		
Rank	Species	Prop-Equiv (ppbC)	Percentage	Species	Prop-Equiv (ppbC)	Percentage
1	Isoprene	16.64	23.7%	Isoprene	12.03	24.9%
2	Monoterpenes	9.38	13.4%	Monoterpenes	8.23	17.0%
3	Propene	6.04	8.6%	*trans*-2-Butene	3.10	6.4%
4	*n*-Butane	5.54	7.9%	Acrolein	3.00	6.2%
5	C_2-Benzenes	4.78	6.8%	Propene	2.92	6.0%
6	Acrolein	4.19	6.0%	C_2-Benzenes	2.61	5.4%
7	Ethene	2.82	4.0%	Toluene	2.59	5.4%
8	*i*-Butane	2.68	3.8%	*n*-Butane	2.25	4.7%
9	Toluene	2.45	3.5%	Ethene	2.05	4.2%
10	Acetaldehyde	2.27	3.2%	Acetaldehyde	1.98	4.1%

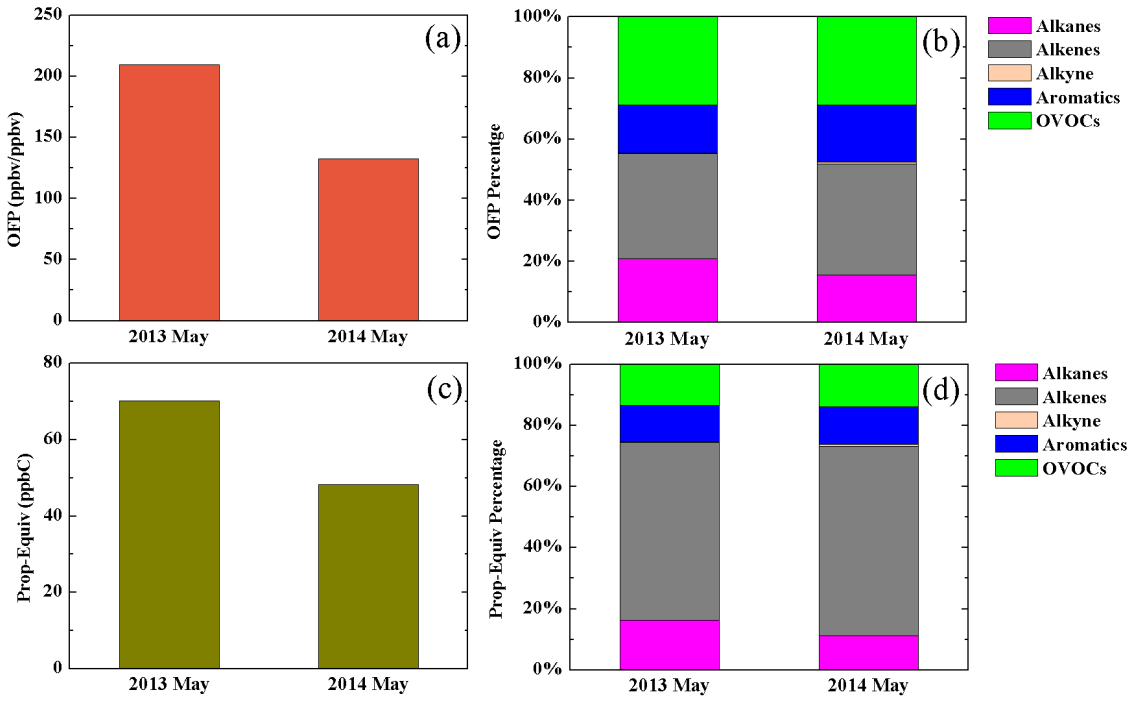

Figure 5.1 OFP and Prop-Equiv of measured VOCs at MK AQMS before and after the LPG CCRP.

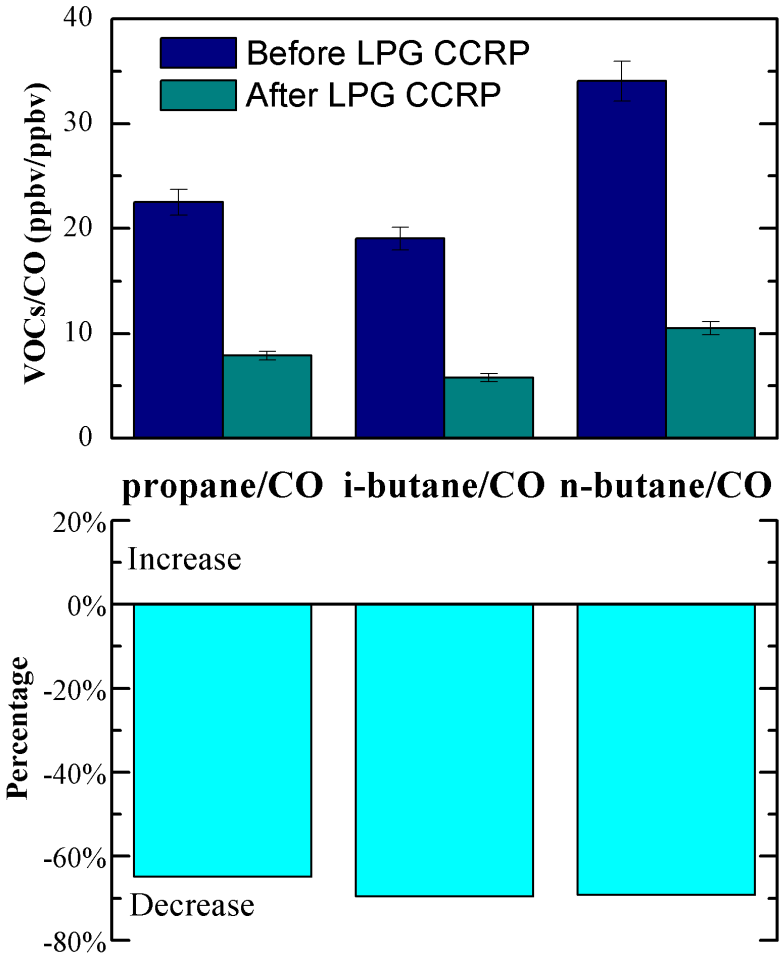

Figure 5.2 The ratios of selected VOCs to CO at MK AQMS before and after the LPG CCRP.

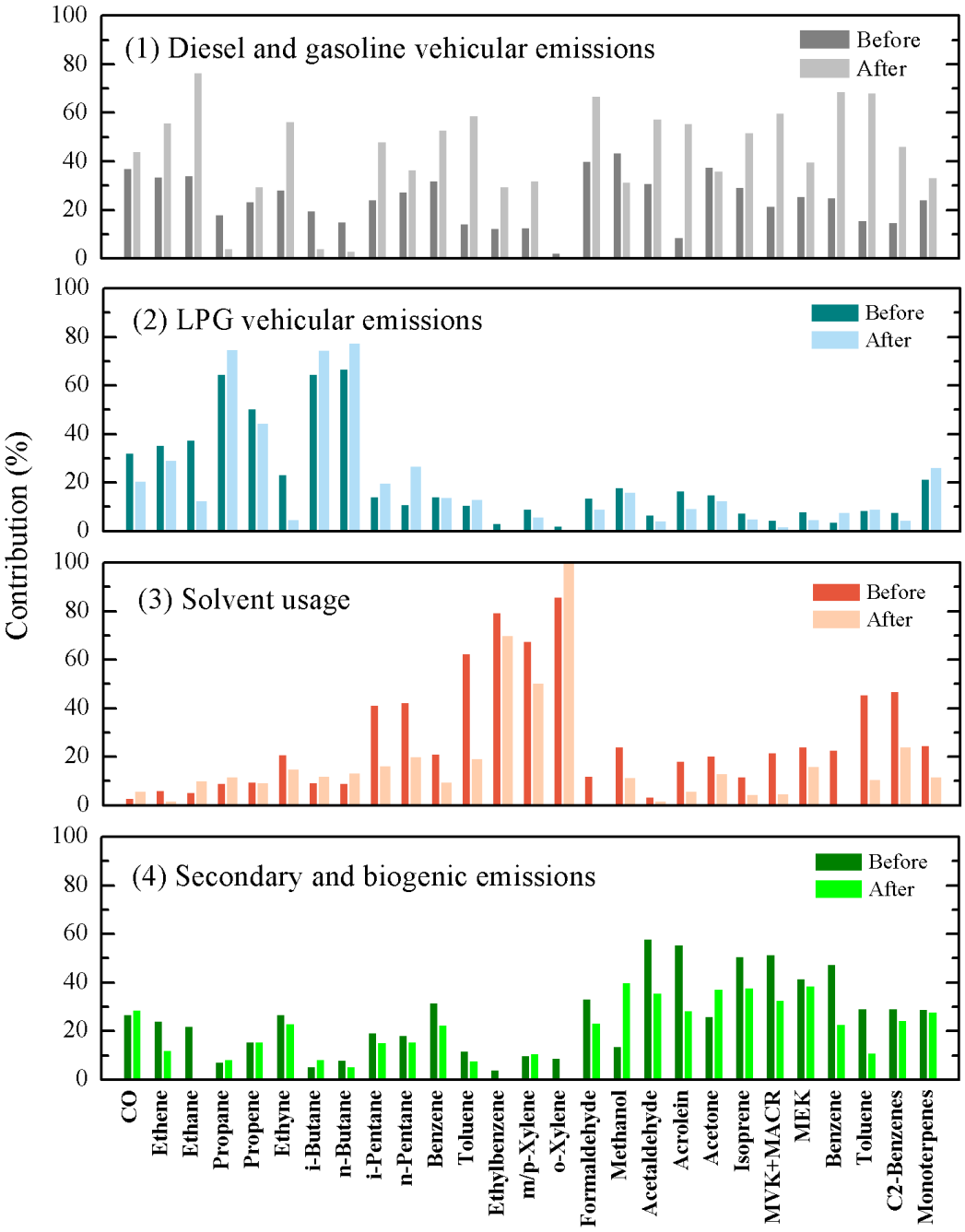

Figure 5.3 Factor profiles (% of species) for VOCs before and after LPG CCRP.

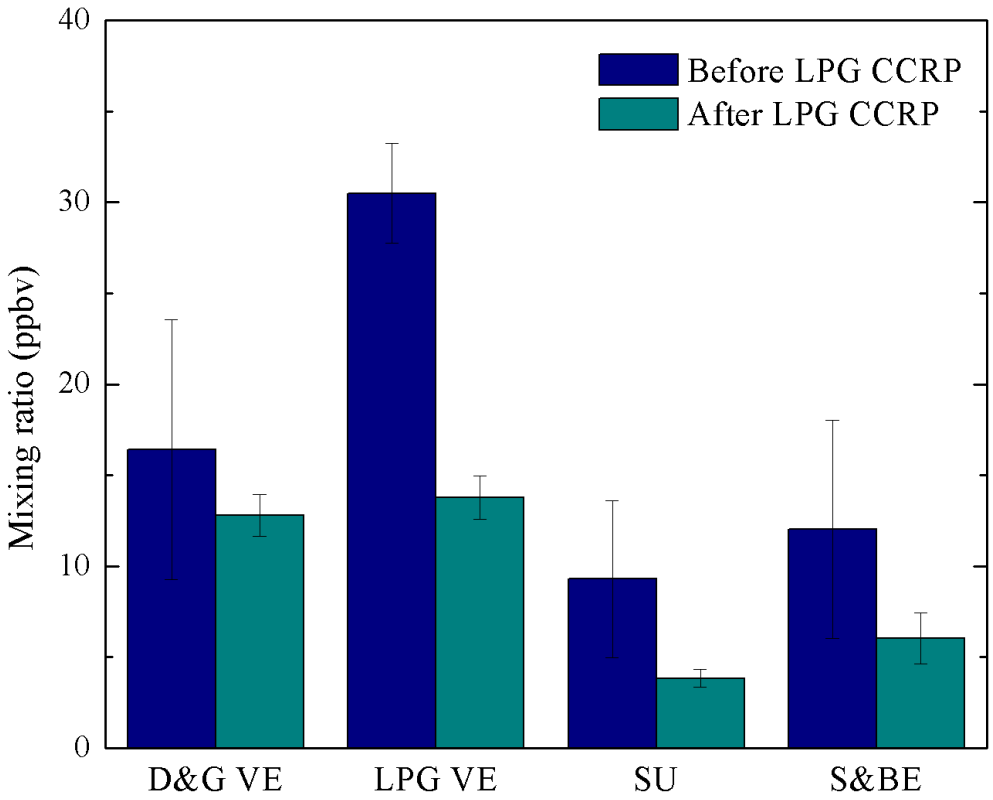

Figure 5.4 Mixing ratios of VOCs from different sources at MK AQMS before and after the LPG CCRP.

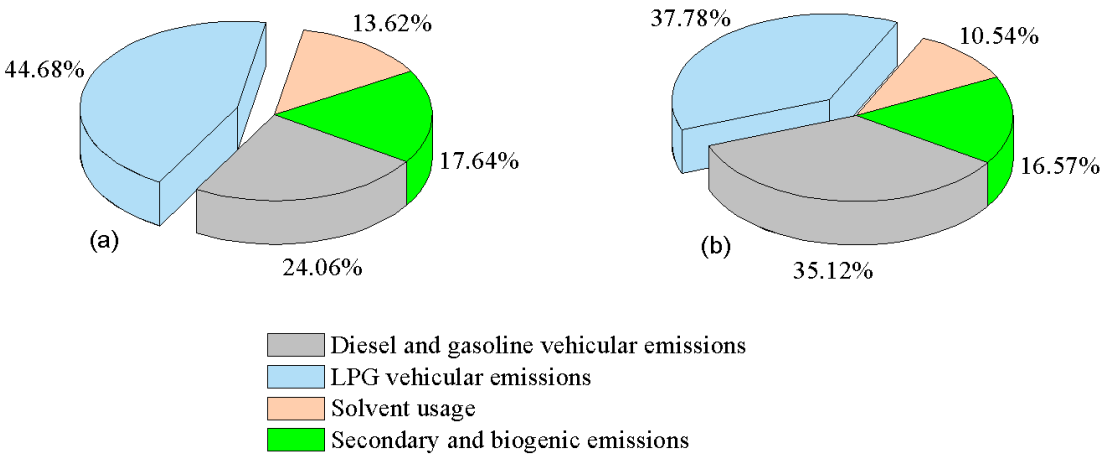

Figure 5.5 Source contributions of each factor to total VOCs at MK AQMS (a) before and (b) after the LPG CCRP.

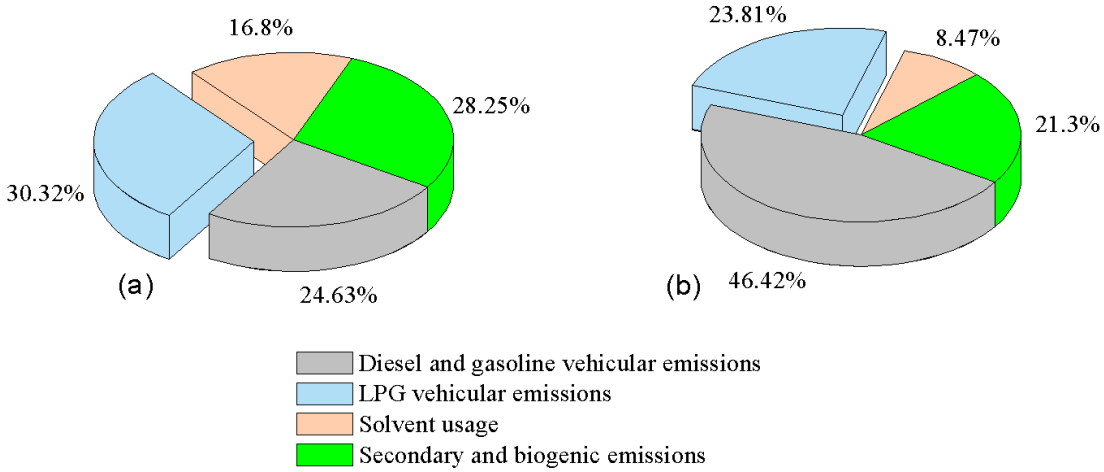

Figure 5.6 Contributions to OFPs from different VOCs emission sources (a) before and (b) after the LPG CCRP based on PMF results.

Chapter 6 Decrease of VOC Emissions from Vehicular Emissions in Hong Kong from a Tunnel Study

6.1 Introduction

VOCs which can be primarily emitted from natural or anthropogenic sources (Atkinson and Arey, 2003; Watson et al., 2001), are important precursors of ground level ozone formation and have adverse effects on human health (Sillman, 2002; von Schneidemesser et al., 2010). Vehicular emission is one of major anthropogenic sources of ambient VOCs in Hong Kong. In 2002–2003, vehicle- and marine vessel-related sources contributed 31–48% of ambient VOC concentrations in Hong Kong, and this contribution increased to 40–54% in 2006–2007 (Lau et al., 2010). Moreover, traffic-related sources including vehicle exhaust, gasoline evaporation and LPG usage contributed 30–60% of ambient VOCs in Hong Kong from 2005 to 2013 through a multi-year study in Hong Kong (Ou et al., 2015).

Over the past twelve years, a series of air pollution control strategies have been undertaken by HKSARG to reduce vehicular emissions in Hong Kong. These measures mainly include: (1) tightening vehicle emission standards, (2) updating vehicle fuel standards, (3) switching diesel vehicles to liquefied petroleum gas (LPG) vehicles, and (4) retrofitting emission control devices (Lau et al., 2015). Euro 3 standard was used before 2003 in Hong Kong, and it was tightened to Euro 5 standard from 2012. Vehicle

fuel standard for diesel was ultra-low sulfur diesel (ULSD, 50 ppm of sulfur) before 2003 and it was updated to Euro 5 diesel standard (10 ppm of sulfur) from 2012. Gasoline fuel was also updated to Euro 5 gasoline standard from 2010. In order to control diesel vehicular emission, nearly 99% taxies were changed from diesel to LPG from August 2000 to the end of 2003. Light buses were also switched from diesel to LPG from August 2002, and about 65% light bus fleets used LPG in 2006. As a result, road transport VOC emissions in Hong Kong decreased gradually from 2003 (7,600 tonnes) to 2015 (4,800 tonnes) even the total vehicle kilometers traveled (VKT) in Hong Kong increased by 18.7% from 2003 to 2015.

Direct measurements in roadway tunnels is one of the methods to determine vehicular emission factors and profiles. Repeated measurements performed at the same tunnel can be used to assess the effectiveness of local vehicular emission control strategies and/or new technologies to reduce vehicular emissions (Stemmler et al., 2005). For instance, a tunnel study was conducted in Gubrist tunnel in Switzerland in 1993 and 2002, and it was found that the emission factors of particular VOCs significantly decreased after nine years, indicating the effectiveness of modern car fleets on reducing VOCs emissions (Staehelin et al., 1995; Stemmler et al., 2005). In Hong Kong, vehicular emission factors and profiles of different VOC groups (alkanes, alkenes, alkynes, aromatic hydrocarbons, and carbonyls) were obtained through a tunnel study in the Shing Mun Tunnel by our group in 2003 (Ho et al., 2009b; Ho et al., 2007). In this study, experiments were repeated in the Shing Mun tunnel in 2015 to evaluate the

vehicular emission reduction after 12 years in Hong Kong. Emission factors of individual VOCs are also updated in this study, which will be useful for speciated VOC inventories and related modelling studies.

6.2 Characteristics of traffic pattern and trace gas concentrations

About 99.7% of total on-road fleets in Hong Kong used the folowing three types of fules, namely LPG (3.1%), gasoline (77.3%) and diesel (19.3%), by the end of Mar 2015 (HKTD, 2015). Total vehicle fleets were classified into NDVs and DVs in this study.

Figure 6.1 shows time series of vehicle numbers, wind speed and CO, NO, and NO_2 concentrations at the outlet sampling site of Shing Mun tunnel during the campain in 2015. The total vehicle number cross the tunnel south bore ranged from 500 to 2300 veh h^{-1} during the daytime. Apparent double-peak pattern was found for the total vehicle number on weekdays, but the morning peak was not obvious on weekends. Moreover, the total vehicle number on weekdends was less than that on weekdays, beacuase there were much less DVs (e.g. sigle deck buses, double deck buses and goods vehicles) on weekends, while the total number of NDVs kept at a similar level both on weekdays and on weekends as shown in Figure 6.1. The average wind speed at the outlet of SM tunnel was about 4.2 m s^{-1}. It can be found that the wind speed maintained at relative stable high level (5.0 m s^{-1}) during the daytime and decreased in the evening when there

were less vehicles, and this is consitent with the study of Stemmler et al. (2005). Apparent double-peak pattern was also found for NDVs during weekdays with the same morning peak (around 8:00) and late afternoon peak (around 18:00) as total vehicle numbers, corresponding to the morning and afternoon rush hours. For DVs, the two peaks were smoother than NDVs' with a later morning peak (9:00 – 10:00) and earlier afternoon peak (15:00 – 16:00).

The temporal pattern of CO is similar to the NDV counts because spark-ignition vehicles have higher CO emission (Kean et al., 2003). NO_x ($NO + NO_2$) concentrations are influenced by both the larger number of NDVs with lower emission factors and the lower number of DVs with higher emission factors. Therefore, their diurnal variations have mixed contributions from NDVs and DVs (Ho et al., 2013; Huang et al., 2015; Wang et al., 2002). The absence of afternoon NO peak on some days could be resulted from the reaction with ozone.

6.3 Diurnal pattern of VOCs at the outlet site

Figure 6.2 shows the diurnal pattern of VOCs at the outlet site of SM tunnel. The highest concentration of total measured VOCs was found during 8:00–10:00 at 102.2 ppb. During 17:00–19:00, the concentration of total measured VOCs was 91.0 ppb. Relative lower levels for total measured VOCs were found during 11:00–13:00 and 14:00–16:00 at 75.4 ppb and 71.3 ppb, respectively. This pattern is consistent with the

diurnal pattern of total vehicle numbers, not only the two peaks occurred at the same periods, but also the morning peak was higher than the late afternoon peak.

The composition of different VOC groups at different sampling periods are plotted in Figure 6.2. Similar group abundances were found at different sampling periods, alkanes were the most abundant group, followed by carbonyls, alkenes, aromatic hydrocarbons and alkyne. Alkanes had much higher concentrations and abundances during 8:00–10:00 (45.71 ppb) and 17:00–19:00 (37.33 ppb) than the other two periods 11:00–13:00 (29.23 ppb) and 14:00–16:00 (27.73 ppb). Aromatic hydrocarbons had the similar diurnal pattern with alkanes, 11.48 ppb during 8:00–10:00, 8.94 ppb 17:00–19:00, 7.73 ppb during 11:00–13:00, and 6.09 ppb during 14:00–16:00. The traffic volume of NDV during the early morning peak (1277 veh h^{-1}) and late afternoon peak (1218 veh h^{-1}) were also much higher than the other two periods (760 - 780 veh h^{-1}). The much higher concentration of alkanes and aromatic hydrocarbons during early morning peak and late afternoon peak could be due to high traffic volume of NDV (about 70% of total vehicles) during these periods as well as NDV's high emission factors of alkanes (56.3 mg veh^{-1} km^{-1}) and aromatic hydrocarbons (12.5 mg veh^{-1} km^{-1}). In contrast, the carbonyl and alkene concentrations were very similar over the four sampling periods; the high volume of NDVs did not cause obviously higher alkene concentrations during 8:00–10:00 and 17:00–19:00. This is likely due to the relatively constant DV traffic volume over the four sampling periods (1325 veh h^{-1}, 1351 veh h^{-1}, 1365 veh h^{-1}, and 1160 veh h^{-1}, respectively) and higher carbonyl and alkene emission factors from DVs (33.85 mg

veh^{-1} km^{-1} for carbonyls, 9.8 mg veh^{-1} km^{-1} for alkenes) than NDVs (8.34 mg veh^{-1} km^{-1} for carbonyls, 8.9 mg veh^{-1} km^{-1} for alkenes).

6.4 Emissions of VOCs at Shing Mun tunnel from 2003 to 2015

In this study, 82 VOC species were quantified in the tunnel air samples. These include 27 C_2–C_{10} alkanes, 21 C_2–C_{10} alkenes, 1 alkyne, 17 aromatic hydrocarbons, and 16 carbonyls.

6.4.1 Concentrations of VOCs

The average concentrations and standard deviations of all the measured VOCs at the inlet and outlet sites of Shing Mun tunnel in 2015 are listed in Table 6.1. In 2015, the concentrations of total measured VOCs at the inlet site and outlet sites of the tunnel were 53.77 ppb, and 84.05 ppb, respectively. Among the 82 compounds, formaldehyde was the most abundant VOC, followed by n-butane, acetaldehyde, ethene, i-butane and propane. For both the inlet site and outlet site of Shing Mun tunnel in 2015, alkanes were the most abundant group with the percentage of 44.7% and 41.1%, respectively, followed by carbonyls (inlet: 22.2%, outlet: 27.7%), alkenes (inlet: 15.8%, outlet: 15.6%), aromatic hydrocarbons (inlet: 10.8%, outlet: 9.9%) and alkyne (inlet: 6.6%, outlet: 5.7%). The inlet and outlet relative contribution were similar indicating that vehicular emissions was the dominant VOC source at the both sampling locations (Ho

et al., 2009b). Net concentrations (average concentrations of outlet minus inlet concentrations for each pair of canister sample) of the measured VOCs are also listed in Table 6.1. For the net concentrations, formaldehyde was still the most abundant species with the value of 5.84 ± 0.94 ppb, followed by n-butane (3.74 ± 2.82 ppb), acetaldehyde (3.04 ± 0.72 ppb), ethene (2.96 ± 1.74 ppb), i-butane (2.56 ± 2.09 ppb), and propane (2.29 ± 1.44 ppb). This indicates that formaldehyde, n-butane, acetaldehyde, ethene, i-butane and propane have the highest emission rates in the vehicular emissions. Based on the net concentrations, the six most abundant species comprised about 67% of the total measured VOC emissions.

Table 6.1 also lists the average concentrations and standard deviations of all the measured VOCs at the inlet and outlet of Shing Mun tunnel in 2003 for comparison (Ho et al., 2009b; Ho et al., 2007). For individual VOC species, Figure 6.3 shows the net concentration of each compound in 2003 and 2015. The net concentration decreased from 2003 to 2015 for almost all measured VOCs. The net concentrations of formaldehyde and ethene, which were the most abundant two species in 2003, decreased by 56.0%, and 65.2% from 2003 to 2015, respectively. The net concentrations of ethyne, 1-butene, and 1-pentene, which are also marker species of diesel fleets exhaust, decreased by 57.1%, 55.7%, and 89.7%, respectively. However, the net concentrations of i-butane and n-butane, which are key components of LPG, were 50.9% and 33.4% higher in 2015 than in 2003, respectively. This should be due to that about 99.8% of taxies were changed from diesel to LPG from 2000 to 2004, and

more than 65% of public light buses were changed from diesel to LPG from 2002 to 2007 (Lau et al., 2015). Based on the licensed number of vehicles by fuel type from the Hong Kong Transport Department, the rate of adoption from diesel to LPG for public light buses increased from 7.5% before the 2003 study to 68.2% before the 2015 study, the rate of adoption from diesel to LPG for taxis increased from 93.4% before the 2003 study to 100% before the 2015 study. Moreover, one previous study at a roadside environment in Hong Kong found the ambient concentrations of propane, i-butane and n-butane increased from 2003 to 2011 with the percentages of 23%, 42%, and 61%, respectively (Huang et al., 2015), which was consistent with the increase of the net concentration of i-butane and n-butane in this study. However, the net concentration of propane, which is another key LPG component, decreased by 4.5% in this study. This may be resulted from the LPG catalytic converter replacement programme for LPG taxies and public light buses from 2013 to 2014 in Hong Kong.

The net concentration of total measured VOCs decreased by 43.4% from 2003 to 2015. For individual VOC groups, the net concentrations of alkanes, alkenes, alkyne, aromatic hydrocarbons, and carbonyls all decreased from 2003 to 2015 with the percentage of 10.8%, 64.9%, 57.1%, 63.3%, and 41.0%, respectively (as shown in Figure 6.5). The net concentration of alkanes did not decrease as significantly as the other groups because of the increase of i-butane and n-butane levels.

6.4.2 Emission factors of VOCs

The average emission factors of all measured VOCs are presented in Table 6.1. The emission factors of several VOCs were zero because their concentrations at the outlet site were less or equal to that at the outlet site. In 2015, n-butane, formaldehyde, acetaldehyde, toluene, i-butane, propane, and ethene had the highest emission factors of 10.2 ± 5.9 mg veh^{-1} km^{-1}, 8.1 ± 1.7 mg veh^{-1} km^{-1}, 6.2 ± 1.8 mg veh^{-1} km^{-1}, 5.8 ± 5.2 mg veh^{-1} km^{-1}, 7.3 ± 4.5 mg veh^{-1} km^{-1}, 4.8 ± 2.4 mg veh^{-1} km^{-1}, and 4.2 ± 2.0 mg veh^{-1} km^{-1}, respectively. In contrast, the five most abundant VOC species for emission factor in 2003, in decreasing order were: formaldehyde (18.8 ± 7.5 mg veh^{-1} km^{-1}), ethene (13.0 ± 4.0 mg veh^{-1} km^{-1}), toluene (12.0 ± 3.9 mg veh^{-1} km^{-1}), n-butane (8.7 ± 3.1 mg veh^{-1} km^{-1}), propane (5.7 ± 2.5 mg veh^{-1} km^{-1}), i-pentane (5.6 ± 2.1 mg veh^{-1} km^{-1}), and acetaldehyde (5.5 ± 2.2 mg veh^{-1} km^{-1}), respectively.

Figure 6.4 compares the emission factors of individual VOCs in 2003 and 2015. The emission factors decreased from 2003 to 2015 for almost all measured VOCs. Formaldehyde, which was the most abundant specie in vehicle emissions in 2003, its emission factor decreased by 57.1% to 2015. As one of the key tracers for diesel vehicular emissions, ethene had the second highest emission factor in 2003, and its emission factor decreased by 67.3% from 2003 to 2015. However, the emission factors of i-butane and n-butane increased from 2003 to 2015 by 32.1% and 17.2%, respectively, while the magnitude of change of their emission factors were much lower

than their net concentrations.

Because of the series of air pollution control measures, the total vehicular emission factors of measured VOCs decreased from 142.8 ± 64.5 mg veh^{-1} km^{-1} in 2003 to 81.0 ± 57.3 mg veh^{-1} km^{-1} in 2015 as shown in Figure 6.5. The emission factor of alkenes decrease the most among the five groups with the percentage of 66.3%, followed by alkyne (61.4%), aromatic hydrocarbons (57.0%), carbonyls (37.8%), and alkanes (21.2%).

6.5 Reconstructed emission factor for NDVs and DVs

The reconstructed emission factors of individual VOCs for NDVs, and DVs based on the MLR method are presented in Table 6.2. The top 4 species of EF_{NDV} were n-butane (18.7 ± 3.9 mg veh^{-1} km^{-1}), i-butane (13.4 ± 3.0 mg veh^{-1} km^{-1}), propane (7.9 ± 1.6 mg veh^{-1} km^{-1}), and i-pentane (4.8 ± 1.1 mg veh^{-1} km^{-1}), respectively. Among the four species, n-butane, i-butane, and propane are major tracers of LPG vehicular emissions (Ling et al., 2011; Liu et al., 2008b; Ou et al., 2015), and i-pentane is one of major tracers of gasoline vehicular emissions (Liu et al., 2008a; Tsai et al., 2006). Figure 6.6 shows the EF_{NDV} and EF_{DV} of specific VOC species in 2003 and 2015. Even though n-butane, i-butane, propane, and i-pentane had the highest EF_{NDV} in 2015, EF_{NDV} of n-butane, i-butane, propane, and i-pentane decreased by 62.3%, 60.6%, 78.4%, and 61.0%, respectively, from 2003 to 2015. The large decrease of EF_{NDV} of these LPG tracers

could be due to the effectiveness of reducing LPG vehicle emissions by the LPG catalytic converter replacement programme even though the total LPG vehicle fleets significantly increased during the past twelve years in Hong Kong. The top five species of EF_{DV} were formaldehyde (13.1 ± 1.3 mg veh^{-1} km^{-1}), acetaldehyde (9.6 ± 1.3 mg veh^{-1} km^{-1}), toluene (8.3 ± 5.6 mg veh^{-1} km^{-1}), ethene (6.0 ± 2.1 mg veh^{-1} km^{-1}), and acetone (4.2 ± 1.0 mg veh^{-1} km^{-1}), respectively. As one of the key tracers of diesel vehicular emissions, ethene had the highest EF_{DV} (25.70 ± 2.62 mg veh^{-1} km^{-1}) in 2003, but the EF_{DV} of ethene has been decreased to 6.0 ± 2.1 mg veh^{-1} km^{-1} (by 76.8%) in 2015. The large decrease of EF_{NDV} and EF_{DV} for these key tracers of LPG, gasoline and diesel demonstrates the effectiveness air pollution control measures in Hong Kong from 2003 to 2015.

6.6 Ozone formation potential of VOCs

MIR method (Carter, 1994) was applied to evaluate the contribution of VOCs from vehicular emissions to OFP in Hong Kong. The top ten species with the highest OFP from vehicular emission in 2003 and 2015 are listed in Table 6.3. Formaldehyde contributed the most to OFP of the measured VOCs in both 2003 (23.9%) and 2015 (22.5%). Due to the large decrease of diesel vehicular emissions, OFP of ethene decreased from 113.9 mgO_3 veh^{-1} km^{-1} in 2003 to 37.2 mgO_3 veh^{-1} km^{-1} in 2015. n-Butane and i-butane, which were in top ten list of OFP in 2015, were not major contributors to total OFP in 2003, because of the increase of their concentrations in

2015 and the decrease of other species as explained before. The total OFP of measured VOCs decreased by 54.5% from 726.0 mg O_3 veh^{-1} km^{-1} to 330.3 mg O_3 veh^{-1} km^{-1} during the past 12 years (shown in Figure 6.7). The contributions of different groups to total OFP in 2003 and 2015 are also shown in Figure 6.7. The contributions by VOC groups to total OFP were different in 2003 and 2015 with the large decrease of alkenes' contribution from 35.0% in 2003 to 24.4% in 2015, and carbonyls became the first contributor in 2015 with the percentage of 37.4%. However, alkenes and hydrocarbon aromatics were always the two major contributors to total OFP from vehicular emissions in Hong Kong in both 2003 and 2015.

6.7 Estimation of road transport VOC emission factor in Hong Kong

From Hong Kong Environmental Protection Department (EPD)'s emission inventory results, total VOC emissions from road transport in Hong Kong was reduced by 36.8% from 2003 (7,600 tonnes) to 2015 (4,800 tonnes) (HKEPD, 2017). A linear trend analysis in Figure 6.8 (a) shows that the annual reduction of road transport VOC emission in Hong Kong was -234 tonnes per year (r^2 = 0.97). Figure 6.8 (b) shows that the annual total VKT in Hong Kong has been linearly increasing at a rate of 1.73×10^8 veh km per year (r^2 = 0.94) (*http://www.td.gov.hk/*). Road transport VOC emission factor of the entire Hong Kong vehicle fleet can be obtained through total VOC emissions from road transport and VKT data based on following equation.

$$EF = \frac{RTVE \times 10^9}{VKT} \qquad (6.1)$$

where EF is emission factor, mg veh^{-1} km^{-1}; RTVE is road transport vehicle emission, tonnes; VKT is vehicle kilometers traveled, veh km.

Total road transport VOC emission factor in Hong Kong from 2003 to 2020 is plotted in Figure 6.9. The total road transport VOC emission factor in Hong Kong from 2016 to 2020 is estimated by the linear regression in Figure 6.8 and equation 6.1. It can be found that total road transport VOC emission factor in Hong Kong decreased by 46.8% from 2003 (679.2 mg veh^{-1} km^{-1}) to 2015 (361.2 mg veh^{-1} km^{-1}). Meanwhile, from the tunnel results in this study, the emission factor of total measured VOCs decreased from 142.8 ± 64.5 mg veh^{-1} km^{-1} in 2003 to 81.0 ± 57.3 mg veh^{-1} km^{-1} in 2015 with the percentage of 43.3%. The decrease percentage was comparable between simulation result (46.8%) and tunnel experiment result (43.3%). However, the estimated total road transport VOC EF in Hong Kong is about 5 times of tunnel experiment result. It should be pointed out that, the tunnel experiments only provide the EFs of vehicles under the tunnel conditions: warmed up engines and cruising speed mostly in the range 60–70 km h^{-1}, while on-road vehicles have a larger varieties of driving conditions including cold starts and stop-and-go. It has been reported that the lower vehicle speed, the higher VOC EFs (Int Panis et al., 2006; Kean et al., 2003). Guo et al. (2011b) reported that the total VOC EFs of gasoline and LPG vehicles under idle state were more than 10 times of that under 70 km h^{-1} in Hong Kong. Considering the huge traffic density in Hong Kong, the average vehicle speed should be less than 60–70 km h^{-1}, which can explain

the 5 times difference between entire fleet estimation and tunnel experiment results. To 2020, the total road transport VOC emission and emission factor is estimated to be 3,803 tonnes, and 279.6 mg veh^{-1} km^{-1}, respectively. Hong Kong committed to reduce total VOC emissions by at least 15% by 2020 as compared to 2010, as part of an emission reduction plan for the PRD region. Assuming the emission trend will remain as found in this study, it is estimated that road transport VOC emission, one of the major sources of VOCs in Hong Kong, can be reduced by 40% from the 2010 level by 2020. Therefore, the reduction of road transport VOC emissions will be a driving contributor for achieving the goal of total VOC reduction in Hong Kong.

6.8 Chapter summary

This study characterized the real-world VOC emissions from on-road vehicles in Hong Kong through a repeated measurements performed at the same tunnel in 2015. Emission profiles and emission factors of VOCs were identified in this study. The temporal patterns of traffic and pollutant concentrations were examined to illustrate the correlations between fleet components and pollutants.

Large decrease of VOC emissions from on-road vehicles was found in Hong Kong from 2003 to 2015 with the total measured VOC emission factor decreased from 142.8 ± 64.5 mg veh^{-1} km^{-1} in 2003 to 81.0 ± 57.3 mg veh^{-1} km^{-1} in 2015. The emission factor of ethene decreased by 67.3% from 2003 to 2015 as a result of diesel vehicular emissions

controls over the past twelve years in Hong Kong. The total OFP of measured VOCs decreased by 54.5% from 2003 (726.0 mgO_3 veh^{-1} km^{-1}) to 2015 (330.3 mgO_3 veh^{-1} km^{-1}). Carbonyls, especially for formaldehyde and acetaldehyde, also contributed a lot to the total VOC mixing ratio and OFP.

Emission factors of individual VOCs were reconstructed in this study. The large decrease of EF_{DV} for ethane and ethyne, and EF_{NDV} for n-butane, i-butane, propane, and i-pentane demonstrated the effectiveness of the series of air pollution control measures conducted by local government during the past years. Total road transport VOC emission has been reduced by more than 36.8% from 2003 to 2015, also demonstrating the effectiveness of air pollution control strategies in Hong Kong. To 2020, total road transport VOC emissions is estimated can be reduced by 40% as compared with 2010, which will help achieve total VOC emission reduction goal set by the emission reduction plan for the PRD region.

Table 6.1 Concentrations and emission factors of VOCs at SM tunnel in 2003 and 2015

VOCs	SMT 2015 (this study)				SMT 2003 (Ho et al., 2009b; Ho et al., 2007)			
	Mixing ratio (ppbv)			Emission Factor	Mixing ratio (ppbv)			Emission Factor
	Inlet	Outlet	Outlet minus inlet	(mg/veh/km)	Inlet	Outlet	Outlet minus inlet	(mg/veh/km)
Alkane								
ethane	3.31±0.87	3.86±0.95	0.55±0.72	0.8±1.1	4.4±1.5	5.5±1.8	1.1±0.55	1.7±0.6
propane	5.23±1.84	7.46±2.47	2.23±1.39	4.5±2.6	5.8±2.8	8.2±4	2.4±1.3	5.7±2.5
i-butane	4.6±2.27	7.28±3	2.68±1.96	7±4.9	3.5±1.8	5.3±2.6	1.7±0.9	5.5±2.2
n-butane	6.1±2.52	9.84±4.17	3.74±2.82	10±6.5	5.7±2.5	8.5±3.7	2.8±1.3	8.7±3.1
i-pentane	1.42±0.72	2.16±0.96	0.74±0.58	2.5±1.9	3.2±1.1	4.6±1.6	1.5±0.66	5.6±2.1
n-pentane	0.52±0.32	0.85±0.61	0.33±0.53	1.1±1.9	0.98±0.31	1.4±0.48	0.45±0.21	1.7±0.6
2,2-dimethyl-butane	0.04±0.02	0.06±0.03	0.02±0.02	0.1±0.1	0.1±0.04	0.13±0.05	0.03±0.05	0.2±0.2
cyclopentane	0.05±0.03	0.07±0.03	0.01±0.04	-0.1±0.4	0.53±0.21	0.81±0.34	0.29±0.15	1±0.4
2,3-dimethylbutane	0.08±0.05	0.14±0.11	0.06±0.11	0.3±0.5	0.14±0.06	0.2±0.09	0.06±0.05	0.3±0.2
2-methylpentane	0.25±0.16	0.41±0.21	0.15±0.12	0.6±0.5	0.94±0.33	1.3±0.47	0.4±0.21	1.8±0.7
3-methylpentane	0.17±0.11	0.25±0.14	0.08±0.06	0.3±0.3	0.67±0.22	0.94±0.31	0.27±0.14	1.2±0.5
n-hexane	0.8±0.73	0.96±0.75	0.16±0.52	0.5±1.9	0.68±0.27	0.98±0.41	0.3±0.2	1.3±0.5
methyl-cyclopentane	0.1±0.06	0.15±0.07	0.06±0.05	0.2±0.2	0.32±0.11	0.47±0.17	0.15±0.07	0.7±0.2
2,4-dimethylpentane	0.03±0.02	0.06±0.03	0.02±0.02	0.1±0.1	0.07±0.03	0.11±0.04	0.03±0.02	0.2±0.1
cyclohexane	0.09±0.08	0.14±0.09	0.04±0.05	0.2±0.2	0.18±0.09	0.24±0.1	0.06±0.04	0.3±0.1
2-methyl-hexane	0.07±0.05	0.1±0.06	0.03±0.03	0.1±0.1	0.39±0.34	0.48±0.18	0.09±0.29	0.7±0.3
2,3-dimethyl-pentane	0.04±0.02	0.06±0.03	0.02±0.02	0.1±0.1	0.07±0.04	0.12±0.07	0.05±0.04	0.3±0.2
3-methyl-hexane	0.14±0.1	0.17±0.1	0.04±0.07	0.2±0.3	0.1±0.03	0.14±0.04	0.04±0.02	0.2±0.1
2,2,4-trimethyl-pentane	0.15±0.07	0.26±0.13	0.11±0.08	0.6±0.5	0.35±0.28	0.49±0.33	0.14±0.25	1±0.7
n-heptane	0.08±0.05	0.12±0.07	0.04±0.04	0.2±0.2	0.43±0.46	0.53±0.2	0.1±0.39	0.9±0.4

methyl-cyclohexane	0.07±0.04	0.1±0.06	0.03±0.04	0.2±0.2	0.22±0.17	0.28±0.11	0.06±0.13	0.4±0.2
2,3,4-trimethyl-pentane	0.05±0.03	0.09±0.05	0.04±0.03	0.2±0.2	0.09±0.05	0.13±0.09	0.04±0.05	0.2±0.2
2-methyl-heptane	0.02±0.01	0.03±0.02	0.01±0.02	0±0.1	0.39±0.34	0.48±0.18	0.09±0.29	0.7±0.3
3-methyl-heptane	0.01±0.01	0.02±0.01	0.01±0.02	0±0.1	0.49±0.76	0.49±0.18	0±0.72	0.8±0.3
n-octane	0.03±0.02	0.04±0.03	0.02±0.03	0.1±0.2	0.15±0.05	0.23±0.08	0.08±0.04	0.5±0.2
n-nonane	0.07±0.07	0.15±0.14	0.08±0.1	0.5±0.7	0.14±0.08	0.24±0.11	0.1±0.05	0.7±0.4
n-decane	0.15±0.11	0.25±0.14	0.1±0.1	0.6±0.6	0.14±0.1	0.25±0.12	0.1±0.07	0.8±0.6
Alkene								
ethene	5.63±1.46	8.66±1.95	2.97±1.72	4.1±2.3	16±4.2	25±7.1	8.5±3.4	13±4
propene	1.62±0.44	2.57±0.66	0.96±0.46	1.9±0.9	4.5±1.1	6.9±1.9	2.4±0.9	5.3±1.5
1-butene	0.56±0.25	0.93±0.43	0.37±0.41	1±1.2	1.7±0.51	2.6±0.85	0.84±0.56	2.5±1.3
1,3-butadiene	0.07±0.08	0.11±0.18	0.05±0.18	0.1±0.5	0.41±0.39	0.36±0.34	-0.05±0.36	0.3±0.6
trans-2-butene	0.07±0.03	0.11±0.04	0.05±0.03	0.1±0.1	0.4±0.13	0.62±0.21	0.22±0.09	0.6±0.2
cis-2-Butene	0.06±0.02	0.1±0.04	0.04±0.02	0.1±0.1	0.29±0.1	0.45±0.16	0.16±0.06	0.5±0.1
3-methyl-1-butene	0.02±0.01	0.04±0.02	0.02±0.01	0.1±0	0.11±0.03	0.17±0.05	0.06±0.02	0.2±0.1
1-pentene	0.08±0.03	0.13±0.05	0.05±0.04	0.2±0.2	0.46±0.34	0.95±0.75	0.5±0.55	1.9±2.1
2-methyl-1-butene	0.06±0.02	0.1±0.05	0.04±0.03	0.1±0.1	0.21±0.08	0.33±0.13	0.12±0.05	0.5±0.2
isoprene	0.07±0.05	0.09±0.08	0.02±0.08	0.1±0.3	0.16±0.34	0.06±0.06	-0.11±0.36	0±0
trans-2-pentene	0.06±0.03	0.11±0.05	0.05±0.03	0.2±0.1	0.27±0.1	0.44±0.17	0.16±0.07	0.6±0.2
cis-2-pentene	0.03±0.01	0.05±0.02	0.02±0.02	0.1±0.1	N.A.	N.A.	N.A.	N.A.
2-methyl-2-butene	0.06±0.02	0.1±0.05	0.04±0.04	0.1±0.1	0.26±0.18	0.4±0.24	0.14±0.13	0.6±0.4
cyclopentene	0.02±0.01	0.04±0.02	0.02±0.01	0.1±0	N.A.	N.A.	N.A.	N.A.
4-methyl-1-pentene	0.02±0.01	0.04±0.02	0.02±0.02	0.1±0.1	0.09±0.03	0.17±0.06	0.07±0.04	0.3±0.1
1-hexene	0.04±0.02	0.07±0.03	0.03±0.03	0.1±0.1	0.13±0.06	0.21±0.11	0.09±0.07	0.4±0.3
trans-2-hexene	0.01±0.01	0.02±0.01	0±0.01	0±0	0.08±0.03	0.14±0.05	0.06±0.02	0.2±0.1
cis-2-hexene	0.01±0	0.01±0.01	0.01±0.01	0±0	0.04±0.02	0.07±0.03	0.03±0.01	0.1±0

3-hexene	0.02±0	0.02±0.01	0±0.01	0±0	0.06±0.02	0.08±0.03	0.03±0.02	0.1±0
α-pinene	0.02±0.01	0.03±0.03	0.02±0.03	0.1±0.2	0.01±0.01	0.01±0.01	0±0.01	0±0
β-pinene	0.01±0.01	0.02±0.03	-0.01±0.01	-0.1±0.1	0.01±0	0.01±0	0±0	0±0
Alkyne								
ethyne	3.53±1.07	4.81±1.41	1.28±0.88	1.5±1.1	7.4±1.8	10±2.6	3±1.3	4±1.3
Aromatic hydrocarbon								
benzene	0.78±0.29	1.16±0.38	0.38±0.25	1.4±0.9	2.5±0.62	3.5±0.92	1.1±0.38	4.5±0.9
toluene	2.25±1.54	4.14±3.04	1.89±2.15	8.6±10.3	6.1±2	8.7±2.8	2.5±1.2	12±3.9
ethyl-benzene	0.29±0.27	0.47±0.56	0.18±0.39	0.7±1.6	0.59±0.21	0.82±0.27	0.24±0.11	1.3±0.4
m/p-xylene	0.55±0.94	1.39±2.51	0.84±1.94	3.4±8.6	1.45±0.46	2.16±0.71	0.67±0.33	3.7±1.3
o-xylene	0.04±0.05	0.08±0.13	0.04±0.1	0.2±0.5	0.64±0.18	0.94±0.31	0.29±0.16	1.6±0.6
styrene	0.28±0.44	0.49±0.75	0.21±0.58	1±2.5	N.A.	N.A.	N.A.	N.A.
isopropylbenzene	0.02±0.02	0.04±0.06	0.02±0.05	0.2±0.4	0.03±0.01	0.05±0.02	0.02±0.01	0.1±0.1
n-propylbenzene	0.03±0.02	0.05±0.04	0.02±0.03	0.1±0.2	0.12±0.04	0.2±0.06	0.07±0.04	0.5±0.2
m-ethyltoluene	0.07±0.06	0.15±0.16	0.08±0.12	0.5±0.7	0.32±0.13	0.53±0.2	0.21±0.18	1.4±0.9
p-ethyltoluene	0.03±0.02	0.07±0.08	0.04±0.07	0.3±0.5	0.13±0.06	0.27±0.23	0.13±0.21	0.7±0.8
1,3,5-trimethyl-benzene	0.03±0.02	0.06±0.04	0.03±0.03	0.2±0.2	0.18±0.07	0.3±0.09	0.12±0.07	0.8±0.4
o-ethyltoluene	0.03±0.02	0.06±0.05	0.03±0.03	0.2±0.2	0.21±0.1	0.38±0.14	0.17±0.14	1±0.7
1,2,4-trimethylbenzene	0.12±0.11	0.29±0.25	0.16±0.17	1±1.1	0.72±0.4	1.2±0.46	0.48±0.46	3±2.4
1,2,3-trimethylbenzene	0.04±0.03	0.07±0.06	0.03±0.04	0.2±0.2	0.28±0.15	0.48±0.19	0.25±0.34	1.4±1.1
m-diethylbenzene	0.01±0	0.01±0.01	0.01±0	0±0	0.03±0.02	0.05±0.02	0.03±0.03	0.2±0.2
p-diethylbenzene	0.01±0.01	0.02±0.02	0.01±0.02	0.1±0.1	0.07±0.06	0.15±0.07	0.08±0.08	0.6±0.4
o-diethylbenzene	0.01±0	0.01±0.02	0±0	0±0	0.02±0.01	0.03±0.01	0.01±0.01	0.1±0.1
Carbonyl								
formaldehyde	6.4±1.03	12.23±1.96	5.84±0.94	8.06±1.65	18.64±5.72	31.9±10.19	13.26±4.52	18.8±7.5
acetaldehyde	2.73±0.64	5.77±1.36	3.04±0.72	6.19±1.77	3.84±1.41	6.55±2.43	2.71±1.21	5.5±2.2

acetone	1.22±0.36	2.02±0.6	0.8±0.24	2.15±0.7	1.03±0.81	2.06±1.5	1.03±0.75	2.9±2.1
acrolein	0.15±0.04	0.35±0.08	0.2±0.05	0.5±0.09	0.13±0.13	0.31±0.18	0.18±0.12	0.4±0.3
propionaldehyde	0.27±0.07	0.45±0.11	0.18±0.04	0.47±0.13	0.26±0.17	0.47±0.26	0.21±0.19	0.6±0.5
crotonaldehyde	0.22±0.05	0.48±0.1	0.26±0.06	0.84±0.2	0.92±0.43	1.63±0.71	0.71±0.48	2.5±1.9
methyl ethyl ketone	0.2±0.11	0.56±0.29	0.35±0.18	1.17±0.62	0.31±0.28	0.62±0.41	0.31±0.23	1.1±0.9
iso-+n-butyraldehyde	0.18±0.05	0.4±0.11	0.22±0.06	0.75±0.25	0.21±0.17	0.41±0.31	0.21±0.16	0.8±0.9
benzaldehyde	0.14±0.03	0.26±0.07	0.12±0.03	0.59±0.17	0.35±0.16	0.54±0.21	0.19±0.05	1±0.7
iso-valeraldehyde	0.16±0.05	0.31±0.1	0.15±0.05	0.59±0.2	0.35±0.2	0.52±0.32	0.17±0.21	0.8±0.9
n-valeraldehyde	0.1±0.04	0.15±0.06	0.05±0.02	0.2±0.08	0.12±0.14	0.17±0.17	0.06±0.11	0.3±0.4
o-tolualdehyde	N.A.	N.A.	N.A.	N.A.	0.02±0.04	0.06±0.06	0.04±0.03	0.1±0.3
m-tolualdehyde	0.03±0.02	0.05±0.03	0.02±0.01	0.11±0.08	0.02±0.04	0.05±0.06	0.03±0.03	0.2±0.3
p-tolualdehyde	0.01±0.01	0.03±0.06	0.03±0.05	0.15±0.28	0.02±0.04	0.05±0.06	0.03±0.03	0.15±0.3
n-hexaldehyde	0.12±0.05	0.19±0.07	0.07±0.03	0.32±0.13	0.07±0.07	0.15±0.07	0.07±0.07	0.44±0.3
2,5-dimethylbenzaldehyde	0.02±0.02	0.04±0.06	0.02±0.04	0.15±0.22	0±0.02	0.04±0.04	0.04±0.02	0.14±0.2

* N.A. – not available

Table 6.2 EF_{NDV} and EF_{DV} of VOCs at Shing Mun tunnel in 2015

VOCs	EF_{NDV}		EF_{DV}		r^2
	avg	s.d.	avg	s.d.	
Alkane					
ethane	0.79	0.55	1.35	0.84	0.62
propane	7.91	1.58	0.00	2.41	0.82
i-butane	13.43	2.97	0.00	4.50	0.74
n-butane	18.69	3.87	0.00	5.86	0.77
i-pentane	4.80	1.13	0.00	1.73	0.71
n-pentane	0.71	1.29	2.09	1.95	0.29
2,2-dimethyl-butane	N.A.	N.A.	N.A.	N.A.	N.A.
cyclopentane	0.14	0.68	0.42	1.08	0.02
2,3-dimethylbutane	N.A.	N.A.	N.A.	N.A.	N.A.
2-methylpentane	0.88	0.30	0.15	0.46	0.64
3-methylpentane	0.47	0.17	0.12	0.26	0.65
n-hexane	3.40	1.22	0.00	1.83	0.43
methyl-cyclopentane	0.24	0.14	0.22	0.21	0.56
2,4-dimethylpentane	N.A.	N.A.	N.A.	N.A.	N.A.
cyclohexane	0.10	0.14	0.33	0.20	0.50
2-methyl-hexane	0.15	0.09	0.17	0.13	0.61
2,3-dimethyl-pentane	N.A.	N.A.	N.A.	N.A.	N.A.
3-methyl-hexane	0.22	0.19	0.38	0.30	0.55
2,2,4-trimethyl-pentane	N.A.	N.A.	N.A.	N.A.	N.A.
n-heptane	0.35	0.17	0.02	0.26	0.49
methyl-cyclohexane	0.11	0.13	0.30	0.19	0.51
2,3,4-trimethyl-pentane	N.A.	N.A.	N.A.	N.A.	N.A.
2-methyl-heptane	0.20	0.07	0.00	0.12	0.39
3-methyl-heptane	0.14	0.07	0.00	0.10	0.35
n-octane	0.34	0.14	0.00	0.21	0.30
n-nonane	0.31	0.52	1.02	0.76	0.40
n-decane	2.93	1.06	0.00	1.57	0.36
Alkene					
ethene	3.11	1.41	5.97	2.10	0.82
propene	2.20	0.61	1.35	0.92	0.81
1-butene	1.05	0.85	1.36	1.29	0.50
1,3-butadiene	N.A.	N.A.	N.A.	N.A.	N.A.
trans-2-butene	0.15	0.05	0.11	0.07	0.79
cis-2-Butene	0.15	0.04	0.03	0.06	0.77
3-methyl-1-butene	0.08	0.03	0.01	0.04	0.65
1-pentene	0.14	0.09	0.26	0.13	0.67
2-methyl-1-butene	0.21	0.06	0.05	0.09	0.71
isoprene	0.11	0.23	0.23	0.34	0.31

trans-2-pentene	0.27	0.06	0.00	0.10	0.73
cis-2-pentene	0.17	0.04	0.00	0.06	0.70
2-methyl-2-butene	0.28	0.07	0.00	0.11	0.67
cyclopentene	0.06	0.03	0.06	0.04	0.68
4-methyl-1-pentene	0.02	0.07	0.20	0.11	0.48
1-hexene	0.15	0.09	0.10	0.14	0.51
trans-2-hexene	0.01	0.02	0.04	0.04	0.29
cis-2-hexene	0.04	0.01	0.00	0.02	0.60
3-hexene	0.08	0.03	0.00	0.04	0.32
a-pinene	0.42	0.15	0.00	0.21	0.38
b-pinene	0.18	0.09	0.00	0.14	0.08
Alkyne					
ethyne	1.39	0.68	1.78	1.02	0.71
Aromatic hydrocarbon					
benzene	1.20	0.61	1.62	0.92	0.70
toluene	4.12	3.69	8.31	5.56	0.54
ethyl-benzene	0.89	1.48	1.44	2.36	0.21
m/p-xylene	3.61	3.30	0.00	5.22	0.10
o-xylene	0.47	0.42	0.09	0.63	0.25
styrene	0.54	1.72	1.84	2.70	0.13
isopropylbenzene	0.01	0.27	0.44	0.39	0.17
n-propylbenzene	0.31	0.15	0.00	0.22	0.39
m-ethyltoluene	0.51	0.49	0.52	0.74	0.32
p-ethyltoluene	0.16	0.34	0.49	0.53	0.24
1,3,5-trimethyl-benzene	N.A.	N.A.	N.A.	N.A.	N.A.
o-ethyltoluene	0.28	0.16	0.09	0.24	0.44
1,2,4-trimethylbenzene	N.A.	N.A.	N.A.	N.A.	N.A.
1,2,3-trimethylbenzene	N.A.	N.A.	N.A.	N.A.	N.A.
m-diethylbenzene	0.13	0.06	0.00	0.09	0.17
p-diethylbenzene	0.17	0.07	0.00	0.10	0.45
o-diethylbenzene	0.13	0.06	0.00	0.10	0.15
Carbonyl					
formaldehyde	2.21	1.00	13.07	1.25	0.97
acetaldehyde	1.12	1.07	9.56	1.33	0.94
acetone	1.55	0.76	4.16	0.95	0.91
acrolein	0.61	0.08	0.36	0.09	0.97
propionaldehyde	0.29	0.17	0.80	0.21	0.88
crotonaldehyde	0.33	0.20	1.07	0.24	0.95
methyl ethyl ketone	0.79	0.43	1.09	0.54	0.77
iso-+n-butyraldehyde	0.26	0.19	1.18	0.24	0.91
benzaldehyde	0.23	0.11	0.71	0.13	0.93
iso-valeraldehyde	0.33	0.12	0.49	0.15	0.89
n-valeraldehyde	0.13	0.07	0.29	0.09	0.86
o-tolualdehyde	N.A.	N.A.	N.A.	N.A.	N.A.

m-tolualdehyde	0.08	0.09	0.26	0.12	0.68
p-tolualdehyde	0.03	0.18	0.29	0.23	0.20
n-hexaldehyde	0.38	0.16	0.52	0.20	0.85
2,5-dimethylbenzaldehyde	N.A.	N.A.	N.A.	N.A.	N.A.

* N.A. – not available

Table 6.3 Top ten species with the highest OFP from vehicular emission in 2003 and 2015 through the tunnel study

2003					2015				
VOCs	**MIR (gO_3 g^{-1})**	**OFP (mgO_3 veh^{-1} km^{-1})**		**Percentage (%)**	**VOCs**	**MIR (gO_3 g^{-1})**	**OFP (mgO_3 veh^{-1} km^{-1})**		**Percentage (%)**
		Average	**S.D.**				**Average**	**S.D.**	
formaldehyde	9.24	173.71	69.30	23.9%	formaldehyde	9.24	74.47	15.25	22.5%
ethene	8.76	113.88	35.04	15.7%	acetaldehyde	6.34	39.26	11.23	11.9%
propene	11.37	60.26	17.06	8.3%	ethene	8.76	37.23	17.55	11.3%
toluene	3.88	46.56	15.13	6.4%	toluene	3.88	22.43	20.25	6.8%
acetaldehyde	6.34	34.87	13.95	4.8%	propene	11.37	21.22	10.02	6.4%
m/p-xylene	7.57	28.01	9.84	3.9%	m/p-xylene	7.57	12.94	32.14	3.9%
1,2,4-trimethylbenzene	8.64	25.92	20.74	3.6%	1-butene	9.42	11.05	10.68	3.3%
1-butene	9.42	23.55	12.25	3.2%	n-butane	1.08	11.01	6.42	3.3%
crotonaldehyde	9.14	22.85	17.37	3.1%	i-butane	1.17	8.50	5.30	2.6%
1,2,3-trimethylbenzene	11.66	16.32	12.83	2.2%	1,2,4-trimethylbenzene	8.64	8.07	9.07	2.4%

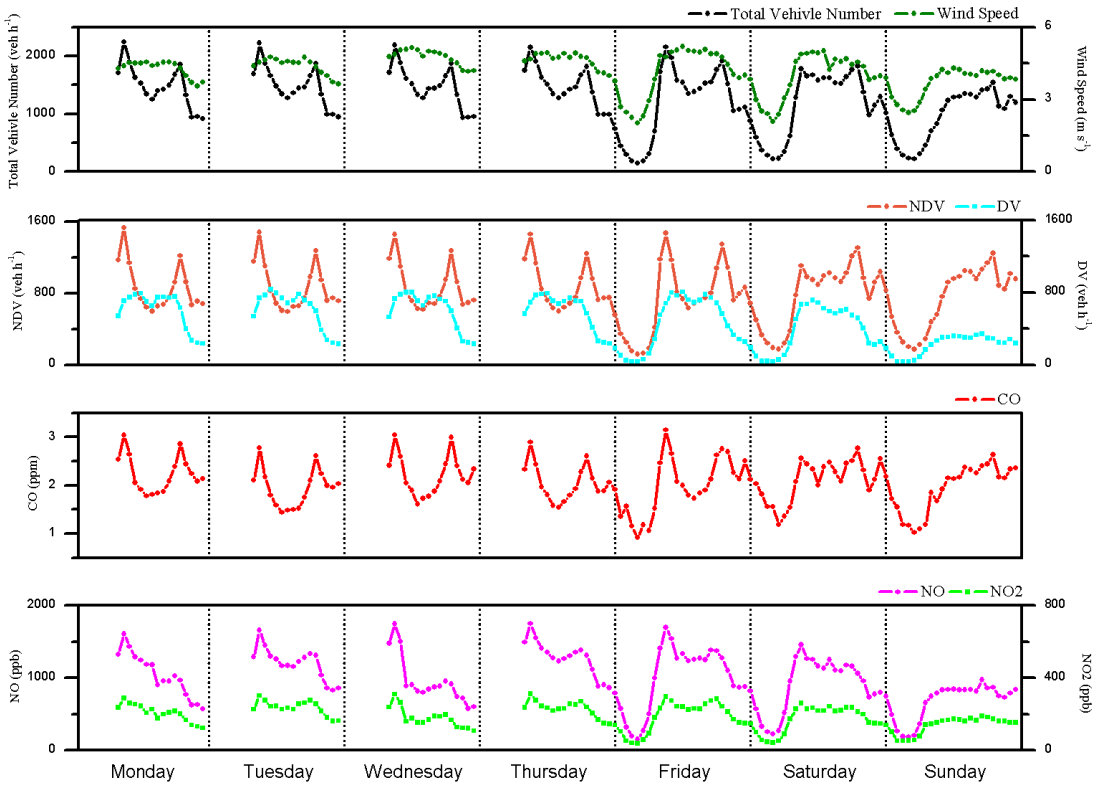

Figure 6.1 Time series of vehicle numbers, wind speed, and trace gases at the outlet site of SM tunnel in January - March 2015.

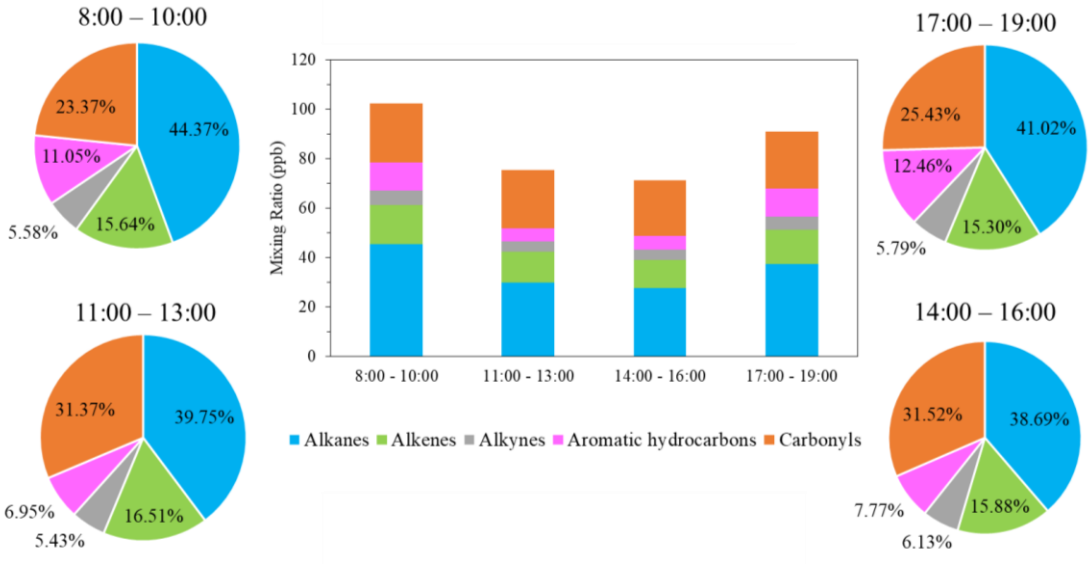

Figure 6.2 Diurnal patterns of VOCs at the outlet site of SM tunnel and their group compositions.

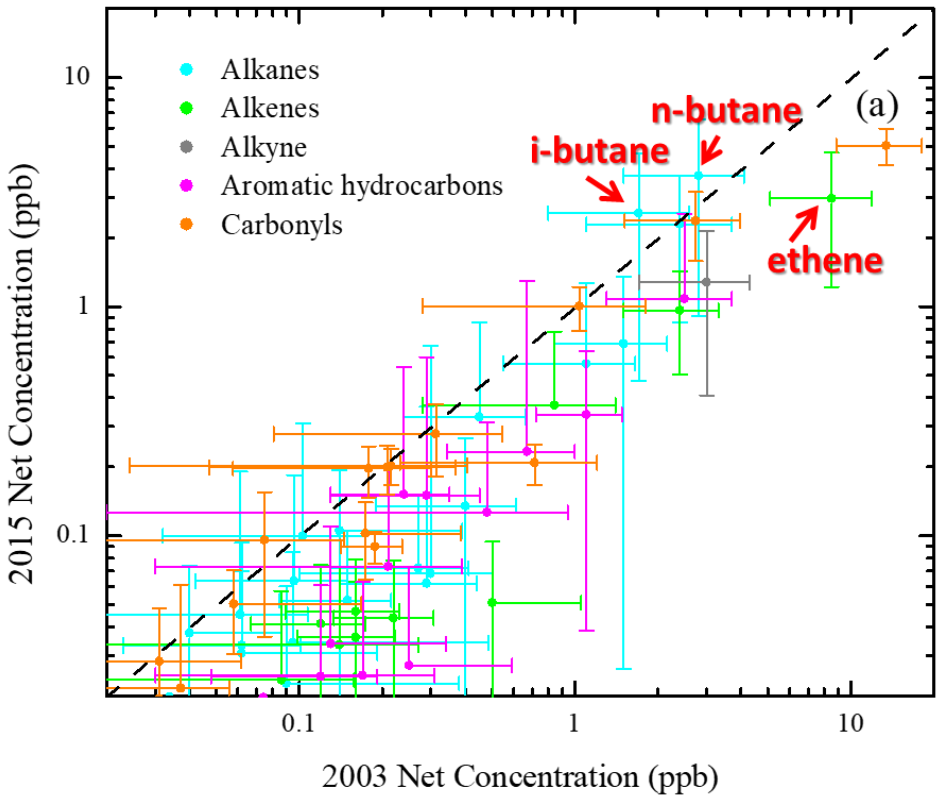

Figure 6.3 Comparison of net concentrations of individual VOCs at Shing Mun tunnel in 2003 and 2015 (error bars stand for one standard deviation).

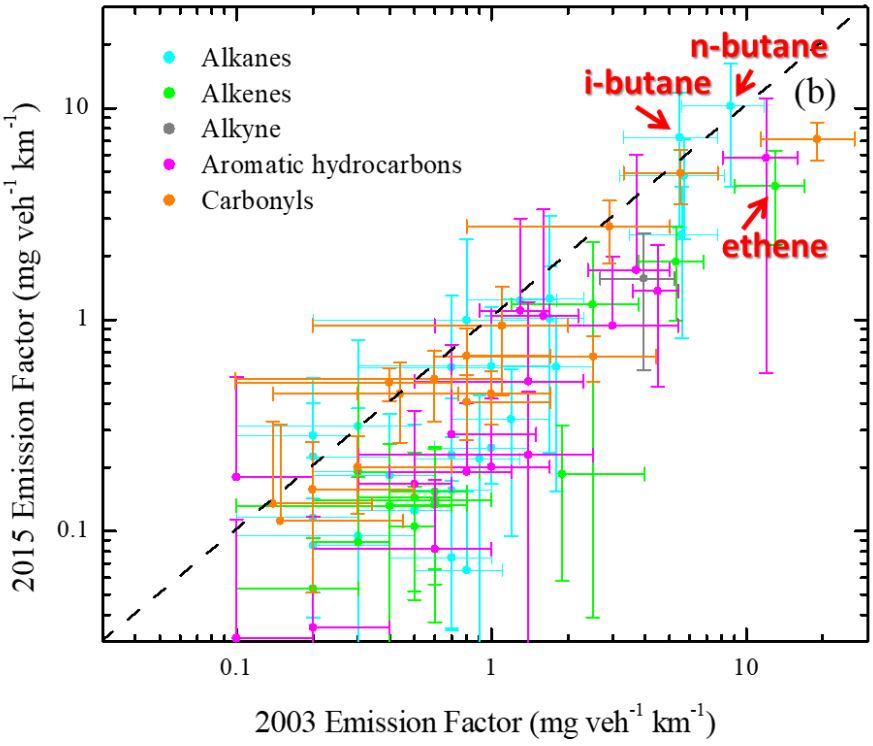

Figure 6.4 Comparison of emission factors of individual VOCs at Shing Mun tunnel in 2003 and 2015 (error bars stand for one standard deviation).

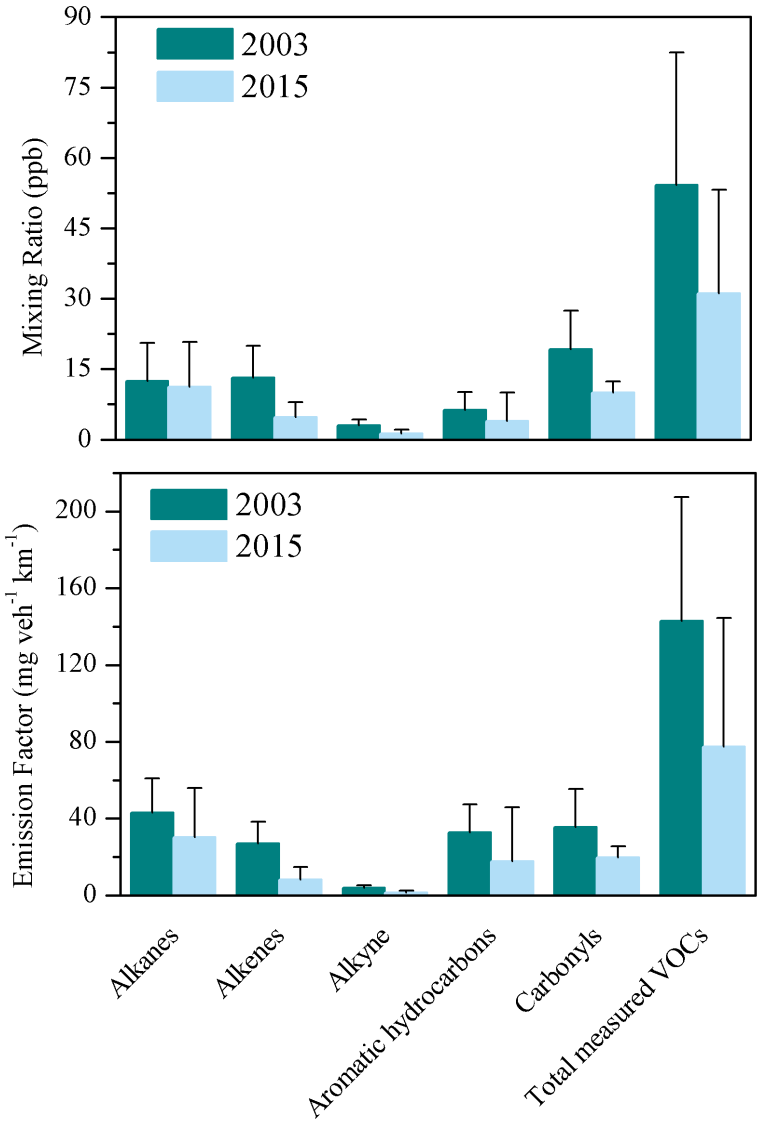

Figure 6.5 Comparison of net concentrations and emission factors of different VOC groups at Shing Mun tunnel in 2003 and 2015 (error bars stand for one standard deviation).

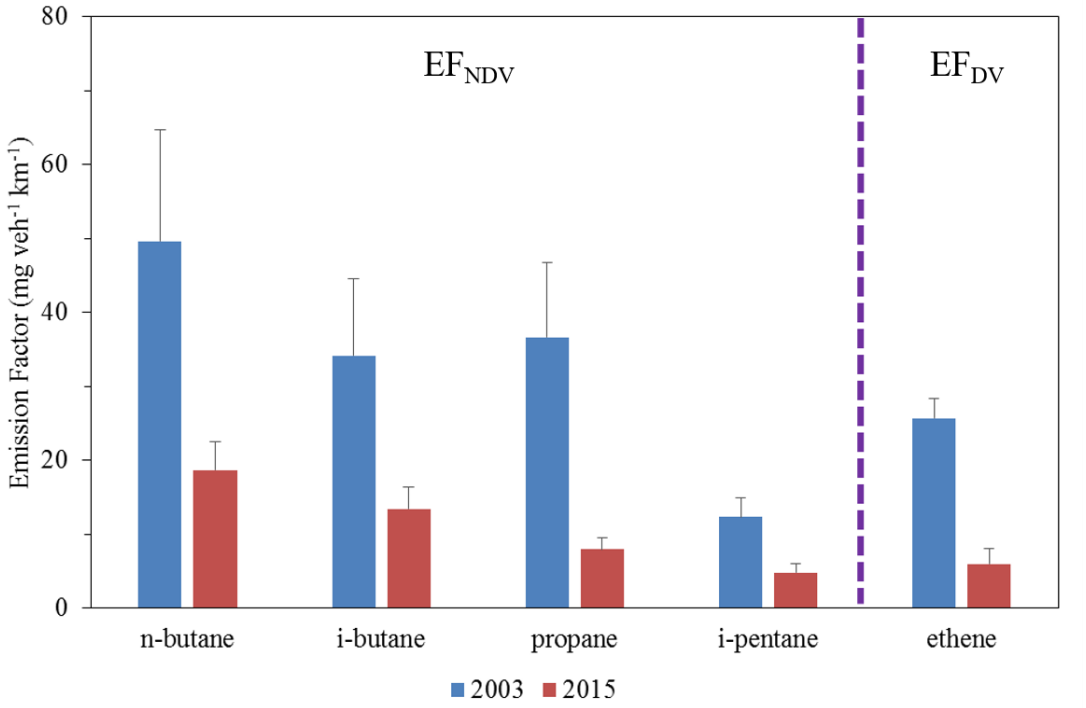

Figure 6.6 EF_{NDV} (left panel) and EF_{DV} (right panel) of specific VOC species through the tunnel study in 2003 and 2015 (error bars stand for one standard deviation).

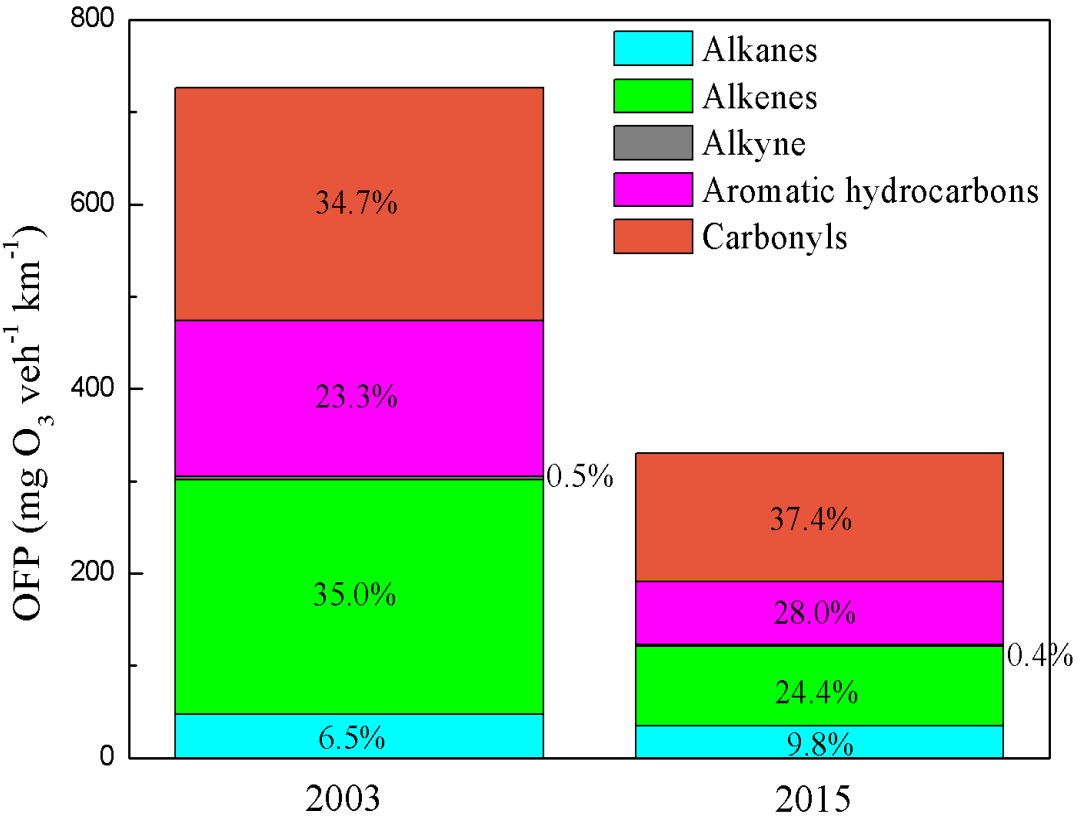

Figure 6.7 OFP of different VOC groups at SM tunnel in 2003 and 2015.

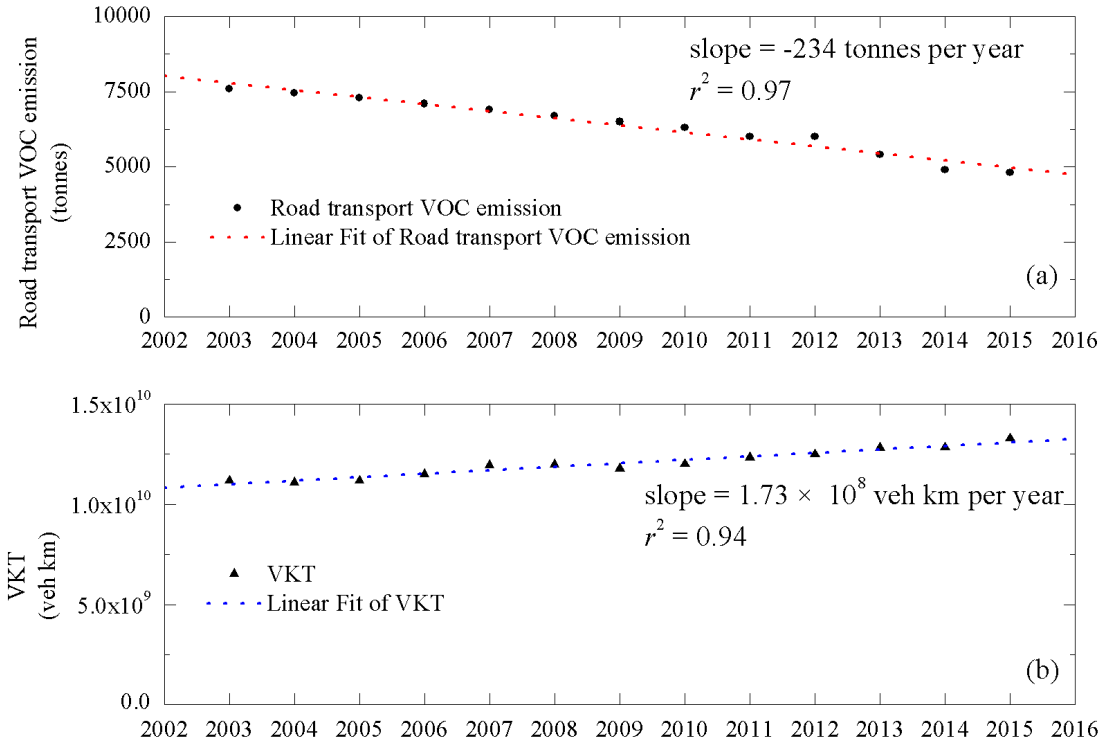

Figure 6.8 Total road transport VOC emission and VKT in Hong Kong and their linear regression with years.

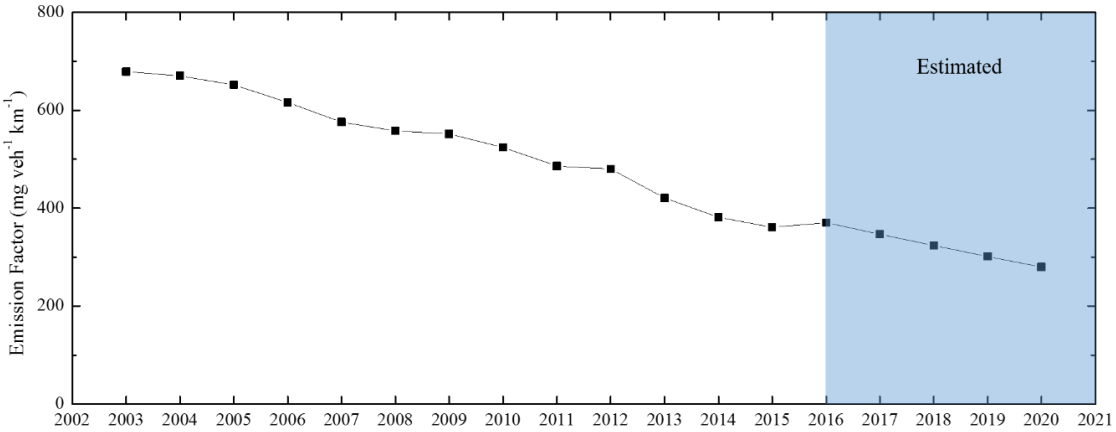

Figure 6.9 Total road transport VOC emission factor in Hong Kong from 2003 to 2020.

Chapter 7 Conclusions

The local government keeps improving the ambient air quality through a series of air pollution control measures since 1999. VOCs and OVOCs, one of the most important air pollutants, their sources varied a lot after the fulfillment of air pollution control programmes. In this study, PTR-MS was firstly used to measure ambient VOCs and OVOCs in Hong Kong, this methodology was validated based on the local environment, and it was applied on investigating roadside VOCs and OVOCs before and after the LPG CCRP from 2013 to 2014. A tunnel study was conducted in 2015 to re-examine the emissions profiles and emission factors of VOCs and OVOCs from on-road vehicles. The latest tunnel study results were compared with previous study at the same tunnel to evaluate the effectiveness of the air pollution control measures conducted during the past twelve years (from 2003 to 2015).

For the measurement of HCHO by PTR-MS, the sensitivity of HCHO was found decreased significantly when ambient RH and/or T varied. The combined effect of RH and T on HCHO measurement was found that the nonlinear surface relationship between $R_{(RH,T)}$, RH, and T through a Poly 2D regression equation $R_{(RH,T)} = 1.63 - 3.81 \cdot 10^{-3} \cdot RH + 1.92 \cdot 10^{-2} \cdot T + 5.10 \cdot 10^{-5} \cdot RH^2 - 6.41 \cdot 10^{-4} \cdot T^2 - 3.76 \cdot 10^{-4} \cdot RH \cdot T$. This method shows good correlation (slope = 1.02, $r = 0.99$) with the correction method by absolute humidity in the reference. Through the field study on VOCs and OVOCs by using PTR-MS at MK AQMS from May 2013 to August 2014, good agreements was

found between PTR-MS and DNPH-HPLC for formaldehyde (slope = 1.00, r = 0.79), acetaldehyde (slope = 1.10, r = 0.75) and MEK (slope = 0.88, r = 0.93). Good agreement was also found for aromatic hydrocarbons (benzene, toluene, and C_2-benzenes) measurements by PTR-MS, on-line GC-FID, and off-line GC-MSD/FID/ECD. Therefore, PTR-MS is applicable on real-time VOC and OVOC measurements in urban roadside areas of Hong Kong.

Roadside VOCs and OVOCs were investigated at MK AQMS from 2013 to 2014 by using PTR-MS coupled with other measurement techniques. It was found that the mixing ratio of total measured VOCs decreased by 36.7% after the LPG CCRP. Propane, i-butane, and n-butane comprised 49% of the total measured VOCs and OVOCs before the LPG CCRP, and the contribution decreased to 34% after the LPG CCRP. The OFPs, rankings and Prop-Equiv concentrations of n-butane and i-butane all decreased significantly after the LPG CCRP. The source apportionment results of roadside VOCs and OVOCs by using PMF model showed that the contribution of LPG vehicular emissions decreased from 44.7% to 37.8% after the LPG CCRP, and the OFP from LPG vehicular emissions also decreased from 8.6 ppbv O_3 $ppbv^{-1}$ to 25.8 ppbv O_3 $ppbv^{-1}$ after the LPG CCRP. The changes on different aspects can indicate that it is effective on reducing LPG vehicular emissions with the fulfillment of LPG CCRP by April 2014.

Furthermore, real-world VOC and OVOC emissions from on-road vehicles in Hong Kong were obtained through the tunnel study in 2015. Large decrease of VOC and

OVOC emissions were found by the following two aspects. On the one hand, the total VOC emission factor decreased from 42.8 ± 64.5 mg veh^{-1} km^{-1} in 2003 to 81.0 ± 57.3 mg veh^{-1} km^{-1} in 2015. On the other hand, the total OFP of measured VOCs decreased from 726.0 mgO_3 veh^{-1} km^{-1} in 2003 to 330.3 mgO_3 veh^{-1} km^{-1} in 2015. Carbonyls (i.e. formaldehyde, acetaldehyde, and acetone etc.) were found to be great contributors to both total VOC missing ratio and total OFP of measured VOCs. By comparing the reconstructed emission factors of those different vehicle types' tracers (ethane, ethyne, propane, i-butane, n-butane, i-pentane) in 2015 and 2003, large decrease of diesel /LPG /gasoline –fueled vehicle emissions can be proved.

All in all, the monitoring results of VOCs and OVOCs at both the urban roadside site and the tunnel site could demonstrate that the series of air pollution control measures undertaken during the past two decades were effective on reducing local vehicular VOC and OVOC emissions and improving the air quality in Hong Kong.

Chapter 8 Significance and Limitations of This Study

The key significance of this study are:

a) It is the first time that the effects of ambient RH and T on formaldehyde measurement by PTR-MS are explored, and a new simulation model is established for the correction of the proton transfer reaction rate coefficient of formaldehyde in this study.

b) PTR-MS was firstly used to measure urban roadside VOCs and OVOCs in Hong Kong, and this relatively new on-line measurement technique could be combined with other traditional measurement techniques to conduct further deeper research on atmospheric chemistry.

c) More accurate source apportionment of VOCs and OVOCs in Hong Kong was obtained by using the real-time VOC and OVOC data from PTR-MS and on-line GC-FID in this study. The data of OVOC species could help to separate secondary emissions in Hong Kong.

d) Updated VOC and OVOC emission profiles and emission factors were obtained through the tunnel study in 2015, which will be useful for speciated VOC inventories and related modelling studies. The large decrease of VOCs and OVOCs from 2003 to 2015 could demonstrate the effectiveness of the air pollution control measures undertaken in Hong Kong during the past twenty years.

Several limitations were still exist in this study:

a) The model PTR-QMS 500 was used in this study on measuring roadside VOCs and OVOCs, but isomers and isobars cannot be separated by this analytical technique.

b) Only 24-h canister and DNPH cartridge samples were collected to do the inter-comparison with PTR-MS data. Higher sampling time resolutions (such as 1-h or 2-h) of these off-line analytical techniques are recommended to get better inter-comparison results.

c) The PMF model was used to do the source apportionment of roadside VOCs and OVOCs in Hong Kong, The source factors resolved by this method could show bias/uncertainty of real-world emissions, and the secondary emission source cannot be separated with the biogenic emission source in this study.

d) The emission factors of VOCs and OVOCs obtained through the tunnel study can only represent the real emission factors under the speed of 60 ~ 70 km h^{-1}, and it cannot totally represent the vehicular emissions all over Hong Kong since on-road vehicles have a larger varieties of driving conditions including cold starts and stop-and-go.

Appendix A: List of Abbreviations

AH	Absolute Humidity
AP-CIMS	Atmospheric Pressure - Chemical Ionization Mass Spectrometer
AQMS	Air Quality Monitoring Station
CCRP	Catalytic Convertor Replacement Programme
CE	Collection Efficiencie
CO	Carbon Monoxide
DNPA	2,4-dinitrophenylazide
DNPH	2,4-Dinitrophenylhydrazine
DOAS	Differential Optical Absorption Spectroscopy
DV	Diesel Vehicle
EB	Environment Bureau
ECD	Electron Capture Detection
EF	Emission factor
EU	European Union
FID	Flame Ionization Detection
GC	Gas Chromatography
GCU	Gas Calibration Unit
H_3O^+	Hydronium Ions
HCHO	Formaldehyde
HKEPD	Hong Kong Environmental Protection Department
HKSARG	Hong Kong Special Administrative Region Government
HKTD	Hong Kong Transport Department
HPLC	High Performance Liquid Chromatography
LOD	Limit of Detection
LPG	Liquefied Petroleum Gas
LST	Local Standard Time
MEK	Methyl Ethyl Ketone
MIR	Maximum Incremental Reactivity
MK	Mong Kok
MLR	Multiple Linear Regression
MSD	Mass Spectrometer Detection
NDV	Non-Diesel Vehicle
NO	Nitrogen Monoxide
NO_2	Nitrogen Dioxide
NO_x	Nitrogen Oxides
OFP	Ozone Formation Potential
OVOCs	Oxygenated Volatile Organic Compounds
PA	Proton Affinity
PCA	Principal Component Analysis
PIT-MS	Proton-transfer Ion Trap - Mass Spectrometer

$PM_{2.5}$	Fine Suspended Particulates
PMF	Positive Matrix Factorization
PRD	Pearl River Delta
PTR-MS	Proton Transfer Reaction–Mass Spectrometry
Qi	Quadrupole Interface
RH	Relative Humidity
RSP	Respirable Suspended Particulates
SIFT-MS	Selected Ion Flow Tube - Mass Spectrometry
SM	Shing Mun
SO_2	Sulphur Dioxide
SOA	Secondary Organic Aerosol
SVOCs	Semi Volatile Organic Compounds
T	Temperature
Td	Townsend
TOF	Time-of-Flight
UCI	University of California, Irvine
ULSD	Ultra-Low Sulfur Diesel
US EPA	United States Environmental Protection Agency
VKT	Vehicle Kilometers Traveled
VMR	Volume Mixing Ratio
VOCs	Volatile Organic Compounds
VVOCs	Very volatile organic compounds
WHO	World Health Organization

Reference

Ambrose, J.L., Haase, K., Russo, R.S., Zhou, Y., White, M.L., Frinak, E.K., Jordan, C., Mayne, H.R., Talbot, R., Sive, B.C., 2010. A comparison of GC-FID and PTR-MS toluene measurements in ambient air under conditions of enhanced monoterpene loading. Atmos. Meas. Tech. 3, 959-980.

Atkinson, R., Arey, J., 2003. Atmospheric Degradation of Volatile Organic Compounds. Chemical Reviews 103, 4605-4638.

Beauchamp, J., Herbig, J., Dunkl, J., Singer, W., Hansel, A., 2013. On the performance of proton-transfer-reaction mass spectrometry for breath-relevant gas matrices. Measurement Science and Technology 24, 125003.

Blake, D.R., Smith, T.W., Chen, T.Y., Whipple, W.J., Rowland, F.S., 1994. Effects of biomass burning on summertime nonmethane hydrocarbon concentrations in the Canadian wetlands. Journal of Geophysical Research: Atmospheres 99, 1699-1719.

Bon, D.M., Ulbrich, I.M., de Gouw, J.A., Warneke, C., Kuster, W.C., Alexander, M.L., Baker, A., Beyersdorf, A.J., Blake, D., Fall, R., Jimenez, J.L., Herndon, S.C., Huey, L.G., Knighton, W.B., Ortega, J., Springston, S., Vargas, O., 2011. Measurements of volatile organic compounds at a suburban ground site (T1) in Mexico City during the MILAGRO 2006 campaign: measurement comparison, emission ratios, and source attribution. Atmos. Chem. Phys. 11, 2399-2421.

Borbon, A., Locoge, N., Veillerot, M., Galloo, J.C., Guillermo, R., 2002. Characterisation of NMHCs in a French urban atmosphere: overview of the main sources. Science of The Total Environment 292, 177-191.

Carter, W.P., 2009. Updated maximum incremental reactivity scale and hydrocarbon bin reactivities for regulatory applications. California Air Resources Board Contract, 07-339.

Carter, W.P.L., 1994. Development of Ozone Reactivity Scales for Volatile Organic Compounds. Air & Waste 44, 881-899.

Chan, C.Y., Chan, L.Y., Wang, X.M., Liu, Y.M., Lee, S.C., Zou, S.C., Sheng, G.Y., Fu, J.M., 2002. Volatile organic compounds in roadside microenvironments of metropolitan Hong Kong. Atmospheric Environment 36, 2039-2047.

Cheng, Y., Lee, S.C., Ho, K.F., Chow, J.C., Watson, J.G., Louie, P.K.K., Cao, J.J., Hai, X., 2010. Chemically-speciated on-road PM2.5 motor vehicle emission factors in Hong Kong. Science of The Total Environment 408, 1621-1627.

Cheng, Y., Lee, S.C., Ho, K.F., Louie, P.K.K., 2006. On-road particulate matter (PM2.5) and gaseous emissions in the Shing Mun Tunnel, Hong Kong. Atmospheric Environment 40, 4235-4245.

Cheng, Y., Lee, S.C., Huang, Y., Ho, K.F., Ho, S.S.H., Yau, P.S., Louie, P.K.K., Zhang, R.J., 2014. Diurnal and seasonal trends of carbonyl compounds in roadside, urban, and

suburban environment of Hong Kong. Atmospheric Environment 89, 43-51.

Christian, T.J., Kleiss, B., Yokelson, R.J., Holzinger, R., Crutzen, P.J., Hao, W.M., Shirai, T., Blake, D.R., 2004. Comprehensive laboratory measurements of biomass-burning emissions: 2. First intercomparison of open-path FTIR, PTR-MS, and GC-MS/FID/ECD. Journal of Geophysical Research: Atmospheres 109.

Colman, J.J., Swanson, A.L., Meinardi, S., Sive, B.C., Blake, D.R., Rowland, F.S., 2001. Description of the Analysis of a Wide Range of Volatile Organic Compounds in Whole Air Samples Collected during PEM-Tropics A and B. Analytical Chemistry 73, 3723-3731.

de Gouw, J., Warneke, C., 2007. Measurements of volatile organic compounds in the earth's atmosphere using proton-transfer-reaction mass spectrometry. Mass Spectrom Rev 26, 223-257.

de Gouw, J.A., Goldan, P.D., Warneke, C., Kuster, W.C., Roberts, J.M., Marchewka, M., Bertman, S.B., Pszenny, A.A.P., Keene, W.C., 2003. Validation of proton transfer reaction-mass spectrometry (PTR-MS) measurements of gas-phase organic compounds in the atmosphere during the New England Air Quality Study (NEAQS) in 2002. Journal of Geophysical Research: Atmospheres 108, 4682.

de Gouw, J.A., Warneke, C., Stohl, A., Wollny, A.G., Brock, C.A., Cooper, O.R., Holloway, J.S., Trainer, M., Fehsenfeld, F.C., Atlas, E.L., Donnelly, S.G., Stroud, V., Lueb, A., 2006. Volatile organic compounds composition of merged and aged forest fire

plumes from Alaska and western Canada. Journal of Geophysical Research: Atmospheres 111, D10303.

Eerdekens, G., Ganzeveld, L., Vilà-Guerau de Arellano, J., Klüpfel, T., Sinha, V., Yassaa, N., Williams, J., Harder, H., Kubistin, D., Martinez, M., Lelieveld, J., 2009. Flux estimates of isoprene, methanol and acetone from airborne PTR-MS measurements over the tropical rainforest during the GABRIEL 2005 campaign. Atmos. Chem. Phys. 9, 4207-4227.

Elliott, L., Longnecker, M.P., Kissling, G.E., London, S.J., 2006. Volatile Organic Compounds and Pulmonary Function in the Third National Health and Nutrition Examination Survey, 1988–1994. Environmental Health Perspectives 114, 1210-1214.

EU, 1999. Council Directive 1999/13/EC of 11 March 1999 on the limitation of emissions of volatile organic compounds due to the use of organic solvents in certain activities and installations.

EU, 2004. Directive 2004/42/CE of the European Parliament and of the Council of 21 April 2004 on the limitation of emissions of volatile organic compounds due to the use of organic solvents in certain paints and varnishes and vehicle refinishing products and amending Directive 1999/13/EC.

Fall, R., Karl, T., Jordan, A., Lindinger, W., 2001. Biogenic C5 VOCs: release from leaves after freeze–thaw wounding and occurrence in air at a high mountain observatory. Atmospheric Environment 35, 3905-3916.

Gouw, J.A.d., Goldan, P.D., Warneke, C., Kuster, W.C., Roberts, J.M., Marchewka, M., Bertman, S.B., Pszenny, A.A.P., Keene, W.C., 2003. Validation of proton transfer reaction-mass spectrometry (PTR-MS) measurements of gas-phase organic compounds in the atmosphere during the New England Air Quality Study (NEAQS) in 2002. Journal of Geophysical Research: Atmospheres 108.

Gouw, J.A.d., Warneke, C., Stohl, A., Wollny, A.G., Brock, C.A., Cooper, O.R., Holloway, J.S., Trainer, M., Fehsenfeld, F.C., Atlas, E.L., Donnelly, S.G., Stroud, V., Lueb, A., 2006. Volatile organic compounds composition of merged and aged forest fire plumes from Alaska and western Canada. Journal of Geophysical Research: Atmospheres 111.

Gouw, J.d., Warneke, C., 2007. Measurements of volatile organic compounds in the earth's atmosphere using proton-transfer-reaction mass spectrometry. Mass Spectrometry Reviews 26, 223-257.

Graus, M., Müller, M., Hansel, A., 2010. High Resolution PTR-TOF: Quantification and Formula Confirmation of VOC in Real Time. Journal of the American Society for Mass Spectrometry 21, 1037-1044.

Grosjean, D., Grosjean, E., Gertler, A.W., 2001. On-Road Emissions of Carbonyls from Light-Duty and Heavy-Duty Vehicles. Environmental Science & Technology 35, 45-53.

Guenther, A., Hewitt, C.N., Erickson, D., Fall, R., Geron, C., Graedel, T., Harley, P., Klinger, L., Lerdau, M., Mckay, W.A., Pierce, T., Scholes, B., Steinbrecher, R.,

Tallamraju, R., Taylor, J., Zimmerman, P., 1995. A global model of natural volatile organic compound emissions. Journal of Geophysical Research: Atmospheres 100, 8873-8892.

Guo, H., Cheng, H.R., Ling, Z.H., Louie, P.K.K., Ayoko, G.A., 2011a. Which emission sources are responsible for the volatile organic compounds in the atmosphere of Pearl River Delta? Journal of Hazardous Materials 188, 116-124.

Guo, H., Lee, S.C., Louie, P.K.K., Ho, K.F., 2004a. Characterization of hydrocarbons, halocarbons and carbonyls in the atmosphere of Hong Kong. Chemosphere 57, 1363-1372.

Guo, H., So, K.L., Simpson, I.J., Barletta, B., Meinardi, S., Blake, D.R., 2007. C1–C8 volatile organic compounds in the atmosphere of Hong Kong: Overview of atmospheric processing and source apportionment. Atmospheric Environment 41, 1456-1472.

Guo, H., Wang, T., Blake, D.R., Simpson, I.J., Kwok, Y.H., Li, Y.S., 2006. Regional and local contributions to ambient non-methane volatile organic compounds at a polluted rural/coastal site in Pearl River Delta, China. Atmospheric Environment 40, 2345-2359.

Guo, H., Wang, T., Simpson, I.J., Blake, D.R., Yu, X.M., Kwok, Y.H., Li, Y.S., 2004b. Source contributions to ambient VOCs and CO at a rural site in eastern China. Atmospheric Environment 38, 4551-4560.

Guo, H., Zou, S.C., Tsai, W.Y., Chan, L.Y., Blake, D.R., 2011b. Emission characteristics of nonmethane hydrocarbons from private cars and taxis at different driving speeds in Hong Kong. Atmospheric Environment 45, 2711-2721.

Haagen-Smit, A.J., 1952. Chemistry and Physiology of Los Angeles Smog. Industrial & Engineering Chemistry 44, 1342-1346.

Hansel, A., Jordan, A., Holzinger, R., Prazeller, P., Vogel, W., Lindinger, W., 1995. Proton transfer reaction mass spectrometry: on-line trace gas analysis at the ppb level. International Journal of Mass Spectrometry and Ion Processes 149-150, 609-619.

Hansel, A., Singer, W., Wisthaler, A., Schwarzmann, M., Lindinger, W., 1997. Energy dependencies of the proton transfer reactions H3O+ + CH2O ⇔ CH2OH+ + H2O. International Journal of Mass Spectrometry and Ion Processes 167-168, 697-703.

Herndon, S.C., Jayne, J.T., Zahniser, M.S., Worsnop, D.R., Knighton, B., Alwine, E., Lamb, B.K., Zavala, M., Nelson, D.D., McManus, J.B., Shorter, J.H., Canagaratna, M.R., Onasch, T.B., Kolb, C.E., 2005. Characterization of urban pollutant emission fluxes and ambient concentration distributions using a mobile laboratory with rapid response instrumentation. Faraday discussions 130, 327-339; discussion 363-386, 519-324.

Herrington, J.S., Fan, Z.-H., Lioy, P.J., Zhang, J., 2007. Low Acetaldehyde Collection Efficiencies for 24-Hour Sampling with 2,4-Dinitrophenylhydrazine (DNPH)-Coated Solid Sorbents. Environmental Science & Technology 41, 580-585.

Herrington, J.S., Hays, M.D., 2012. Concerns regarding 24-h sampling for formaldehyde, acetaldehyde, and acrolein using 2,4-dinitrophenylhydrazine (DNPH)-coated solid sorbents. Atmospheric Environment 55, 179-184.

HKEPD, 2017. 2015 Hong Kong Emission Inventory Report.

HKTD, 2014. The Annual Traffic Census 2014.

HKTD, 2015. The Annual Traffic Census 2015.

Ho, K.F., Ho, S.S.H., Lee, S.C., Cheng, Y., Chow, J.C., Watson, J.G., Louie, P.K.K., Tian, L., 2009a. Emissions of gas- and particle-phase polycyclic aromatic hydrocarbons (PAHs) in the Shing Mun Tunnel, Hong Kong. Atmospheric Environment 43, 6343-6351.

Ho, K.F., Ho, S.S.H., Lee, S.C., Louie, P.K.K., Cao, J.J., Deng, W.J., 2013. Volatile Organic Compounds in Roadside Environment of Hong Kong. Aerosol Air Qual. Res. 13, 1331-1347.

Ho, K.F., Lee, S.C., Guo, H., Tsai, W.Y., 2004. Seasonal and diurnal variations of volatile organic compounds (VOCs) in the atmosphere of Hong Kong. Science of The Total Environment 322, 155-166.

Ho, K.F., Lee, S.C., Ho, W.K., Blake, D.R., Cheng, Y., Li, Y.S., Ho, S.S.H., Fung, K., Louie, P.K.K., Park, D., 2009b. Vehicular emission of volatile organic compounds (VOCs) from a tunnel study in Hong Kong. Atmospheric Chemistry and Physics 9,

7491-7504.

Ho, K.F., Lee, S.C., Louie, P.K.K., Zou, S.C., 2002. Seasonal variation of carbonyl compound concentrations in urban area of Hong Kong. Atmospheric Environment 36, 1259-1265.

Ho, K.F., Sai Hang Ho, S., Cheng, Y., Lee, S.C., Zhen Yu, J., 2007. Real-world emission factors of fifteen carbonyl compounds measured in a Hong Kong tunnel. Atmospheric Environment 41, 1747-1758.

Ho, S.S.H., Chow, J.C., Watson, J.G., Ip, H.S.S., Ho, K.F., Dai, W.T., Cao, J.J., 2014. Biases in ketone measurements using DNPH-coated solid sorbent cartridges. Analytical Methods 6, 967-974.

Ho, S.S.H., Ho, K.F., Lee, S.C., Cheng, Y., Yu, J.Z., Lam, K.M., Feng, N.S.Y., Huang, Y., 2012. Carbonyl emissions from vehicular exhausts sources in Hong Kong. J. Air Waste Manage. Assoc. 62, 221-234.

Huang, X., Zhang, Y., Yang, W., Huang, Z., Wang, Y., Zhang, Z., He, Q., Lü, S., Huang, Z., Bi, X., Wang, X., 2017. Effect of traffic restriction on reducing ambient volatile organic compounds (VOCs): Observation-based evaluation during a traffic restriction drill in Guangzhou, China. Atmospheric Environment 161, 61-70.

Huang, Y., Ho, S.S.H., Ho, K.F., Lee, S.C., Yu, J.Z., Louie, P.K.K., 2011. Characteristics and health impacts of VOCs and carbonyls associated with residential cooking activities

in Hong Kong. Journal of Hazardous Materials 186, 344-351.

Huang, Y., Ling, Z.H., Lee, S.C., Ho, S.S.H., Cao, J.J., Blake, D.R., Cheng, Y., Lai, S.C., Ho, K.F., Gao, Y., Cui, L., Louie, P.K.K., 2015. Characterization of volatile organic compounds at a roadside environment in Hong Kong: An investigation of influences after air pollution control strategies. Atmospheric Environment 122, 809-818.

Inomata, S., Tanimoto, H., Kameyama, S., Tsunogai, U., Irie, H., Kanaya, Y., Wang, Z., 2008a. Technical Note: Determination of formaldehyde mixing ratios in air with PTR-MS: laboratory experiments and field measurements. Atmos. Chem. Phys. 8, 273-284.

Inomata, S., Tanimoto, H., Kameyama, S., Tsunogai, U., Irie, H., Kanaya, Y., Wang, Z., 2008b. Technical Note: Determination of formaldehyde mixing ratios in air with PTR-MS: laboratory experiments and field measurements. Atmospheric Chemistry and Physics 8, 273-284.

Inomata, S., Tanimoto, H., Kato, S., Suthawaree, J., Kanaya, Y., Pochanart, P., Liu, Y., Wang, Z., 2010. PTR-MS measurements of non-methane volatile organic compounds during an intensive field campaign at the summit of Mount Tai, China, in June 2006. Atmospheric Chemistry and Physics 10, 7085-7099.

Int Panis, L., Broekx, S., Liu, R., 2006. Modelling instantaneous traffic emission and the influence of traffic speed limits. Science of The Total Environment 371, 270-285.

Jobson, B.T., McCoskey, J.K., 2010. Sample drying to improve HCHO measurements by PTR-MS instruments: laboratory and field measurements. Atmos. Chem. Phys. 10, 1821-1835.

Jobson, B.T., Volkamer, R.A., Velasco, E., Allwine, G., Westberg, H., Lamb, B.K., Alexander, M.L., Berkowitz, C.M., Molina, L.T., 2010. Comparison of aromatic hydrocarbon measurements made by PTR-MS, DOAS and GC-FID during the MCMA 2003 Field Experiment. Atmos. Chem. Phys. 10, 1989-2005.

Jordan, A., Haidacher, S., Hanel, G., Hartungen, E., Märk, L., Seehauser, H., Schottkowsky, R., Sulzer, P., Märk, T.D., 2009. A high resolution and high sensitivity proton-transfer-reaction time-of-flight mass spectrometer (PTR-TOF-MS). International Journal of Mass Spectrometry 286, 122-128.

Kampa, M., Castanas, E., 2008. Human health effects of air pollution. Environmental Pollution 151, 362-367.

Kato, S., Miyakawa, Y., Kaneko, T., Kajii, Y., 2004. Urban air measurements using PTR-MS in Tokyo area and comparison with GC-FID measurements. International Journal of Mass Spectrometry 235, 103-110.

Kean, A.J., Harley, R.A., Kendall, G.R., 2003. Effects of Vehicle Speed and Engine Load on Motor Vehicle Emissions. Environmental Science & Technology 37, 3739-3746.

Kerns, W.D., Pavkov, K.L., Donofrio, D.J., Gralla, E.J., Swenberg, J.A., 1983. Carcinogenicity of Formaldehyde in Rats and Mice after Long-Term Inhalation Exposure. Cancer Research 43, 4382-4392.

Kuster, W.C., Jobson, B.T., Karl, T., Riemer, D., Apel, E., Goldan, P.D., Fehsenfeld, F.C., 2004. Intercomparison of Volatile Organic Carbon Measurement Techniques and Data at La Porte during the TexAQS2000 Air Quality Study. Environmental Science & Technology 38, 221-228.

Lau, A.K.H., Yuan, Z., Yu, J.Z., Louie, P.K.K., 2010. Source apportionment of ambient volatile organic compounds in Hong Kong. Science of The Total Environment 408, 4138-4149.

Lau, C.F., Rakowska, A., Townsend, T., Brimblecombe, P., Chan, T.L., Yam, Y.S., Močnik, G., Ning, Z., 2015. Evaluation of diesel fleet emissions and control policies from plume chasing measurements of on-road vehicles. Atmospheric Environment 122, 171-182.

Lee, S.C., Chiu, M.Y., Ho, K.F., Zou, S.C., Wang, X., 2002. Volatile organic compounds (VOCs) in urban atmosphere of Hong Kong. Chemosphere 48, 375-382.

Lelieveld, J., Evans, J.S., Fnais, M., Giannadaki, D., Pozzer, A., 2015. The contribution of outdoor air pollution sources to premature mortality on a global scale. Nature 525, 367.

Li, J., Xie, S.D., Zeng, L.M., Li, L.Y., Li, Y.Q., Wu, R.R., 2015. Characterization of ambient volatile organic compounds and their sources in Beijing, before, during, and after Asia-Pacific Economic Cooperation China 2014. Atmos. Chem. Phys. 15, 7945-7959.

Lindinger, W., Hansel, A., Jordan, A., 1998. On-line monitoring of volatile organic compounds at pptv levels by means of proton-transfer-reaction mass spectrometry (PTR-MS) medical applications, food control and environmental research. International Journal of Mass Spectrometry and Ion Processes 173, 191-241.

Ling, Z.H., Guo, H., 2014. Contribution of VOC sources to photochemical ozone formation and its control policy implication in Hong Kong. Environmental Science & Policy 38, 180-191.

Ling, Z.H., Guo, H., Cheng, H.R., Yu, Y.F., 2011. Sources of ambient volatile organic compounds and their contributions to photochemical ozone formation at a site in the Pearl River Delta, southern China. Environmental Pollution 159, 2310-2319.

Ling, Z.H., Guo, H., Zheng, J.Y., Louie, P.K.K., Cheng, H.R., Jiang, F., Cheung, K., Wong, L.C., Feng, X.Q., 2013. Establishing a conceptual model for photochemical ozone pollution in subtropical Hong Kong. Atmospheric Environment 76, 208-220.

Liu, Y., Shao, M., Fu, L., Lu, S., Zeng, L., Tang, D., 2008a. Source profiles of volatile organic compounds (VOCs) measured in China: Part I. Atmospheric Environment 42, 6247-6260.

Liu, Y., Shao, M., Lu, S., Chang, C.-C., Wang, J.-L., Fu, L., 2008b. Source apportionment of ambient volatile organic compounds in the Pearl River Delta, China: Part II. Atmospheric Environment 42, 6261-6274.

Louie, P.K.K., Ho, J.W.K., Tsang, R.C.W., Blake, D.R., Lau, A.K.H., Yu, J.Z., Yuan, Z., Wang, X., Shao, M., Zhong, L., 2013. VOCs and OVOCs distribution and control policy implications in Pearl River Delta region, China. Atmospheric Environment 76, 125-135.

Lyu, X.P., Guo, H., Simpson, I.J., Meinardi, S., Louie, P.K.K., Ling, Z.H., Wang, Y., Liu, M., Luk, C.W.Y., Wang, N., Blake, D.R., 2016. Effectiveness of replacing catalytic converters in LPG-fueled vehicles in Hong Kong. Atmospheric Chemistry and Physics 16, 6609-6626.

Mader, P.P., MacPhee, R.D., Lofberg, R.T., Larson, G.P., 1952. Composition of Organic Portion of Atmospheric Aerosols in the Los Angeles Area. Industrial & Engineering Chemistry 44, 1352-1355.

Manousakas, M., Papaefthymiou, H., Diapouli, E., Migliori, A., Karydas, A.G., Bogdanovic-Radovic, I., Eleftheriadis, K., 2017. Assessment of PM2.5 sources and their corresponding level of uncertainty in a coastal urban area using EPA PMF 5.0 enhanced diagnostics. Science of The Total Environment 574, 155-164.

Mielke, L.H., Erickson, D.E., McLuckey, S.A., Müller, M., Wisthaler, A., Hansel, A., Shepson, P.B., 2008. Development of a Proton-Transfer Reaction-Linear Ion Trap Mass

Spectrometer for Quantitative Determination of Volatile Organic Compounds. Analytical Chemistry 80, 8171-8177.

Min, S., Bin, W., Sihua, L., Bin, Y., Ming, W., 2011. Effects of Beijing Olympics Control Measures on Reducing Reactive Hydrocarbon Species. Environmental Science & Technology 45, 514-519.

Müller, K., Haferkorn, S., Grabmer, W., Wisthaler, A., Hansel, A., Kreuzwieser, J., Cojocariu, C., Rennenberg, H., Herrmann, H., 2006. Biogenic carbonyl compounds within and above a coniferous forest in Germany. Atmospheric Environment 40, 81-91.

Nelson, P.F., Quigley, S.M., 1983. The m,p-xylenes:ethylbenzene ratio. A technique for estimating hydrocarbon age in ambient atmospheres. Atmospheric Environment (1967) 17, 659-662.

Norris, G., Duvall, R., Brown, S., Bai, S., 2014. EPA Positive Matrix Factorization (PMF) 5.0 fundamentals and User Guide Prepared for the US Environmental Protection Agency Office of Research and Development, Washington, DC. Inc., Petaluma.

Ou, J., Guo, H., Zheng, J., Cheung, K., Louie, P.K.K., Ling, Z., Wang, D., 2015. Concentrations and sources of non-methane hydrocarbons (NMHCs) from 2005 to 2013 in Hong Kong: A multi-year real-time data analysis. Atmospheric Environment 103, 196-206.

Paatero, P., 2000. User's guide for positive matrix factorization programs PMF2 and

PMF3. Helsinki: University of Helsinki.

Paatero, P., Tapper, U., 1994. Positive matrix factorization: A non-negative factor model with optimal utilization of error estimates of data values. Environmetrics 5, 111-126.

Pierson, W.R., Brachaczek, W.W., 1982. Particulate Matter Associated with Vehicles on the Road. II. Aerosol Science and Technology 2, 1-40.

Pierson, W.R., Gertler, A.W., Robinson, N.F., Sagebiel, J.C., Zielinska, B., Bishop, G.A., Stedman, D.H., Zweidinger, R.B., Ray, W.D., 1996. Real-world automotive emissions—Summary of studies in the Fort McHenry and Tuscarora mountain tunnels. Atmospheric Environment 30, 2233-2256.

Rogers, T.M., Grimsrud, E.P., Herndon, S.C., Jayne, J.T., Kolb, C.E., Allwine, E., Westberg, H., Lamb, B.K., Zavala, M., Molina, L.T., Molina, M.J., Knighton, W.B., 2006. On-road measurements of volatile organic compounds in the Mexico City metropolitan area using proton transfer reaction mass spectrometry. International Journal of Mass Spectrometry 252, 26-37.

Sahu, L.K., 2012. Volatile organic compounds and their measurements in the troposphere. Current Science 102, 1645-1649.

Seila, R.L., Main, H.H., Arriaga, J.L., Martínez V, G., Ramadan, A.B., 2001. Atmospheric volatile organic compound measurements during the 1996 Paso del Norte Ozone Study. Science of The Total Environment 276, 153-169.

Shao, P., An, J., Xin, J., Wu, F., Wang, J., Ji, D., Wang, Y., 2016. Source apportionment of VOCs and the contribution to photochemical ozone formation during summer in the typical industrial area in the Yangtze River Delta, China. Atmospheric Research 176-177, 64-74.

Sillman, S., 2002. Chapter 12 The relation between ozone, NOx and hydrocarbons in urban and polluted rural environments, in: Austin, J., Brimblecombe, P., Sturges, W. (Eds.), Developments in Environmental Science. Elsevier, pp. 339-385.

Simpson, I.J., Blake, N.J., Barletta, B., Diskin, G.S., Fuelberg, H.E., Gorham, K., Huey, L.G., Meinardi, S., Rowland, F.S., Vay, S.A., Weinheimer, A.J., Yang, M., Blake, D.R., 2010. Characterization of trace gases measured over Alberta oil sands mining operations: 76 speciated C2-C10 volatile organic compounds (VOCs), CO2, CH4, CO, NO, NO2, NO, O3 and SO2. Atmos. Chem. Phys. 10, 11931-11954.

Slowik, J.G., Vlasenko, A., McGuire, M., Evans, G.J., Abbatt, J.P.D., 2010. Simultaneous factor analysis of organic particle and gas mass spectra: AMS and PTR-MS measurements at an urban site. Atmos. Chem. Phys. 10, 1969-1988.

Smith, D., Španěl, P., 2005. Selected ion flow tube mass spectrometry (SIFT-MS) for on-line trace gas analysis. Mass Spectrometry Reviews 24, 661-700.

So, K.L., Wang, T., 2004. C3–C12 non-methane hydrocarbons in subtropical Hong Kong: spatial–temporal variations, source–receptor relationships and photochemical reactivity. Science of The Total Environment 328, 161-174.

Spanel, P., Smith, D., 2008. Quantification of trace levels of the potential cancer biomarkers formaldehyde, acetaldehyde and propanol in breath by SIFT-MS. Journal of breath research 2, 046003.

Sprung, D., Jost, C., Reiner, T., Hansel, A., Wisthaler, A., 2001. Acetone and acetonitrile in the tropical Indian Ocean boundary layer and free troposphere: Aircraft-based intercomparison of AP-CIMS and PTR-MS measurements. Journal of Geophysical Research: Atmospheres 106, 28511-28527.

Staehelin, J., Schläpfer, K., Bürgin, T., Steinemann, U., Schneider, S., Brunner, D., Bäumle, M., Meier, M., Zahner, C., Keiser, S., Stahel, W., Keller, C., 1995. Emission factors from road traffic from a tunnel study (Gubrist tunnel, Switzerland). Part I: concept and first results. Science of The Total Environment 169, 141-147.

Stavrakou, T., Müller, J.F., De Smedt, I., Van Roozendael, M., van der Werf, G.R., Giglio, L., Guenther, A., 2009. Evaluating the performance of pyrogenic and biogenic emission inventories against one decade of space-based formaldehyde columns. Atmos. Chem. Phys. 9, 1037-1060.

Stemmler, K., Bugmann, S., Buchmann, B., Reimann, S., Staehelin, J., 2005. Large decrease of VOC emissions of Switzerland's car fleet during the past decade: results from a highway tunnel study. Atmospheric Environment 39, 1009-1018.

Sulzer, P., Hartungen, E., Hanel, G., Feil, S., Winkler, K., Mutschlechner, P., Haidacher, S., Schottkowsky, R., Gunsch, D., Seehauser, H., Striednig, M., Jürschik, S., Breiev, K.,

Lanza, M., Herbig, J., Märk, L., Märk, T.D., Jordan, A., 2014. A Proton Transfer Reaction-Quadrupole interface Time-Of-Flight Mass Spectrometer (PTR-QiTOF): High speed due to extreme sensitivity. International Journal of Mass Spectrometry 368, 1-5.

Tang, J.H., Chan, L.Y., Chan, C.Y., Li, Y.S., Chang, C.C., Liu, S.C., Wu, D., Li, Y.D., 2007. Characteristics and diurnal variations of NMHCs at urban, suburban, and rural sites in the Pearl River Delta and a remote site in South China. Atmospheric Environment 41, 8620-8632.

Tsai, W.Y., Chan, L.Y., Blake, D.R., Chu, K.W., 2006. Vehicular fuel composition and atmospheric emissions in South China: Hong Kong, Macau, Guangzhou, and Zhuhai. Atmos. Chem. Phys. 6, 3281-3288.

USEPA, 1999. EPA Method TO-11A: Determination of Formaldehyde in Ambient Air Using Adsorbent Cartridge Followed by High Performance Liquid Chromatography (HPLC). U.S. Environmental Protection Agency.

USEPA, 2009. United States Environmental Protection Agency, Technology transfer Network/National Ambient Air Quality Standards, Ozone Implementation: Definition of Volatile Organic Compounds (VOC).

Vlasenko, A., Macdonald, A., Sjostedt, S., Abbatt, J., 2010. Formaldehyde measurements by Proton transfer reaction–Mass Spectrometry (PTR-MS): correction for humidity effects. Atmos. Meas. Tech. 3, 1055-1062.

von Schneidemesser, E., Monks, P.S., Plass-Duelmer, C., 2010. Global comparison of VOC and CO observations in urban areas. Atmospheric Environment 44, 5053-5064.

Wang, B., Liu, Y., Shao, M., Lu, S., Wang, M., Yuan, B., Gong, Z., He, L., Zeng, L., Hu, M., Zhang, Y., 2016. The contributions of biomass burning to primary and secondary organics: A case study in Pearl River Delta (PRD), China. Science of The Total Environment 569-570, 548-556.

Wang, C., Wu, S., Zhou, S., Wang, H., Li, B., Chen, H., Yu, Y., Shi, Y., 2015. Polycyclic aromatic hydrocarbons in soils from urban to rural areas in Nanjing: Concentration, source, spatial distribution, and potential human health risk. Science of The Total Environment 527-528, 375-383.

Wang, M., Zeng, L., Lu, S., Shao, M., Liu, X., Yu, X., Chen, W., Yuan, B., Zhang, Q., Hu, M., Zhang, Z., 2014. Development and validation of a cryogen-free automatic gas chromatograph system (GC-MS/FID) for online measurements of volatile organic compounds. Analytical Methods 6, 9424-9434.

Wang, T., Cheung, T.F., Li, Y.S., Yu, X.M., Blake, D.R., 2002. Emission characteristics of CO, NOx, SO2 and indications of biomass burning observed at a rural site in eastern China. Journal of Geophysical Research: Atmospheres 107, ACH 9-1-ACH 9-10.

Wang, T., Wei, X.L., Ding, A.J., Poon, C.N., Lam, K.S., Li, Y.S., Chan, L.Y., Anson, M., 2009. Increasing surface ozone concentrations in the background atmosphere of Southern China, 1994–2007. Atmos. Chem. Phys. 9, 6217-6227.

Wang, X., Wu, T., 2008. Release of Isoprene and Monoterpenes during the Aerobic Decomposition of Orange Wastes from Laboratory Incubation Experiments. Environmental Science & Technology 42, 3265-3270.

Ware, J.H., Spengler, J.D., Neas, L.M., Samet, J.M., Wagner, G.R., Coultas, D., Ozkaynak, H., Schwab, M., 1993. Respiratory and Irritant Health Effects of Ambient Volatile Organic CompoundsThe Kanawha County Health Study. American Journal of Epidemiology 137, 1287-1301.

Warneke, C., de Gouw, J.A., Lovejoy, E.R., Murphy, P.C., Kuster, W.C., Fall, R., 2005. Development of Proton-Transfer Ion Trap-Mass Spectrometry: On-line Detection and Identification of Volatile Organic Compounds in Air. Journal of the American Society for Mass Spectrometry 16, 1316-1324.

Warneke, C., Gouw, J.A., Holloway, J.S., Peischl, J., Ryerson, T.B., Atlas, E., Blake, D., Trainer, M., Parrish, D.D., 2012. Multiyear trends in volatile organic compounds in Los Angeles, California: Five decades of decreasing emissions. Journal of Geophysical Research: Atmospheres 117.

Warneke, C., Roberts, J.M., Veres, P., Gilman, J., Kuster, W.C., Burling, I., Yokelson, R., de Gouw, J.A., 2011a. VOC identification and inter-comparison from laboratory biomass burning using PTR-MS and PIT-MS. International Journal of Mass Spectrometry 303, 6-14.

Warneke, C., van der Veen, C., Luxembourg, S., de Gouw, J.A., Kok, A., 2001.

Measurements of benzene and toluene in ambient air using proton-transfer-reaction mass spectrometry: calibration, humidity dependence, and field intercomparison. International Journal of Mass Spectrometry 207, 167-182.

Warneke, C., Veres, P., Holloway, J.S., Stutz, J., Tsai, C., Alvarez, S., Rappenglueck, B., Fehsenfeld, F.C., Graus, M., Gilman, J.B., de Gouw, J.A., 2011b. Airborne formaldehyde measurements using PTR-MS: calibration, humidity dependence, inter-comparison and initial results. Atmos. Meas. Tech. 4, 2345-2358.

Warneke, C., Veres, P., Holloway, J.S., Stutz, J., Tsai, C., Alvarez, S., Rappenglueck, B., Fehsenfeld, F.C., Graus, M., Gilman, J.B., de Gouw, J.A., 2011c. Airborne formaldehyde measurements using PTR-MS: calibration, humidity dependence, inter-comparison and initial results. Atmos. Meas. Tech. 4, 2345-2358.

Watson, J.G., Chow, J.C., Fujita, E.M., 2001. Review of volatile organic compound source apportionment by chemical mass balance. Atmospheric Environment 35, 1567-1584.

Wisthaler, A., Apel, E.C., Bossmeyer, J., Hansel, A., Junkermann, W., Koppmann, R., Meier, R., Müller, K., Solomon, S.J., Steinbrecher, R., Tillmann, R., Brauers, T., 2008. Technical Note: Intercomparison of formaldehyde measurements at the atmosphere simulation chamber SAPHIR. Atmos. Chem. Phys. 8, 2189-2200.

World Health, O., 1989. Indoor air quality: Organic pollutants. Environmental Technology Letters 10, 855-858.

Xue, L., Wang, T., Louie, P.K.K., Luk, C.W.Y., Blake, D.R., Xu, Z., 2014. Increasing External Effects Negate Local Efforts to Control Ozone Air Pollution: A Case Study of Hong Kong and Implications for Other Chinese Cities. Environmental Science & Technology 48, 10769-10775.

Yuan, B., Koss, A.R., Warneke, C., Coggon, M., Sekimoto, K., de Gouw, J.A., 2017. Proton-Transfer-Reaction Mass Spectrometry: Applications in Atmospheric Sciences. Chemical Reviews 117, 13187-13229.

Yuan, B., Shao, M., Gouw, J., Parrish, D.D., Lu, S., Wang, M., Zeng, L., Zhang, Q., Song, Y., Zhang, J., Hu, M., 2012. Volatile organic compounds (VOCs) in urban air: How chemistry affects the interpretation of positive matrix factorization (PMF) analysis. Journal of Geophysical Research: Atmospheres 117.

Yuan, Z., Yadav, V., Turner, J.R., Louie, P.K.K., Lau, A.K.H., 2013a. Long-term trends of ambient particulate matter emission source contributions and the accountability of control strategies in Hong Kong over 1998–2008. Atmospheric Environment 76, 21-31.

Yuan, Z., Zhong, L., Lau, A.K.H., Yu, J.Z., Louie, P.K.K., 2013b. Volatile organic compounds in the Pearl River Delta: Identification of source regions and recommendations for emission-oriented monitoring strategies. Atmospheric Environment 76, 162-172.

Zhang, J., Smith, K.R., 2003. Indoor air pollution: a global health concern. British Medical Bulletin 68, 209-225.

Zhang, Y., Wang, X., Blake, D.R., Li, L., Zhang, Z., Wang, S., Guo, H., Lee, F.S.C., Gao, B., Chan, L., Wu, D., Rowland, F.S., 2012. Aromatic hydrocarbons as ozone precursors before and after outbreak of the 2008 financial crisis in the Pearl River Delta region, south China. Journal of Geophysical Research: Atmospheres 117.